Safety Analysis of Highway Curves Where Crashes Occur in South Carolina

FINAL REPORT

Prepared by:

Wayne Sarasua
Pamela Murray-Tuite
Farhad Farzinpour
Glenn Department of Civil Engineering
Clemson University

Kweku Brown
William J. Davis
Emmett Davis Dept. of Civil, Environmental & Construction Engineering
The Citadel

FHWA-SC-26-01

February 1, 2026

Sponsoring Agencies:

South Carolina Department of Transportation
Office of Materials and Research
1406 Shop Road
Columbia, SC 29201

Federal Highway Administration
South Carolina Division
Strom Thurmond Federal Building
1835 Assembly Street, Suite 1270
Columbia, SC 29201

Technical Report Documentation Page

1. Report No FHWA-SC-26-01	2. Government Accession No.	3. Recipient's Catalog No.
4. Title and Subtitle Safety Analysis of Highway Curves Where Crashes Occur in South Carolina		5. Report Date February 1, 2026 6. Performing Organization Code
7. Author/s W. Sarasua, P. Murray-Tuite, F. Farzinpour, K. Brown, W. Davis		8. Performing Organization Report No.
9. Performing Organization Name and Address Glenn Department of Civil Engineering 110 Lowry Hall Clemson, SC 29634		10. Work Unit No. (TRAIS) 11. Contract or Grant No. SPR No. 771
12. Sponsoring Organization Name and Address South Carolina Department of Transportation Office of Materials and Research 1406 Shop Road Columbia, SC 29201		13. Type of Report and Period Covered Final Report 14. Sponsoring Agency Code
15. Supplementary Notes		

16. Abstract

The design of highway curves has significant impact on traffic safety. More than 25% of fatal crashes in the United States occur on horizontal curves, and the crash rate for curves is approximately three times higher than other highway sections. Furthermore, crashes are over 4 times more likely to be fatal on horizontal curve sections compared to similar highway tangent sections. These statistics underscore the critical need to identify and mitigate the specific risks associated with driving on curved sections, particularly in the context of Vision Zero goals for zero roadway fatalities. This research focuses on a detailed analysis of curves where vehicle crashes occur in South Carolina. Eight years of crash data and an inventory of circular curves including Rieker CARS data are analyzed to identify trends and the effectiveness of countermeasures. The research achieved several objectives including identifying potential locations of compliance issues related to curve signage and also identifying curve locations of highest crash frequency that can benefit from potential countermeasures. The research required innovative data development methods vital to achieve the objectives.

17. Key Words Highway Curves, Rieker CARS, curve radius, curve super elevation	18. Distribution Statement No restrictions. This document is available to the public through the National Technical Information Service, Springfield, VA 22161.		
19. Security Classification (of this report) Unclassified	20. Security Classification (of this page) Unclassified	21. No. Of Pages	22. Price

Form DOT F 1700.7 (8-72)   Reproduction of form and completed page is authorized

DISCLAIMER

The contents of this report reflect the views of the author who is responsible for the facts and the accuracy of the data presented herein. The contents do not necessarily reflect the official views or policies of the South Carolina Department of Transportation or the Federal Highway Administration. This report does not constitute a standard, specification, or regulation.

The State of South Carolina and the United States Government do not endorse products or manufacturers. Trade or manufacturer's names appear herein solely because they are considered essential to the object of this report.

ACKNOWLEDGMENTS

The research team acknowledges the South Carolina Department of Transportation and the Federal Highway Administration for supporting and funding this project. We extend our thanks to the project Steering and Implementation Committee members: Eugene Taylor (Chair), Edward Hunt, and Sarah Ives. Thanks also to Andrew Stokes who reviewed the draft.

The authors would like to thank the following civil engineering students who worked on this project: Henry Turner, John Penna, Nelson Essien, Pratiksha Paudel, Bayezid Islam, Nelson Ativor, Eric Thompson-Vazquez, McKenna Adams, and Genevieve Harris. Their tireless efforts were instrumental in the successful outcome of this research.

EXECUTIVE SUMMARY

The design of highway curves has significant impact on traffic safety. More than 25% of fatal crashes in the United States occur on horizontal curves, and the crash rate for curves is approximately three times higher than other highway sections. Furthermore, crashes are over 4 times more likely to be fatal on horizontal curves compared to similar highway tangent sections. South Carolina has the second highest fatality rate per hundred million vehicle miles traveled and the fourth highest fatality crash rate per 100,000 population in the country based on 2023 fatal crash data. Because of the high proportion of crash fatalities that occur on highway curves, research that can potentially reduce fatality rates is significant. This research explores methods to improve horizontal curve safety.

While there has been a great deal of research on highway curve safety and applicable countermeasures, there is still a substantial gap in the knowledge base concerning highway curve safety related to the methodology for assessing curve related crashes. Previous research has almost uniformly relied on crash codes and aggregate data. The innovative GIS techniques used in this research to associate crashes with curve buffers allow for statewide analysis and screening of curve crash incidence. Further, published highway crash countermeasures for curves from other states and jurisdictions are not calibrated for South Carolina. The modeling aspects of this research provide more appropriate crash modification factors for certain countermeasures.

The researchers developed a GIS based workflow for determining signing needs and compliance for horizontal curves. The workflow is based on using the AASHTO design equation and the TTI equation to determine the advisory speed for a curve. The workflow uses the GIS centerline database that was populated with curve attributes (curve radius, super elevation) using automated methods. The GIS automated method for determining advisory speeds is novel and efficient, requiring no additional field data collection. It provides comparable advisory speed results to Rieker CARS. The Rieker mandatory signage requirements were updated to reflect more appropriate posted speed limits.

The safety analysis of this research investigated the relationship between geometric design features of highway curves and the frequency and severity of crashes. The analysis used a population sample of curves in South Carolina that was only limited by the radius and proximity to intersections. The negative binomial crash analysis indicated that traffic volume, radius, and posted speed limit were significant estimators for total crashes, severe crashes, and single vehicle crashes. Grade was significant for single-vehicle crashes. Superelevation was significant for rural 2-lane severe crashes (fatal and incapacitating injury). Crash modification factors were developed for all of the significant parameters except for traffic volume.

The results of the research will have significant benefits for SCDOT and the traveling public, as well as other DOTs. Direct benefits to SCDOT include increased safety on highway curves through highly targeted countermeasures. Enhanced safety includes reduced crash frequency, reduced crash rates, and reduced crash severity. This final report includes a workflow that can be followed by SCDOT to facilitate future highway curve safety analysis and prioritize investment in highway curves to enhance safety in the most efficient manner. Other products of this research include several digital files provided to SCDOT:

- *A table of locations of highway curves that may not meet 2023 MUTCD standards for mandated highway curve signage.* The list includes three categories of signage: 1) curve warning; 2) curve warning with advisory speed; and 3) curve warning with advisory speed and chevron signs.

- *Tables of curves with highest crash frequency and potential countermeasures.* The tables include curve attributes, number of crashes by year, number of fatal and severe crashes, and potential countermeasures.

- *Linear referenced curve database of attributes.* This database includes curve radii for 54,000 highway curves the state. Most of these curves include superelevation and grade data extracted from aerial LiDAR.

- *ArcGIS feature class of improved highway curve signage with improved geocoding.* The speed limit and curve signage provided by SCDOT underwent a positional accuracy assessment. Milepoints were corrected for 12,500 signs (24% of the provided signs) and geographic coordinates were corrected for 4,500 signs (9% of the provided signs).

- *Speed limit database.* Prior to this research, posted speed limit data was available for only one-third of state highway mileage. The accuracy of these posted speed limits was estimated at 86%. Using a hybrid methodology developed by the researchers, posted speed limits data is now available for over 90% of state highway mileage with an estimated accuracy of 88%.

- *ArcGIS feature class of curve buffers.* When overlaid with crash data, these buffers can be used to identify curves with greatest crash frequency based on the curve safety analysis workflow.

The research recommendations revolve around all of the products of this research. In the near-term, SCDOT should focus on MUTCD sign compliance by making use of the list of locations that may be in need of signage. An obvious benefit is enhanced safety from new signage. New signage should also be an initial consideration at curves with a high frequency of crashes if signage is listed as a potential countermeasure.

The tables of roadway curves with highest crash frequency should be scrutinized and prioritized for potential funding of countermeasures. The potential reduction in crashes will be of significant benefit to SCDOT and the traveling public.

The researchers strongly recommend that SCDOT takes advantage of the data products of this research including curve attributes, greatly expanded posted speed limit data, and the improved curve sign inventory. The availability of these data should be communicated department wide to maximize the utility of the data.

Periodic use of the curve safety workflow should be used to identify future curve safety needs while also providing “after” data for monitoring the effectiveness of countermeasures.

TABLE OF CONTENTS

DISCLAIMER ..... **ii**

ACKNOWLEDGMENTS ..... **iii**

EXECUTIVE SUMMARY ..... **iv**

Chapter 1: INTRODUCTION **1**

1.1 Background 1

1.2 Problem Statement 1

1.3 Research Objectives 1

1.4 Significance of Work 2

1.5 Report Organization 3

Chapter 2: LITERATURE REVIEW AND SURVEY OF STATES **4**

2.1 Literature Review 4

2.1.1 Crash Frequency and Crash Rate 4

2.1.2 Crash Types 4

2.1.3 Curve Characteristics 5

2.1.4 Crash Severity 5

2.1.5 Highway Curve Crash Reporting 5

2.1.6 Countermeasures 6

2.1.7 Crash Prediction Models 6

2.1.8 Highway Curve Signage Requirements 7

2.1.9 Determining Highway Curve Advisory Speeds 8

2.1.10 Collection of Curve Attributes 8

2.2 Survey of State Transportation Agencies 9

Chapter 3: DATA COLLECTION PROCEDURES AND DATA SUMMARY **11**

3.1 Data Requirements ... 11

3.1.1 Crash Data and Preprocessing ... 11

3.1.2 SCDOT's Roadway Centerline and Road Inventory Management System (RIMS).. 11

3.1.3 SCDOT's Sign Inventory ... 12

3.1.4 Rieker CARS System ... 13

3.2 Collection of Horizontal Curve Radius (and an initial attempt at Superelevation) ... 13

3.2.1 Rieker CARS System ... 14

3.2.2 GIS Automated Method ... 14

3.2.3 Google Earth Approach ... 17

3.2.4 Mobile Lidar ... 18

3.2.5 Comparative Approach ... 18

3.2.6 Comparison of Rieker CARS, automated GIS, and manual Google Earth Methods . 19

3.2.7 Comparison with Mobile Lidar Scanning ... 26

3.2.8 Discussion of Comparative Results ... 26

3.2.9 Rieker Superelevation ... 29

3.2.10 Comparison of Extraction Methods with Mobile LiDAR Data ... 29

3.3 Superelevation ... 29

3.4 Posted Speed Limit ... 32

3.4.1 Extracting Posted Speed Limits from Signs ... 33

3.4.2 Extracting Posted Speed Limits from Crash Reports ... 34

Chapter 4: IDENTIFICATION OF HIGHWAY CURVE ADVISORY SPEEDS ... 38

4.1 Workflow for Determining Highway Curve Advisory Speeds ... 38

4.2 Selecting Curves ... 40

4.3 Design Equation Attributes ... 41

4.3.1 Curve Attributes ... 41

4.3.2 Friction Coefficient and Tangent 85th Percentile Speed ... 41
4.4 Identification of Horizontal Curve Advisory Signage using GIS ... 41
4.4.1 Comparison of GIS Generated Advisory Speeds with the Rieker Speeds ... 41
4.4.2 Comparison of GIS Generated Advisory Signage with SCDOT Actual Signage ... 46
4.4.3 Discussion of Comparative Results ... 50
4.5 Using the Results ... 52
Chapter 5: SAFETY ANALYSIS OF HIGHWAY CURVES ... 54
5.1 Introduction ... 54
5.2 Preparing for the Safety Analysis ... 54
5.2.1 Populating Data into GIS ... 54
5.2.2 Selecting and Stratifying Curves ... 54
5.2.3 Crash Preprocessing and Assigning Crashes to Curves ... 55
5.3 Safety Analysis using GIS ... 56
5.3.1 Statistical Analysis of Curve Crashes ... 56
5.3.2 Development of Crash Modification Factors ... 59
5.3.3 Development of a Crash Modification Factor for Grade ... 61
5.3.4 Crash Severity ... 62
5.3.5 Summary ... 64
Chapter 6: IDENTIFICATION OF HIGH CRASH LOCATIONS AND COUNTERMEASURE STUDY ... 65
6.1 Identification of Curves with the Highest Frequency of Crashes ... 65
6.2 Highway Curve Countermeasures ... 65
6.3 Applying Suggested Countermeasures to Curves ... 67
6.4 Recommended SCDOT Workflow ... 69
Chapter 7: CONCLUSIONS AND RECOMMENDATIONS ... 70

7.1 Highway Curve Safety 70

7.2 Identification of Horizontal Curve Advisory Signage 70

7.3 Safety Analysis of Horizontal Curves using GIS 70

7.4 Benefits of This Research and Research Products 71

7.5 Research Products 71

7.6 Recommendations 72

REFERENCES 73

APPENDIX A A-1

Survey of State Agencies A-1

LIST OF FIGURES

Figure 2-1 Methods used by states to determine highway curve advisory speeds 10

Figure 3-1 Example of resultant curve wedges from the GIS automated method....................... 15

Figure 3-2 Unprocessed and processed curve wedge examples 16

Figure 3-3 Chord length (C) and middle ordinate distance (M) measured in Google Earth 17

Figure 3-4 Curve radius estimation method.. 17

Figure 3-5 Creating an isosceles triangle in Google Earth to calculate the radius 18

Figure 3-6 Parkway in Anderson, SC that includes MLS data 19

Figure 3-7 Rieker CARS curve overlapping with two automated GIS curves 20

Figure 3-8 Graph of Rieker CARS data versus automated GIS method 23

Figure 3-9 Graph of the manual Google Earth method vs Rieker CARS data 24

Figure 3-10 Graph of the manual Google Earth method vs automated GIS method................... 25

Figure 3-11 Quality level of available aerial LiDAR data in South Carolina 31

Figure 3-12 RANSAC roadway plane fitting to determine superelevation and grade 32

Figure 3-13 Coverage of the RIMS Segments with speed limit data 33

Figure 3-14 Conceptual diagram of the Hidden Markov Model for speed limit inference 35

Figure 3-15 Coverage of segments created based on hybrid approach 37

Figure 4-1 Workflow and screening methodology for determining highway curve advisory speeds for South Carolina state highways 39

Figure 4-2 Section of road in SC with tight curves. The highlighted curve has a length just over 100’ 40

Figure 4-3 Rieker minimum advisory speed vs GIS generated advisory speed (AASHTO) 43

Figure 4-4 Rieker minimum advisory speed vs GIS generated advisory speed (TTI) 44

Figure 4-5 GIS generated (TTI) vs GIS generated advisory speed (AASHTO).......................... 45

Figure 4-6 MUTCD Curve signage selection criteria (6) 47

Figure 4-7 Breakdown of advisory speed signage in South Carolina 51

Figure 4-8 Rieker and AASHTO advisory speeds with corresponding signage requirement 52

Figure 4-9 Curve location that meets mandatory sign requirements based on two out of three methods 53

Figure 5-1 Associating crashes with curves using a curve buffer 56

Figure 5-2 SPF for R2U and U2U curves 59

Figure 5-3 CMF for change in radius 60

Figure 5-4 CMF for change in posted speed limit 61

Figure 5-5 CMF for change in grade 62

Figure 5-6 CMF for change in speed limit 63

Figure 5-7 CMF for change in superelevation 64

Figure 6-1 Fork Shoals Rd in Simpsonville, July 2016 68

Figure 6-2 Fork Shoals Rd in Simpsonville, June 2021 with safety improvements 68

Figure 6-3 Workflow for statewide safety screening of highway curves 69

LIST OF TABLES

Periodic use of the curve safety workflow can be used to identify future curve safety needs while also provide “after” data for monitoring the effectiveness of countermeasures.

Table 3-1 Summary statistics of radii (ft) generated by each method 20

Table 3-2 Paired t-test results 22

Table 3-3 Radius MAPD between methods. Columns are the reference 25

Table 3-4 Radius median of absolute percentage deviations. Columns are the reference............ 25

Table 3-5 East West Parkway horizontal curve data from various methods 27

Table 3-6 East West Parkway horizontal curve data and percent errors 28

Table 3-7 Effects of a radius deviation of 10% on speed change 29

Table 4-1 Paired t-test results of the comparison between advisory speed methods.................... 45

Table 4-2 Curve comparison of Rieker required sign locations compared to field inventory sign data 48

Table 4-3 Curve comparison of field inventory signage w/AASHTO, TTI, adjusted Rieker 49

Table 4-4 Curve comparison of field inventory signage w/AASHTO, TTI (expanded dataset).. 50

Table 5-1 Roadway group types and definition in Highway Safety Manual, 2010...................... 55

Table 5-2 Negative binomial estimation results for crashes on curves (R2U right, U2U left)..... 58

Table 5-3 Negative binomial estimation results combined (R2U and U2U)............................... 58

Table 5-4 Negative binomial estimation results for severe crashes on curves 62

Table 6-1 Potential countermeasures for R2U roads 66

Table 6-2 Potential countermeasures for U2U roads 67

CHAPTER 1: INTRODUCTION

1.1 Background

The design of highway curves has significant impact on traffic safety. More than 25% of fatal crashes in the US occur on horizontal curves *(Torbic et al. 2004)*, and the crash rate for curves is approximately three times higher than other highway sections *(Glennon et al. 1985)*. Furthermore, crashes are over 4 times more likely to be fatal on horizontal curve sections compared to similar highway tangent sections *(Farzinpour et al. 2024)*. Research has shown that a key contributor to highway curve related crashes is excessive vehicle speed *(Rasdorf et al. 2010; Milstead et al. 2011)*. South Carolina is no exception to this. Identifying the hazards of driving on horizontal curves and mitigating them is a big part of achieving the goal of Vision Zero (*USDOT, 2022*). These statistics underscore the critical need to identify and mitigate the specific risks associated with driving on curved sections, particularly in the context of Vision Zero goals for zero roadway fatalities. This research titled: "Safety Analysis of Highway Curves Where Crashes Occur in South Carolina" explores highway curve safety and methods to improve horizontal curve safety.

1.2 Problem Statement

A recent study conducted by this research team of over 900 South Carolina fatal crashes showed that nearly 20 percent occurred on highway horizontal curves *(Zou et al. 2022)*. The study further identified that 25% of the curves where these crashes occurred may have had design speeds less than the posted speed limit and 47% of the curves have a design speed less than 5 mph above the speed limit. Prior research on operating speeds indicates that drivers tend to drive at least 7-10 mph above the posted speed limit *(AASHTO, 2010)*. With design speeds below or right at the posted speed limit, excess speed of any level can become problematic. This research focuses on a detailed analysis of curves where vehicle crashes occur in South Carolina. The existing inventory of circular curves along with crashes are analyzed to identify trends and the effectiveness of countermeasures. There are some acknowledged systematic issues with the Rieker CARS (Curves Advisory Reporting Service) South Carolina highway curve inventory. Some of Rieker data issues are corrected as part of this research. These issues include locations identified as curves that are actually turns at intersections and correcting attributes used to determine curve warning advisory speeds based on criteria from the Manual on Uniform Traffic Control Devices (MUTCD) *(2009)*. MUTCD compliance issues related to horizontal alignment warning information is a specific concern of SCDOT. This research will help to address that concern.

1.3 Research Objectives

The overall goal of this research is to enhance safety on highway curves in South Carolina. There are several research objectives that are discussed in the following paragraphs.

Objective 1 Develop a highway curves safety analysis work flow. This research includes a highway curves safety analysis workflow that can be used to provide SCDOT with a systematic means to identify curves that may have opportunities for potential safety enhancements. The workflow uses existing SCDOT data sources including road characteristics data (RIMS), curve inventory ("cleaned" Rieker CARS, and new curve data created as part of this research), and crash data. Speed limit data and available highway curve sign inventory data are also used.

Objective 2 – Determine significant contributing factors to curve crashes and why some curves have a higher crash frequency. Identification of factors that contribute to curve related crashes is critical for identifying and prioritizing countermeasures. In some cases, curves with similar radii may have very different crash frequency. The research uses statistical methods to determine the most significant factors that contribute to highway curve crashes and their severity.

Objective 3 – Develop a prioritized list of highway curves with a high crash frequency and associated countermeasures. The overall goal of this project is to enhance safety on highway curves in South Carolina. To do this, countermeasures will need to be implemented at highway curve locations that are identified as having the highest frequency and severity of crashes. The literature review has identified a number of potential countermeasures. The research has recalibrated some of the countermeasures based on South Carolina data as well as developing additional countermeasures which is a product of Objective 2.

Objective 4 – Identify curve locations that may need additional review with regard to signage based on MUTCD guidelines. The 2009 MUTCD established a compliance date of December 31, 2019 for highway alignment warning signs. Highway curve requirements in Section 2C identifies the selection, location, and spacing of signs as well as instances where they are required, recommended, or optional. While South Carolina has been very proactive in meeting MUTCD guidelines, compliance issues may exist. This research attempts to identify curve locations that may need additional signage or signage modifications based on MUTCD guidelines. This objective was updated based on 2023 MUTCD guidance *(2023)*.

Objective 5 – Improve the existing circular curve inventory. SCDOT has an existing curve database that was created using Rieker CARS (Curves Advisory Reporting Service) data. While the inventory is critical to this research, there are several issues that are addressed. One example is that several entries in the database are not highway curves but rather curves created by the inventory vehicle making turns at intersections. The Rieker inventory is cleaned to address these issues. This objective was updated during the research to include a database of highway curve radii generated by a consultant using the SCDOT digital centerline map. This database is much more extensive than the Rieker data in terms of included curves however it required a great deal of manual cleaning to make it more usable.

Objective 6 – Review the accuracy and completeness of crashes on highway curve reporting and suggest future data collection and records management improvements. The basis for SCCATTS crash data is defined by the South Carolina TR-310 crash report manual, which contains a single field (road character) that indicates if the section is straight or a curve and if it is level, on-grade, or at the crest of a hill. The crash report coding doesn't directly indicate if the curve may have contributed to the crash, although some curve details may be in the police narrative. The researchers reviewed curve crash data to allow the researchers to ascertain if curve information is coded consistently among jurisdictions.

1.4 Significance of Work

While there has been a great deal of research on highway curve safety and applicable countermeasures, there is still a significant need for this research. A substantial gap in the knowledge base concerning highway curve safety is related to the methodology for assessing curve related crashes. Previous research has almost uniformly relied on crash codes and aggregate data. The innovative GIS techniques used in this research to associate crashes with curve buffers allows for verification of crash report coding related to curves, and the completeness of the curve inventory. It is anticipated that this verification process will be important for improving crash reporting related to highway curves and the usefulness of the crash inventory.

South Carolina is unique in its fatal crash incidence characteristics. It has the second highest fatality rate per hundred million vehicle miles traveled and the fourth highest fatality crash rate per 100,000 population in the country based on 2023 fatal crash data. Because of the high proportion of crash fatalities that occur on highway curves, research that can potentially reduce fatality rates is significant.

Published highway crash countermeasures for curves from other states and jurisdictions are not calibrated for South Carolina. The modeling aspects of this research will help to determine more appropriate crash modification factors for certain countermeasures.

1.5 Report Organization

This report is divided into seven chapters:

- Chapter 2 presents recent literature on GIS methods to determine horizontal curve attributes, advisory signing, and safety analysis for a statewide roadway network. Chapter 2 also summarizes the team's survey of states with questions related to highway curves safety.
- Chapter 3 provides a detailed description of data and data development.
- Chapter 4 discusses the use of the data products discussed in Chapter 3 to determine statewide advisory speeds for curves. These speeds along with posted speed limits and existing sign inventory data are used to identify MUTCD compliance issues.
- Chapter 5 presents the safety analysis used to determine crash modification factors for different curve crash countermeasures.
- Chapter 6 discusses locations of highest crash incidence along with potential countermeasures.
- Chapter 7 gives recommendations and conclusions.

CHAPTER 2: LITERATURE REVIEW AND SURVEY OF STATES

2.1 Literature Review

Previous highway safety studies have shown that crashes on roadway sections with horizontal curves exhibit a higher crash severity than similar highway tangent alignment sections *(Glennon et al. 1985; Rasdorf et al. 2010; Gooch et al. 2018)*. Recent research at Clemson University using 2022 crash data indicated that crashes are over 4 times more likely to be fatal on horizontal curve sections compared to similar highway tangent sections *(Farzinpour et al. 2024)*. Furthermore, the research also determined that one of the primary contributing factors to fatal crashes on curve sections is excessive vehicle speed.

In 2020, over 5.25 million crashes were reported by the police, causing 38,824 deaths and over 2.28 million injuries on roads and streets within the United States *(Stewart, 2022)*. Horizontal curves are among the most vulnerable sites for crash occurrence *(Buddhavarapu et al., 2013)*. More than a quarter of fatal crashes are associated with horizontal curve sections with the majority being roadway departures *(FHWA, 2022; Donnell et al., 2019).*

2.1.1 Crash Frequency and Crash Rate

Crash frequency is a widely used indicator of crash occurrence. It is defined as the number of crashes occurring on a roadway segment, or at an intersection during a given time period. To normalize crash frequency, crash rate is frequently used in safety analysis to examine the impacts of factors that may contribute to a crash *(AASHTO, 2010)*. The primary factor to normalize crash frequency is traffic volume, thus crash rates are typically given as the crash frequency divided by the vehicle miles traveled.

A comprehensive, four-state study by (*Glennon et al., 1985)* found that the average crash rate for horizontal curves on two-lane rural highways is three times higher than on tangent road segments. This study also found that the average single-vehicle run-off-road crash rate was four times higher on horizontal curves than on tangent segments. The severity of roadway departure crashes on horizontal curves was also higher than roadway departure crashes on tangent segments. A more recent study by *(Rasdorf et al., 2010)* found similar results. An analysis of North Carolina crash data found that curve collisions have more than three times the fatality rate of collisions on all roads statewide. One study on different combinations of horizontal and vertical curve alignments found that crash frequency increases with decreasing horizontal curve radius, decreasing horizontal curve length, increasing grade difference, and increasing percent grade *(Bauer and Harwood, 2014).*

2.1.2 Crash Types

Crash types are identified in virtually all state crash reports, and there is strong agreement in the literature that single-vehicle crashes are the most predominant type of horizontal curve related crash. One study indicated that nearly 80 percent of horizontal fatal crashes were single vehicle while roughly 10 percent were head-on collisions. Virtually all curve related single-vehicle crashes involve leaving the roadway and striking trees, utility poles, rocks, or other fixed objects or overturning. Curve related head-on collisions are the result of one vehicle drifting into the opposing lane when a driver tries to cut the curve or redirect the vehicle after having run onto the shoulder *(Torbic et al., 2004)*.

2.1.3 Curve Characteristics

During the past several decades, improving safety at horizontal curvature has been critical to researchers and transportation agencies. Researchers have identified several geometric factors that influences safety on horizontal curves *(Donnell et al., 2019; Zegeer et al,1992; Khan et al, 2012)*. These include curve radius, superelevation, grade within the curve, upstream and downstream tangent lengths, shoulder type and shoulder width, available clear zone, and surface width and surface type. Studies have shown that tighter radii are associated with higher crash rates. Superelevation helps a vehicle to resist centripetal force. Longer tangent lengths help vehicles to better prepare for or recover from curves. Obstacles in the clear zones can be hazardous because of the probability of vehicles exiting the roadway because they are unable to safely navigate the curve. Highway curves are typically circular curves. Circular curves without spiral transitions can be challenging for drivers on roads with narrow lane widths. This is because of a driver's tendency to move laterally in the lane. Thus, a driver may start high on a curve, transition to the low side, and move back to the high side while leaving the curve.

Numerous researchers have pursued deeper understanding of the relationships between curve design parameters, traffic, and human driving behavior related to curve crashes. One repeat finding is the inverse relationship between curve radius and crash rate – as the curve radius decreases, the crash rate increases *(Elvik 2013)*. Explanations state that as the lateral acceleration required to navigate tighter curves increases, the vehicle handling capabilities and driver comfort thresholds can be exceeded, which can lead to a higher likelihood of single-vehicle crashes, particularly run-off-road incidents. This inverse relationship strengthens as the radius drops below 656 ft *(Elvik, 2013)* Another study *(Hummer et al. 2010)* found significant increases in crash frequency when the radius dropped below 2000 ft. In addition to this inverse relationship, *(Puersaud, 2000)*, and *(Khan, 2012)*, also found positive relationships between crashes, traffic volume, and curve length.

2.1.4 Crash Severity

Crash records provide information about the consequences of crashes—namely, whether the crash results in property damage, injuries, or fatalities. This type of information is commonly used in the literature to identify crash severity. There is consensus in the literature that curve related crashes are typically more severe than crashes not occurring on a curve. A recent study done by the researchers in South Carolina indicated that, based on 2019 crash data, fatal crashes are more than 4 times likely to occur on highway curves than non-fatal crashes. A closer look identified the top two contributing factors (including primary and other contributing factors) for curve-related fatal crashes were driving under the influence and speeding *(Zou, 2022)*.

2.1.5 Highway Curve Crash Reporting

South Carolina crash reports (Form TR-310) follow the Model Minimum Uniform Crash Criteria (MMUCC) guidelines *(NHTSA, 2012)*. A crash report includes a variety of different characteristics and data elements including crash data elements, personal data elements, roadway data elements and several other elements. Crash reports offer very little information about curves in the coded information beyond whether or not a crash occurred in a curve. Super elevation, curve radius, and the presence of highway advisory speed or other warning signage are not included unless the reporting officer includes this information in a narrative or sketch.

2.1.6 <u>Countermeasures</u>

There have been a number of studies to assess countermeasure effectiveness on curves experiencing excessive crash rates. The NCHRP Report 500, Volume 7 *(2004)*, identifies several strategies to address the specific safety problem at horizontal curves. These strategies meet one of the following two objectives: 1) reduce the likelihood of a vehicle leaving its lane at a horizontal curve; and 2) minimize the damaging consequences of a vehicle leaving the roadway at a horizontal curve. Another publication, Low-Cost Treatments for Horizontal Curve Safety *(Albin et al., 2016)*, provides practical information on where, when, and how to apply the safety countermeasure including examples and costs. Another important source for countermeasures related to curves is the FHWA CMF Clearinghouse which contains a number of potential countermeasures along with their corresponding CMF value. One CMF is based on increasing curve radius. Another considers radius, posted speed, and superelevation *(Donnell, 2019)*. A CMF by *(Baur, Harwood, 2014)* is based on horizontal curve and grade combinations. Other researchers have also worked on methods for increasing horizontal curve safety. Head-on collisions are of significant concern when it comes to horizontal curve safety. A study by Ghalehni and Boroujerdian *(Ghalehni et al. 2023)* recommends using rumble strips and friction treatment to help keep vehicles in their lane. Because of the magnitude of roadway departures at horizontal curves, countermeasures include increasing clear zone width, making the roadside/clearzone slope traversable, or installing barriers to protect vehicles from greater hazards *(Donnell et al., 2019)*. Babic and Brjs *(Babic et al. 2021)* conducted a simulator study and found that unique pavement markings combined with signage increased a driver's ability to stay in their travel lines.

2.1.7 <u>Crash Prediction Models</u>

Many of the CMFs discussed in the previous section are based on crash prediction models developed by different researchers, e.g. *(Donnell, 2019; Baur and Harwood, 2014)*. (*Persaud, et al, 2000)* developed an empirical Bayes-based procedure for prioritizing potential treatment sites on the basis of crashes that may be classified as occurring because of the presence of curves. The attractiveness of their procedure is enhanced by the fact that the data and calculations are also a part of the evaluation of treatment that may be applied to a particular site. Gooch, et al *(2018)* developed a model for safety performance functions (SPFs) for horizontal curves. Previous approaches have used SPFs for tangent sections and then applied a CMF to determine a base expected number of crashes for horizontal curves. This may not be appropriate because of the differences between highway curve and tangent sections. Several researchers have argued that the choice of SPF affects the identification of important crash prediction variables as well as the estimation of crash severity *(Gooch, 2018; Wang, 2016; and Russo, 2016).* The literature indicates that horizontal curve length and volume should be considered in the SPF for horizontal curves *(Gooch, 2018)*.

Within the suite of Highway Safety Manual *(2014)* crash prediction models, only the rural two-lane undivided roadway type includes horizontal curves as a significant factor for crash prediction. Within the segmentation process, horizontal curves are separated from tangent sections. Data elements needed for the curve section predictions include: AADT (vpd), lane width (ft), shoulder width (ft), shoulder type, length of horizontal curve (mi), radius (ft), presence or absence of spiral transition curve, superelevation, grade (percent), driveway density (driveways/mi), roadside hazard rating, and the presence or absence of centerline rumble strips, short four-lane section, two-way left-turn lane, segment lighting and automated speed enforcement. The base condition for the model is a straight tangent section, thus if present, a crash modification factor (CMF) must be applied. The published curve CMF is derived from *(Zegeer et al. 1992)* and includes the length of curve, curve radius, and an indicator for presence of spiral transitions. CMFs can go as high as 6.0 for a 250 ft radius with a curve length of 0.05 mi. Significant increases are generally seen with radius below 1000 ft. A separate CMF for superelevation requires the actual superelevation rate and any differential between the minimum AASHTO superelevation and the available superelevation. If the superelevation meets or exceeds the minimum, the CMF is set to 1. If the superelevation is not adequate, the CMF will be above one and indicate increased crash predictions.

While still the predominant resource for safety prediction, the Highway Safety Manual models are approaching two plus decades in age. Other researchers have built upon these models and identified several factors influencing curve crashes. One study on different combinations of horizontal and vertical curve alignments found that crash frequency increases with decreasing horizontal curve radius, decreasing horizontal curve length, increasing grade difference, and increasing percent grade *(Bauer, 2014)*. A follow-on study by (*Saleem, Persaud, 2017*) estimated CMFs for flattening horizontal curves with respect to approach grades and deflection angles. Up to 50% reduction in crashes can be obtained by doubling the radius when deflection angles approach 120 degrees on a moderate approach grade. Another study (*Gooch, 2018*) looked at the degree of curvature in relation to the proximity of adjacent curves within three-quarters of a mile and found a negatively correlated relationship with crash frequency. (*Sil, 2020*) found that curve radius significantly influences vehicle operating speed at the center of the curve, which in turn affects crash risk. Increases in traffic volumes have been significantly associated with increases in truck crashes on curves as well as overall crashes, further total ADT is related to motorcycle crashes on curves *(FHWA, 2021)*. Fitzpatrick et al. *(2010*) found that with similar driveway density, there is no significant difference in crash rates on curves and tangents. While this research did remove curve sections adjacent or overlapping with intersection areas, driveway crashes were not removed.

2.1.8 Highway Curve Signage Requirements

The Manual on Uniform Traffic Control Devices *(MUTCD, 2009; MUTCD 2023)* provides guidance on the use of signage to advise motorists of a change in the roadway alignment and help motorists negotiate roadway curves at safe operating speeds. Section 2C.06, Table 2C-4 of the MUTCD *(2023)* identifies selection, location (e.g., advance placement distance), and spacing of warning signs at horizontal curves, as well as roadways where traffic control devices (e.g., signs) are required, recommended, or optional. The use of these signs on roads is based on the speed differential between the horizontal curve's advisory speed and the roadway's posted speed limit, statutory speed limit, or the 85th-percentile speed on the approach to the curve. Table 2C-6 provides guidance for the use of advisory speed signs. For local roads or roads with ADT less than 1000, the MUTCD allows for use of highway warning signs for changes in horizontal alignment based on engineering judgement, except as required on freeways and expressways.

2.1.9 Determining Highway Curve Advisory Speeds

A comprehensive review of methods to determine curve advisory speeds can be found in Dixon et al, 2008*)*. Though many methods exist, the MUTCD *(2023)* acknowledges several approaches, including the accelerometer, a ball bank indicator, and the AASHTO design equation *(Kronicz, 2016)*. The AASHTO design equation method is based on Equation 2-1 which is generally used to estimate a minimum radius given the roadway design speed.

$$R = \frac{v^2}{15(e+f)} \qquad (2\text{-}1)$$

In this equation, *R* (feet) is the minimum radius of the curve, *v* (mph) is the design speed, *e* (ratio to 1) is the design superelevation rate, and *f* is the design friction coefficient. If the radius of a curve is known, design speed can be calculated by substituting values for *R, e*, and *f.* This equation can also be used for determining highway curve advisory speed *(Glennon et al., 1985) (Tsai, 2021),* which is used in this study along with the posted speed limit to determine highway curve signage requirements.

During the development of a statewide approach, the Texas Transportation Institute (TTI) found that neither the accelerometer nor ball bank indicator produced consistent values for advisory speeds *(Milstead, 2011)*. They ultimately settled on an alternative design equation, where the advisory speed can be calculated from various curve parameters *(Milstead, 2011)*. The MUTCD *(2023)* also identifies the design equation method as one of the acceptable methods for determining advisory speed but does not specifically refer to the TTI method. The TTI method design equation is given in **Section 4-1**.

2.1.10 Collection of Curve Attributes

Accurate determination of highway curve attributes including radius, superelevation, and length is essential for geometric design, safety analysis, and asset management. Curve radius and superelevation influence vehicle dynamics, sight distance, and crash risk, making its collection a priority for transportation agencies. Several methods—ranging from traditional surveying to advanced remote sensing—are employed to capture this critical parameter.

Historically, curve radius data has been derived from highway design plans and as-built drawings. Engineers extract geometric details such as tangent lengths, deflection angles, and chord lengths to compute radius using trigonometric formulas. Field surveys using total stations or tape-based methods remain accurate but are labor-intensive and time-consuming, particularly for large networks *(Ural et al. 2015)*. Modern practices leverage Global Positioning System (GPS) and Geographic Information System (GIS) technologies to automate curve identification and radius calculation. GPS trajectory data combined with GIS basemaps enables algorithms to detect curve segments and compute radii across extensive networks. Recent studies have demonstrated large-scale horizontal curve inventories using regression algorithms applied to open GIS datasets *(Kronicz et al. 2016).*

Light Detection and Ranging (LiDAR) technology, particularly mobile LiDAR mounted on survey vehicles can provide highly accurate georeferenced three-dimensional data in the form of a point cloud that has numerous applications in transportation. The adoption of mobile LiDAR technology by transportation agencies has significantly increased over the past decade. Research studies have identified several benefits associated with the implementation of LiDAR technology *Chang, 2014)* and how transportation agencies can potentially use LiDAR for many applications including extraction of lane markings *(Guan, 2014) (Ma et al. 2019)*, evaluation of pavement friction *(Du, 2019)*, and extraction and assessment of road geometry including both horizontal *(Shalkamy, 2020)* and vertical alignment *(Holgado-Barco, 2014)*, and roadway cross section *(Holgado-Barco, 2014) (Shams et al. 2018)*. One benefit of using Mobile LiDAR is that precise measurements of longitudinal lines can be made. Data collected by GPS will only collect positional information along the survey vehicles path which can vary within a travel lane. Mobile LiDAR systems can collect a road's entire right-of-way in a single pass. By leveraging the longitudinal line data, the actual location of the center of a travel lane or the centerline of the roadway can be determined. Shams et al (*Shams et al. 2018)* determined that Mobile LiDAR can collect both curve radii and superelevation data to a high degree of accuracy. The study indicated that the cost of this collection is significant and requires extensive point cloud processing to extract curve information.

Photogrammetry using aerial or drone imagery is increasingly applied for highway design and monitoring. Unmanned Aerial Vehicles (UAVs) equipped with high-resolution cameras capture overlapping images, which are processed into orthomosaics and 3D models. Ground control points enhance positional accuracy, enabling reliable extraction of horizontal alignment and curve geometry. This method is particularly useful for large-scale or hard-to-access areas and offers cost savings compared to traditional surveys *(Zulkipli & Tahar, 2018; Ferrer-González et al. 2020).*

2.2 Survey of State Transportation Agencies

The researchers conducted a survey of state transportation agencies to determine their methods for identifying advisory speeds on highway curves. Questions were also asked on whether the state's roadway characteristics database included curve radius and super elevation which are two parameters required for using the design method to determine advisory speed. Twenty-eight states responded to the survey. **Figure 2-1** shows the methods used by states who replied to the survey to determine highway advisory speeds. Most states indicated that they use more than one method. The survey indicates that twelve states use the design method to determine advisory speeds, however only six states indicated that the design method was their primary method. The majority of states use the ball bank indicator as their primary method. Twelve states indicated that they have curve radius as one of the attributes included in their road characteristics database and eight states also have superelevation data. Of the twelve states that maintain curve radius data in their road characteristics database, eight of these states indicated that they use their curve radius data for determining highway advisory speeds. In all cases, superelevation is field collected.

Details of the survey along with a summary of the state responses are provided in **Appendix A**

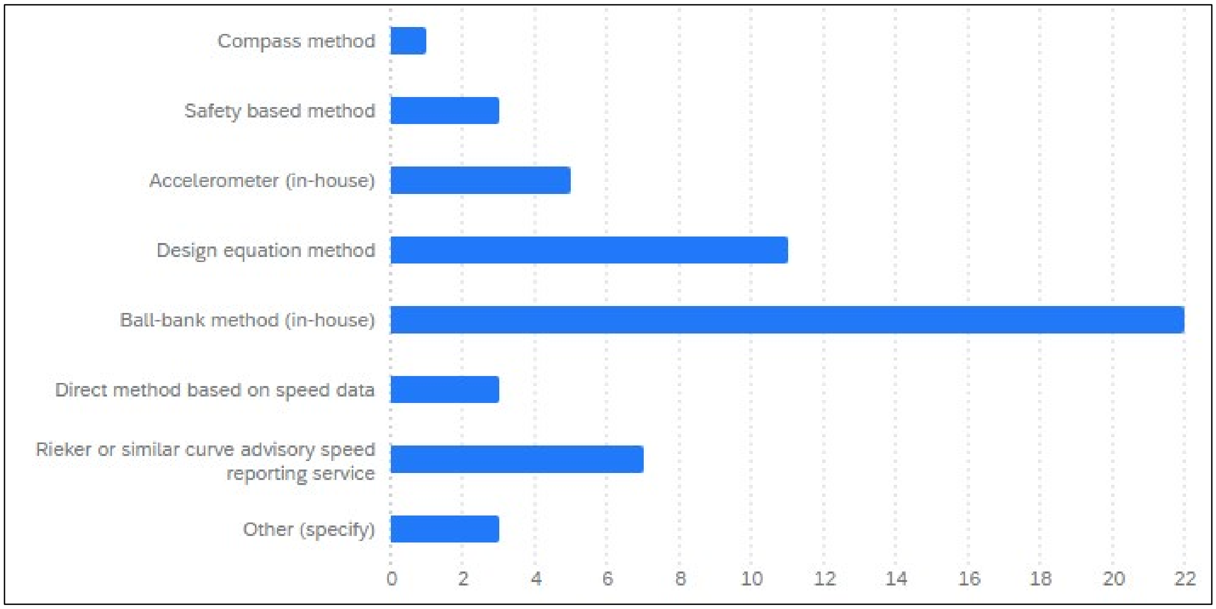

Figure 2-1 Methods used by states to determine highway curve advisory speeds

CHAPTER 3: DATA COLLECTION PROCEDURES AND DATA SUMMARY

3.1 Data Requirements

There were numerous data elements required to complete this research. Some data was provided by SCDOT and used as is. Several data elements required different levels of processing before they were used. Others were collected from other sources. This Chapter discusses the different data acquired, processed, and used on this project

3.1.1 Crash Data and Preprocessing

Eight years of crash data from 2017-2024 was provided by SCDOT. This crash data included over 1.22 million records. Crashes were filtered to remove any crashes where there were inconsistencies between their geographic coordinates and the roadways listed in the crash report. This was only a very small proportion of crashes.   South Carolina crash reports (Form TR-310) follow the Model Minimum Uniform Crash Criteria (MMUCC) guidelines *(NHTSA, 2012)*. A crash report includes a variety of different characteristics and data elements, including crash data elements, personal data elements, and roadway data elements. Crash reports offer very little information about curves beyond whether or not a crash occurred in a curve. Super elevation, curve radius, and the presence of highway advisory speed or other warning signage are not included unless the reporting officer includes this information in a narrative or diagram.

The association of crashes to curves is discussed in Chapter 5. Our research found that many crashes associated with curves were not coded as curves in the crash report. Additionally, there were other instances where the crash report indicated the crash occurred on a curve, however our data processing association did not show this. There were many reasons for this. Our research only associated crashes with curves if the curve radii were between 300' and 1500'. Crashes near the tangent section of curves may or may not be coded as curves based on the discretion of the officer. In summary, our research indicated that only a small number of curve related crashes were miscoded when overlooking subjective choices.

3.1.2 SCDOT's Roadway Centerline and Road Inventory Management System (RIMS)

Roadway centerline geometry was obtained from the SCDOT GIS portal. The centerline layer was projected to NAD 1983 State Plane South Carolina (US Feet) so that it would be consistent with other datasets and suitable for subsequent geometric calculations. The original centerline file consisted of polyline features with several key attributes, including County Name, Route Type Name, Route Number, Route Direction, RouteID, and Route LRS (RouteLRS).

Using these fields, individual polylines were assembled into continuous routes. In particular, the combination of County Name, Route Type Name, Route Number, and Route Direction was used to construct a RouteID that would be compatible in format with other data sources used in the study. RouteLRS, together with the beginning and ending milepoints for each polyline, was then used to define a linear referencing system along each route.

Additional roadway attributes were obtained from SCDOT's Roadway Information Management System (RIMS). From RIMS, the researchers relied on three main groups of variables. For route identification and referencing, the researchers used County Name, Route Type Name, Route Number, Route Direction, RouteLRS, and Begin/End MilePoint. Cross-section and median characteristics were captured through Median Type Name, Median Width, Number of Left Lanes, Number of Right Lanes, Total Number of Lanes, Left Surface Width, and Right Surface Width. Finally, regulatory characteristics were represented by the Regulatory Speed Limit field.

The combination of County Name, Route Type Name, Route Number, and Route Direction from RIMS was again used to generate a RouteID consistent with the RouteID schema in the centerline data. Using this constructed RouteID together with RouteLRS and the Begin/End MilePoint values, the RIMS attributes were joined to the centerline routes. The lane counts and surface widths were later used to compute the effective radius of curves, while median type, median width, and lane configuration contributed to the definition of roadway and curve classes (for example, rural two-lane undivided "R2U" and related categories). The Regulatory Speed Limit field was taken as the posted speed limit for each segment.

Both RouteID and RouteLRS were retained throughout processing because different supporting datasets referenced routes using different keys. Some external tables were indexed by RouteID, whereas others relied on RouteLRS and milepoints. Keeping both identifiers available allowed for consistent linking and joining across all datasets without repeated reformatting or loss of information.

Statewide functional classification data were also obtained from SCDOT. This file was joined with the RIMS data set using the linear referencing and included functional class (e.g. minor and major collector, etc) and area type (rural or urban). These attributes were later combined with median type (divided versus undivided) and the number of lanes to assign a final classification to each curve segment, providing a consistent typology of roadway context for subsequent analysis.

3.1.3 SCDOT's Sign Inventory

The researchers requested a subset of the SCDOT sign inventory for use in this research. The signs requested were all posted speed limit signs and curve related signs. The curve related signs included curve warning signs, curve chevrons, and advisory speed signs.

An initial review of the sign inventory revealed inconsistencies in Route ID formatting as well as numerous typographical errors. These issues were corrected on a case-by-case basis in order to develop a standardized set of Route IDs. A similar standardization procedure was applied to the centerline database so that Route ID conventions would be consistent across both the sign inventory and the roadway network data. Once the attribute fields were standardized, the signs were mapped in ArcGIS using their supplied geographic coordinates. Visual inspection suggested substantial positional error in many instances. Some signs appeared in implausible locations, including the Atlantic Ocean, or clustered well outside the roadway right of way. To evaluate and correct these errors in a more systematic manner, an accuracy assessment was carried out by comparing the coordinate-based locations with linear-referenced locations derived from the recorded mile points. For each sign, the distance between the coordinate-based point and the mile-point-based point was computed, and the records were then grouped according to this discrepancy. The resulting segmentation and associated correction procedures were as follows:

Spatially validated records: The largest group, approximately 67% of the dataset (34,200 signs), exhibited a separation of less than 200 feet between the coordinate-based and mile-point-based locations. Given this relatively small discrepancy, these records were judged to be spatially reliable and were retained without modification.

Coordinate-based corrections: A second subset, roughly 24% of the dataset (12,500 signs), showed discrepancies greater than 200 feet. Spot checks within this group indicated that, in most cases, the geographic coordinates appeared credible while the recorded mile points were inconsistent with the roadway geometry. For this subset, the provided coordinates were therefore treated as the primary locational reference and were used to compute and assign corrected mile points.

Outlier resolution: The remaining 9% of the dataset (4,500 signs) contained more severe inconsistencies involving both mile points and Route IDs, often placing the sign locations far from any plausible match on the roadway network. Examination of these records suggested that the coordinates were particularly susceptible to human entry errors, whereas the inventory-based Route IDs and mile points were more frequently reasonable. For most of these signs, acceptable locations were recovered by replotting them using the inventory Route ID and mile point attributes rather than the supplied coordinates. However, approximately 1,500 signs could not be reconciled because their Route IDs were absent from the centerline database or their mile points lay outside the valid range for the corresponding route. As neither the coordinate information nor the linear-referencing data provided a verifiable location, these records were tagged as unreliable and were skipped from the final segmentation process.

3.1.4 Rieker CARS System

In 2019, the South Carolina Department of Transportation (SCDOT) contracted with a consultant to collect horizontal curve information using the Rieker CARS system. The Rieker CARS System is a dashboard mounted roadway survey system that includes a GPS and a digital ball bank indicator. Data can be collected in a single data collection run or pass while driving at highway speeds. Rieker analysts post-process raw GPS positional data and digital ball bank inclination data for selected points that are used to delineate each horizontal curve. The point attributes are entered into a computer model to extract horizontal curve radius and superelevation, as well as calculation of a corresponding advisory speed. The CARS system's use of a digital ball bank indicator complies with methodologies recommended by the FHWA for setting advisory speeds on curves *(Milstead, 2011)*. Research conducted by (*Green et al. 2016)* found that the CARS system is an effective method for identifying horizontal curve advisory speeds at a wide scale along highway routes and across highway networks.

3.2 Collection of Horizontal Curve Radius (and an initial attempt at Superelevation)

One of the objectives of this research is related to highway curve signage compliance. The Rieker data included signage requirements based on MUTCD standards. As a means to verify the Rieker curve signage requirements, the AASHTO and TTI design equations are used as an alternative to determine highway curve advisory speeds on the project. The objective is to apply these equations on a network wide basis to estimate advisory speeds for each curve. The curve attributes needed are radius, superelevation, and friction coefficient (*f*). This section describes the different methods used for extracting horizontal curve radius and comparing the methods for accuracy. The methods were initially selected based on roadway datasets available in South Carolina. The Rieker CARS System is one of the data sets. A manually derived calculation method for determining curve radius was also included for comparison purposes as identified in the literature *(Farzinpour et al. 2024; Tsai et al. 2021)*. Superelevation extracted from Rieker data was also evaluated.

3.2.1 Rieker CARS System

As part of the Rieker data collection the consultant identified curve radii and superelevation data for approximately 25,000 curves. A subset of the data determined for horizontal curves is included in the comparison of the methods used for this study to determine the accuracy of the curve radii. The Rieker CARS radii are representative of the travel lane in the direction of travel of the survey vehicle. At least two passes, one in each direction, are made for each curve. An estimate of the centerline radius for non-freeways is the average of the two directions. This average is what is used in the comparison. It is noteworthy that a GIS road characteristics database is usually spatially represented by the roadway centerline. While most attributes are usually the same for both directions (including curve attributes such as super elevation), there can be differences. For example, the number of lanes can vary by direction. In this case, there may be a separate attribute column for each direction. Curve radii by direction can be calculated based on offset from the centerline using lane width and median width attributes.

3.2.2 GIS Automated Method

In a separate application, SCDOT contracted with a GIS consultant who used customized data processing programming scripts to extract curve radii from SCDOT centerline data. Horizontal curves in ArcGIS are represented as one or more alignment segments that have a series of closely spaced shape points. The consultant's approach for generating curve wedges and extracting horizontal curve radii is similar to a previous method (*Li et al. 2012)* where deflection angles between adjacent pairs of shape points are analyzed. The Pennsylvania Department of Transportation has also used this approach *(Kronicz, 2016) FHWA (2019)*. The consultant's programming scripts generated an ArcGIS shape file for over 350,000 curve "wedges" that included the point of curvature (PC) station, point of tangency (PT) station, and radius, as numeric attributes. **Figure 3-1** shows an example of the resultant curve wedges. One issue with the reliability of this method is that perceived changes in measured radii resulted in delineation of an excessive number of compound curves. This is due to imperfections in the digital centerline. A closer examination of a sample of the wedge curves compared with Google Earth imagery and, in some cases, SCDOT design plans, indicate that highway alignments depicted using digital centerlines routinely deviate from identifying a commonly intended consistent radius dimension extending across the entire length of curve.

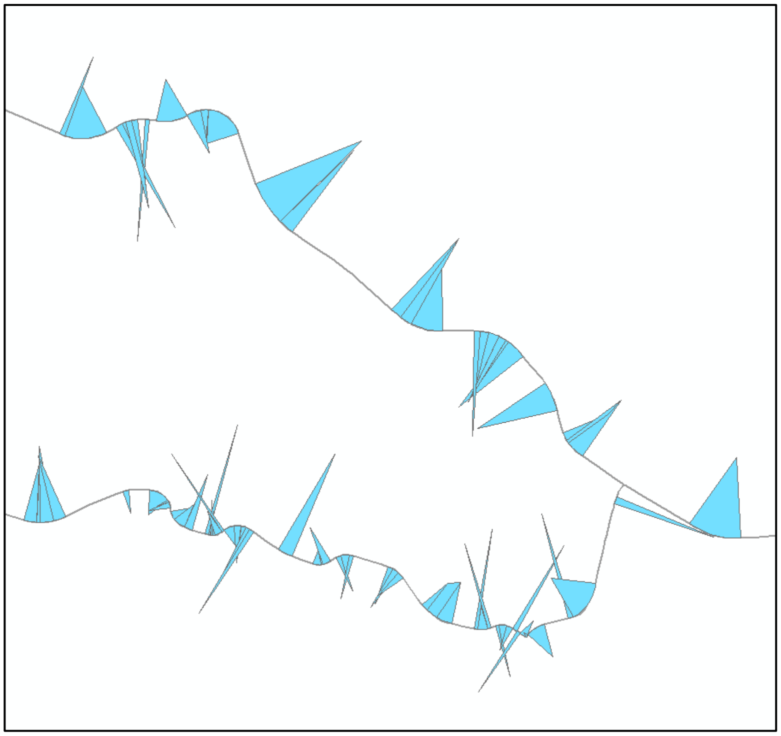

Figure 3-1 Example of resultant curve wedges from the GIS automated method

In general, highway horizontal curves are simple curves designed with a consistent radius, extending for the entire length of curve and successive curves are generally balanced to provide a smooth-riding transition from one curve to the next AASHTO *(2018)*. An exception is for spiral transition curves that are used infrequently for open roadway alignments or for compound curves which are used for specific design objectives or site constraints, and typically not used where simple curves are applicable AASHTO *(2018)*, MassDOT (2024), Indiana DOT (2013). Compound curves are typically used for transitioning low- speed roads at intersections (e.g., ramps) and are usually not recommended for sharp curves Montana DOT *(2016)*.

To smooth the curves along the length of curve, Clemson researchers developed an ArcGIS Python script toolbox to process the wedges combining them to generate a single curve with a fixed radius. This process is conducted on a curve-by-curve basis with the analyst subjectively choosing which combination of curve wedges should be included to generate a single radius curve extending across the entire length of curve. The analysis procedure uses a Google Earth image background as reference for visual verification to ensure ground proofing. Curves where the GIS centerline did not match well with the Google Earth image were given a special code to indicate that additional verification and processing of the curve was necessary. In some cases the curves needed to be manually edited to reflect a realignment from new construction as represented in recent Google Earth imagery. Other potential sources of ground truth for verification purposes could include available as-built plans, aerial LiDAR, and low altitude photogrammetry.

A number of processing scripts were developed to address the variety of differing curve wedge issues. The first processing script was developed to address the issue of gaps between multiple curve wedges and was dubbed GapRemover. The analyst selects two curve wedges from the GIS dataset and the processing script retrieves the curve IDs and associated metadata of the selected polygons, including their Linear Referencing System (LRS) values start mile points (PC_MP), and end mile points (PT_MP). The tool identifies the gap distance between the two curve wedges and determines the required length of the new wedge polygon with curvature influenced by the largest curve wedge selected.

Upon verifying there are no gaps in between the curve wedges on a specific curve, the analyst proceeds to use another processing script in the toolbox dubbed Integrate tool to transform multiple curve wedges occurring along an obvious curve section into one single and continuous curve wedge. The analyst selects all of the curve wedges on the curve section and the processing script conducts geometric calculations using the chord length and the length of curve to back-calculate the radius as well as location of the PC and PT mile points. Based on results of these calculations the processing script then determines the total length of chord and total length of curve. **Figure 3-2a** shows one highway curve with several different curve wedges, each with a very different radius, and **Figure 3-2b** shows the resulting wedge processed by custom scripts.

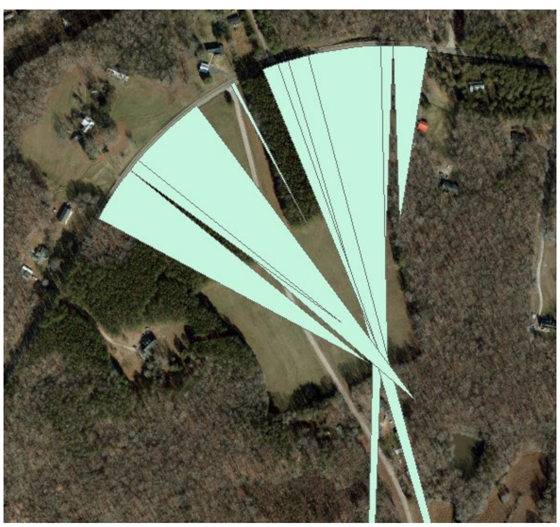

Figure 3-2 a Multiple wedges along a curve due to imperfections in the digital centerline

Figure 3-2 b Processed wedge image Source: ESRI, Maxar, Earthstar Geographics, and the GIS User Community

3.2.3 Google Earth Approach

The third approach for estimating curve radius was calculated by determining measurements within Google Earth. Google makes no claims to the accuracy of Google Earth maps, however based on information readily available from user community groups, relative accuracy of about 3' per 1000' feet can be expected at the highest resolution.

To estimate curve radius, a chord length (C) and middle ordinate distance (M) are measured in Google Earth relative to the vehicle trajectory along the center of the travel lane (**Figure 3-3**). The actual long chord (LC) is not needed to estimate radius. Only a chord along the curve is required. Ideally, a chord length as long as possible is preferred to minimize error, however, it is difficult to precisely estimate the location of a curve's point of curvature (PC) and point of tangency (PT). The curve radius can be estimated using the Pythagorean Theorem with the variables identified in **Figure 3-4**, and by using Equations 3-1 and 3-2.

$$R^2 = (R - M)^2 + (\frac{C}{2})^2 \qquad (3\text{-}1)$$

$$R = \frac{1}{2}M + \frac{C^2}{8M} \qquad (3\text{-}2)$$

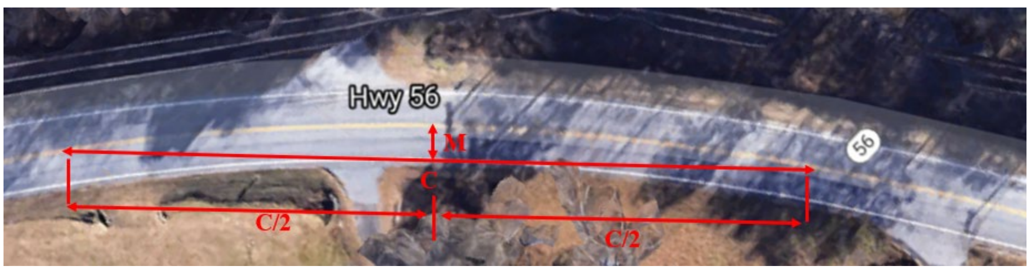

Figure 3-3 Chord length (C) and middle ordinate distance (M) measured in Google Earth

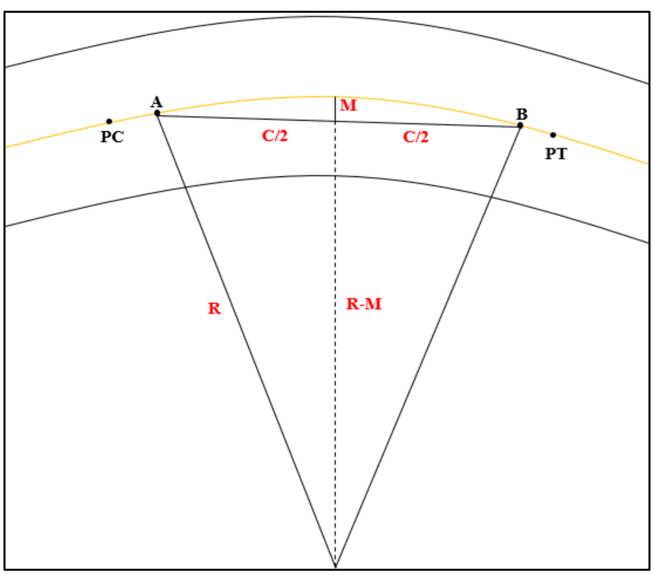

Figure 3-4 Curve radius estimation method

After testing with Google Earth, the manual method was modified slightly. After drawing C in Google Earth to get its length, the chord line will disappear when starting to draw a separate line representing M. Thus, a visual estimate of the center of C is needed. An easier method is to draw an isosceles triangle as shown in **Figure 3-5**. Google Earth includes the C midpoint location that provides an accurate visual reference so a vertex can be moved to make sure that the triangle looks correct. Then, using C and the area of the triangle provided by Google Earth, M can be calculated. Both methods (measuring C and M directly versus drawing the triangle) compared favorably during testing however the triangle method was deemed more efficient and less prone to error.

Figure 3-5 Creating an isosceles triangle in Google Earth to calculate the radius

3.2.4 Mobile Lidar

A limited amount of Mobile LiDAR data was available for use on this project. This data was from a previous SCDOT research project that was conducted by Clemson and the Citadel. It was collected by different vendors along two highway corridors in the upstate of South Carolina. Radius and superelevation were two primary data elements extracted from the mobile LiDAR point clouds and were found to be very accurate compared to ground truth conventional survey.

3.2.5 Comparative Approach

The comparison between the Rieker CARS method, the GIS automated method, and the manual Google Earth method were conducted for Pickens County in the upstate of South Carolina. This county was chosen because of the mileage of hilly terrain. The three different datasets were reconciled so that a direct comparison could be made between the three methods. Of the over 800 Rieker CARS curves in Pickens County, just over 500 are used in the comparison. The difference was due to various reasons. First, the GIS automated method only included curves with radii less than 1500’ because a primary use of the curve information is for setting advisory speeds. Roads with radii greater than 1500’ will have design speeds of at least 60 MPH which will be higher than the posted speed limit in most cases. Of the 800 Rieker CARS curves, just over 200 had radii over 1500’. The remaining Rieker CARS curves that were not represented in the comparison did not have corresponding GIS generated curve data. In many of these cases, the Rieker CARS curve had a radius just over 1500' while the automated GIS curve was likely just under 1500' and was filtered.

The mobile LiDAR comparison was only conducted for a small number of curves on a multilane parkway in Anderson, South Carolina. The parkway was manually surveyed for ground truth purposes. The comparison included multiple parameters because in addition to radius, the Mobile LiDAR data can be used to calculate the roadway's cross slope and superelevation. Five different vendors participated in the MLS data collection. **Figure 3-6** shows the section of parkway used in the MLS comparison. The Rieker CARS curves are shown in red. Only two of the curves have useable automated GIS wedges. The other curves' radii wedges were filtered because of their large radii.

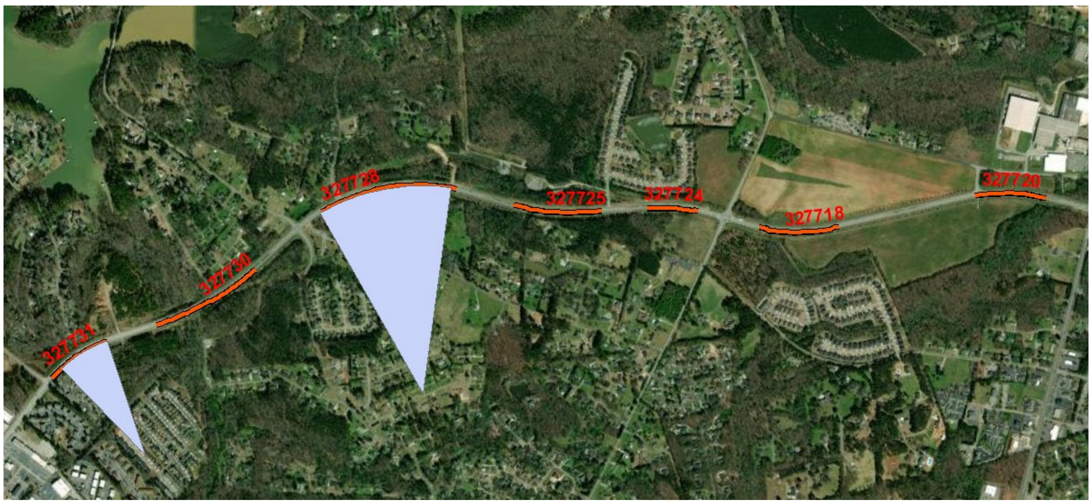

Figure 3-6 Parkway in Anderson, SC that includes MLS data

3.2.6 Comparison of Rieker CARS, automated GIS, and manual Google Earth Methods

An initial comparison between the Rieker CARS radii data and the GIS automated method showed a number of outliers that were individually checked to identify if the deviation was due to a curve matching problem or some other issue. As observed, most of the outliers were due to curve mismatching. In some cases, a Rieker CARS curve extended longer than the actual curve which caused it to overlap significantly with one automated GIS generated curve and partially with another (**Figure 3-7**). In these cases, the mismatched curves were removed so that each Rieker CARS curve is paired with only one GIS generated curve.

Figure 3-7 Rieker CARS curve overlapping with two automated GIS curves

Table 3-1 presents the summary statistics of radii generated by each method. The Rieker CARS approach had the highest minimum radius and the highest maximum radius. The automated GIS approach had the lowest minimum radius, while the Google Earth approach had the lowest maximum radius. The standard deviation values are relatively large which is due, in part, to the remaining outliers. In the standard deviation, the deviations from the mean (residuals) are squared, so large deviations are weighted more heavily. Thus, outliers heavily influence values.

Table 3-1 Summary statistics of radii (ft) generated by each method

	N	Minimum	Maximum	Mean	Std. Deviation
Rieker CARS Radius	471	63.23	2264.80	763.14	423.37
Automated GIS Radius	471	57.30	2055.76	744.55	390.97
Google Earth	471	60.34	1839.83	718.01	399.22

Table 3-2 presents the results of statistical paired t-tests to determine whether the differences in means vary across the approaches. When examining the entire dataset, the differences between each pair of approaches are statistically significant. Consistent with the summary statistics, the Rieker CARS data produces longer radii than the other two approaches. The automated GIS approach is also longer than the Google Earth approach. However, when examining only the lower quartile (based on the Rieker CARS measurements), the results are different. The average Rieker CARS measurement is lower than the automated GIS estimated radius. In the lower-middle and upper-middle quartiles, the Rieker CARS and automated GIS approaches are not statistically different, but the other pairs are and follow the previous trend. At the upper quartile, however, the Rieker CARS radius is larger than both automated GIS and Google Earth radius

estimates. Automated GIS and Google Earth radius estimates are not significantly different at these larger values.

Figures 3-8,9, and 10 show comparison graphs of the different methods. There are 471 data points for each graph. **Figure 3-8** shows a comparison graph of how well the automated GIS method (x axis) predicts the Rieker CARS data (y axis). The fitted line to the graph shows a constant of -10.361 and a slope of 1.0389. The R^2 is 0.920. Ideally, if the data perfectly matched, the constant would be 0 and the slope would be 1. A closer look at the statistics related to the graph indicate that the constant is not statistically significant at 95% confidence ($p=0.05$) but the slope (coefficient) is (t-stat=83.389). **Figure 3-9** shows a comparison graph of how well the Rieker CARS data predicts the manual Google Earth method. The fitted line to the graph provides a constant of 25.107 and the slope is 0.908. The R^2 is 0.9272. The statistics indicate that both the constant and slope are statistically significant at 95% confidence ($p=0.05$). **Figure 3-10** shows a comparison graph of how well the automated GIS method predicts the manual Google Earth method. The fitted line to the graph provides a constant of -17.829 and the slope is 0.988. The R^2 is 0.9368. The constant is not statistically significant.

The mean absolute percentage deviation (MAPD) is a common metric of model prediction accuracy. It is especially useful in this comparative analysis because it is easily understood irrespective of the magnitude of the radius. It is given by Equation 3-3, as follows:

$$MAPD = \frac{100}{n}\sum_{t=1}^{n}\left|\frac{A_t - F_t}{A_t}\right| \qquad (3\text{-}3)$$

Where:

- n is the number of fitted points;
- A_t is the reference value for observation t;
- F_t is the forecasted or comparison value.

Table 3-3 shows the MAPD values of the comparisons between methodologies. It shows that the methods are, on average, within about 10% of each other. The dataset for Pickens County was partially cleaned of outliers. Because of the number of matching errors, additional outliers are likely but were not identified because of the size of the dataset. While some outliers are included in the graphs, to give a more representative picture of the comparison, the median of the absolute percentage deviations was calculated. A percent deviation is calculated by taking the absolute value of the difference between a reference value and a comparison value divided by the reference value. **Table 3-4** shows the medians of the absolute percent deviations of the comparisons between methodologies. It shows that the 50^{th} percentile of the percent deviations are less than 8% in all comparisons.

Table 3-2 Paired t-test results

Complete Dataset		Paired Differences: Mean	Paired Differences: Std. Deviation	Paired Differences: Std. Error Mean	95% Confidence Interval of the Difference: Lower	95% Confidence Interval of the Difference: Upper	t	df	Significance: One-Sided p	Significance: Two-Sided p
Pair 1	Rieker CARS R – Automated GIS R	18.597	120.396	5.548	7.696	29.498	3.352	470	0.000	0.001
Pair 2	Rieker CARS R – Google Earth R	45.131	114.565	5.279	34.758	55.504	8.549	470	0.000	0.000
Pair 3	Automated GIS R – Google Earth R	26.534	100.453	4.629	17.438	35.629	5.732	470	0.000	0.000
Lower Quartile of Rieker CARS										
Pair 1	Rieker CARS R – Automated GIS R	-16.371	42.269	3.875	-24.044	-8.697	-4.225	118	0.000	0.000
Pair 2	Rieker CARS R – Google Earth R	6.185	32.620	2.990	0.264	12.107	2.068	118	0.020	0.041
Pair 3	Automated GIS R – Google Earth R	22.556	37.281	3.418	15.788	29.323	6.600	118	0.000	0.000
Lower-Middle Quartile of Rieker CARS										
Pair 1	Rieker CARS R – Automated GIS R	-6.616	75.284	6.990	-20.462	7.230	-0.947	115	0.173	0.346
Pair 2	Rieker CARS R – Google Earth R	30.253	83.253	7.730	14.941	45.564	3.914	115	0.000	0.000
Pair 3	Automated GIS R – Google Earth R	36.869	72.170	6.701	23.595	50.142	5.502	115	0.000	0.000
Upper-Middle Quartile of Rieker CARS										
Pair 1	Rieker CARS R – Automated GIS R	9.671	99.906	9.158	-8.465	27.807	1.056	118	0.147	0.293
Pair 2	Rieker CARS R – Google Earth R	53.330	100.375	9.201	35.108	71.551	5.796	118	0.000	0.000
Pair 3	Automated GIS R – Google Earth R	43.659	98.298	9.011	25.815	61.503	4.845	118	0.000	0.000
Upper Quartile of Rieker CARS										
Pair 1	Rieker CARS R – Automated GIS R	88.240	185.140	17.116	54.339	122.141	5.155	116	0.000	0.000
Pair 2	Rieker CARS R – Google Earth R	91.154	176.052	16.276	58.918	123.391	5.601	116	0.000	0.000
Pair 3	Automated GIS R – Google Earth R	2.915	153.272	14.170	-25.151	30.980	0.206	116	0.419	0.837

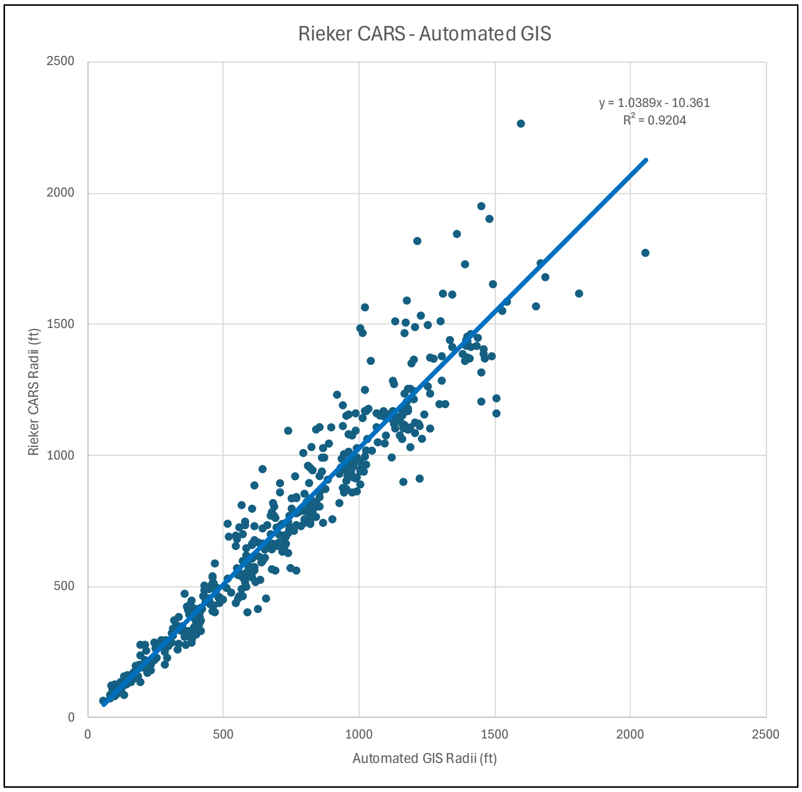

Figure 3-8 Graph of Rieker CARS data versus automated GIS method

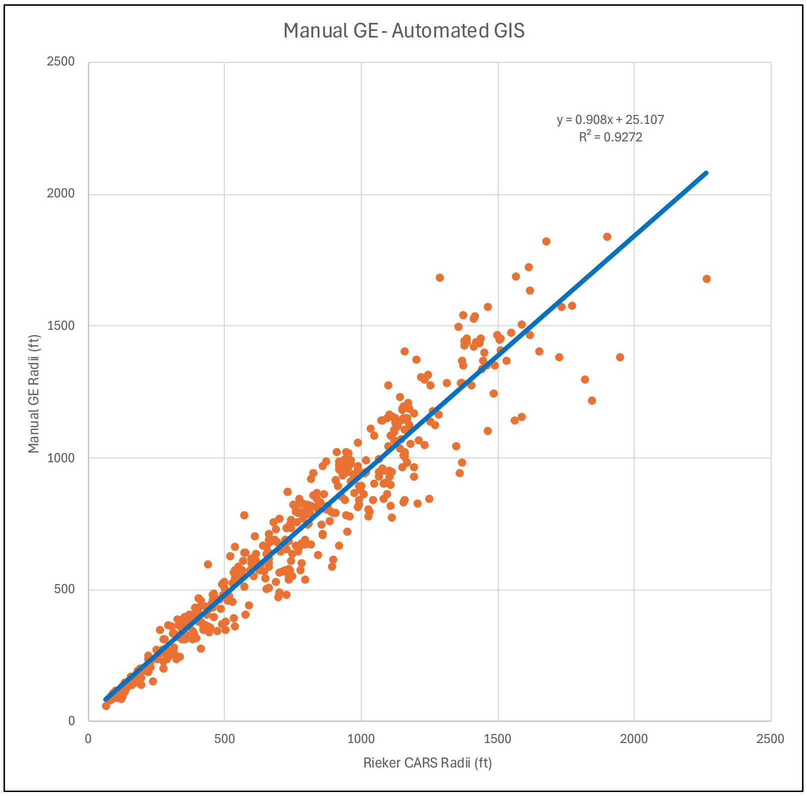

Figure 3-9 Graph of the manual Google Earth method vs Rieker CARS data

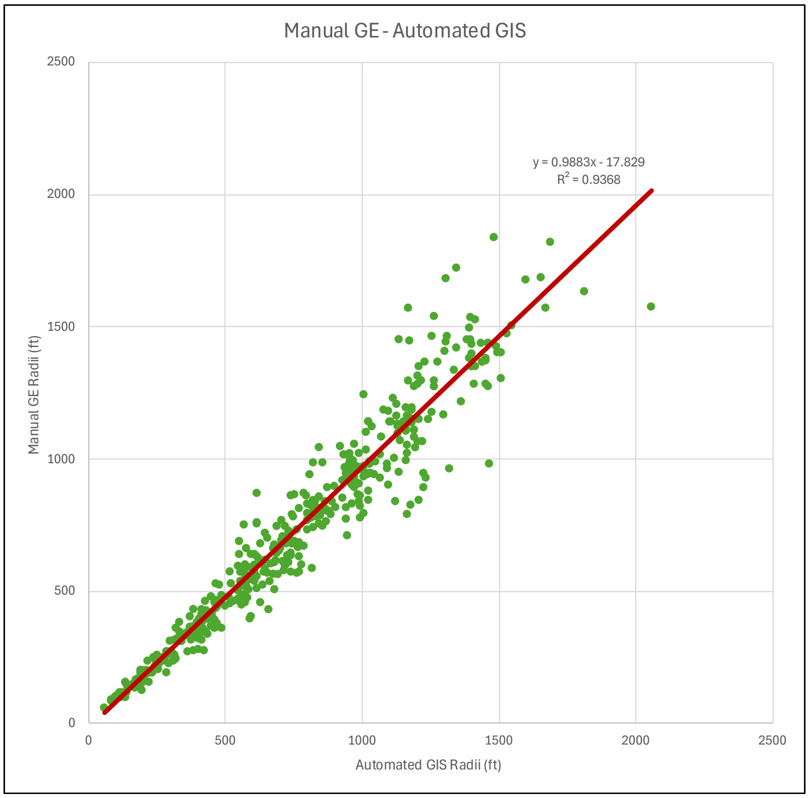

Figure 3-10 Graph of the manual Google Earth method vs automated GIS method

Table 3-3 Radius MAPD between methods. Columns are the reference

Average of Deviations	Rieker CARS	Automated GIS	Manual GE
Rieker CARS	0	10.69%	11.96%
Automated GIS	10.38%	0	10.78%
Manual GE	10.35%	9.63%	0

Table 3-4 Radius median of absolute percentage deviations. Columns are the reference

Medians of Deviations	Rieker CARS	Automated GIS	Manual GE
Rieker CARS	0.00%	7.74%	7.79%
Automated GIS	7.95%	0.00%	7.56%
Manual GE	7.68%	7.46%	0.00%

3.2.7 Comparison with Mobile Lidar Scanning

Horizontal curve data collected using a traditional manual field survey conducted along the alignment of East West Parkway in Anderson, SC is presented as the basis for comparison with data determined using curve data collection methods, as summarized in **Table 3-5**. To further understand differences between data collection methods, **Table 3-6** provides a summary of percent differences in comparison to traditional manual field survey collected values. Of the five MLS vendors who participated in the previous SCDOT data collection rodeo, Vendor B is used as the basis for comparison as the best performing vendor, although similar results were obtained by all five vendors The variable of primary interest is horizontal radius as this variable is directly related to design speed of the curve. As shown in **Table 3-6**, collection of radius data using MLS produced four values that were overestimated and three values that were underestimated for all seven curves. Collection of radius data using the Rieker CARS method produced all seven values that were overestimated. Collection of radius data using the manual Google Earth method produced six values that were overestimated and one value that was underestimated. Furthermore, average absolute percent error for radius per curve for each method is as follows: 1.) MLS, 0.33% error per curve (n=7); 2.) Rieker CARS, 1.69% error per curve (n=7); 3.) Automated GIS, 1.69% error per curve (n=2); and 4.) Manual Google Earth, 1.97% error per curve (n=7).

Both MLS and Rieker CARS provides a value for superelevation for each curve it surveys. As shown in **Table 3-5** for extraction of superelevation (e), data using LiDAR produced 5 values that were overestimated and 2 values that were underestimated for all seven curves. Extraction of superelevation (e) data using the Rieker CARS method produced all seven (7) values that were overestimated. Furthermore, as shown in **Table 3-6** average absolute percent error for superelevation (e) per curve for each method is as follows: 1.) LiDAR, 2.42% error per curve (n=7); and 2.) Rieker CARS, 35.89% error per curve (n=7).

3.2.8 Discussion of Comparative Results

The results show that all of the methods are typically within 10% of each other for the Pickens County data (n=471) and the Anderson data indicated that the Google manual method data was within 2% of surveyed ground truth (6 out of 7) for relatively large radius curves. This is promising because the value of M decreases with increasing radius which makes it difficult to estimate M accurately with large radius curves. Thus, it seems reasonable to assume that improved results with the manual method would be achieved with smaller radii. There is a question regarding the significance of errors in radius estimates for different applications. A primary use of radius would be setting advisory speeds on curves. As presented in Chapter 2, Equation 3-4 is generally used to estimate roadway design speed *(Gooch, 2016)* and is also used in the design method for determining highway curve advisory speeds *(Torbic, 2004)*.

$$R = \frac{v^2}{15(e+f)} \qquad (3\text{-}4)$$

In this equation, *R* (feet) is the radius of the curve, *v* (mph) is the design speed, *e* (ratio to 1) is the design superelevation rate, and *f* is the design friction coefficient. If the radius of a curve is known, design speed can be calculated by substituting values for *R, e*, and *f.* This equation can also be used for determining highway curve advisory speeds *(Torbic, 2004)*. Design friction coefficients (*f*) are a function of speed and can be determined from AASHTO design guidelines *(2018)*. A conservative value of 0.04 (4%) was used for superelevation (e).

Table 3-5 East West Parkway horizontal curve data from various methods

E-W Parkway Alignment	Curve Variable	Field Survey	LiDAR Vendor B	Rieker CARS Data	Automated GIS	Manual GE
Curve 1	R (ft)	1432.40	1423.07	1442.17	1501.96	1345.40
	L (ft)	857.36	847.62	859.00	675.19	
	e (%)	4.73	4.86	4.22		
Curve 2	R (ft)	3819.72	3830.26	3866.47		3846.97
	L (ft)	1630.10	1633.20	1370.00		
	e (%)	2.45	2.41	3.77		
Curve 3	R (ft)	2291.83	2287.84	2335.67	2590.46	2324.46
	L (ft)	2349.10	2335.57	1787.00	1700.62	
	e (%)	3.68	3.67	4.16		
Curve 4	R (ft)	2864.79	2865.99	2873.93		2910.83
	L (ft)	1052.17	1049.37	1171.00		
	e (%)	2.83	2.95	3.99		
Curve 5	R (ft)	1909.86	1902.72	1962.63		1948.39
	L (ft)	698.65	697.29	661.00		
	e (%)	3.94	4.01	5.82		
Curve 6	R (ft)	2291.83	2306.64	2360.70		2303.36
	L (ft)	1144.89	1153.50	987.00		
	e (%)	3.09	3.27	4.32		
Curve 7	R (ft)	2291.83	2294.70	2336.53		2325.56
	L (ft)	1057.44	1066.37	813.00		
	e (%)	3.40	3.43	4.93		

For a design speed of 50 MPH, the friction coefficient is 0.14 and minimum design radius is 926 feet assuming a superelevation (0.04). If the radius of the data is 10% lower than actual (833 feet), the corresponding design speed would be 47 MPH. **Table 3-7** presents the results for other speeds and assumes a conservative estimate of superelevation to be 0.04 in all cases. The table indicates that a 10% reduction in radius corresponds to a 5.1% reduction in design speed.

While the deviations can be significant, all three methods can be used for screening purposes to identify candidate locations in need of curve warning and advisory speed signage. Rieker is already used for this purpose by many DOTs. For South Carolina, Rieker and the automated GIS method are most feasible for screening purposes because this data is available for all counties. **Table 3-7** indicates that a 10% radius deviate corresponds to design/advisory speed deviation of 2 to 3 MPH depending on the magnitude of the design speed. In practice, advisory speeds are rounded to 5 mph increments. DOTS may choose to be more conservative and/or conduct further study for curves that are close to a threshold for mandatory signage based on MUTCD guidelines. Curve warning signs are only required if advisory speeds are at least 10 MPH lower than the actual speed limit; and advisory speed signs are only required if advisory speeds are at least 15 MPH lower than the actual speed limit. Further, the radii values can also potentially be useful for crash analysis and preliminary design work. Field confirmation can be done for selected curves depending on the application.

Table 3-6 East West Parkway horizontal curve data and percent errors

E-W Parkway Alignment	Curve Variable	Field Survey	LiDAR Vendor B	Rieker CARS Data	Automated GIS	Manual GE
Curve 1	R (ft)	1432.4	-0.65%	0.68%	4.86%	-6.07%
	L (ft)	857.36	-1.14%	0.19%	-21.25%	
	e (%)	4.73	2.64%	-10.78%		
Curve 2	R (ft)	3819.72	0.28%	1.22%		0.71%
	L (ft)	1630.1	0.19%	-15.96%		
	e (%)	2.45	-1.63%	53.88%		
Curve 3	R (ft)	2291.83	-0.17%	1.91%	13.03%	1.42%
	L (ft)	2349.102	-0.58%	-23.93%	-27.61%	
	e (%)	3.68	-0.27%	13.04%		
Curve 4	R (ft)	2864.79	0.04%	0.32%		1.61%
	L (ft)	1052.172	-0.27%	11.29%		
	e (%)	2.83	4.24%	40.99%		
Curve 5	R (ft)	1909.86	-0.37%	2.76%		2.02%
	L (ft)	698.647	-0.19%	-5.39%		
	e (%)	3.94	1.78%	47.72%		
Curve 6	R (ft)	2291.83	0.65%	3.01%		0.50%
	L (ft)	1144.889	0.75%	-13.79%		
	e (%)	3.09	5.66%	39.81%		
Curve 7	R (ft)	2291.83	0.13%	1.95%		1.47%
	L (ft)	1057.44	0.84%	-23.12%		
	e (%)	3.4	0.74%	45.00%		

Table 3-7 Effects of a radius deviation of 10% on speed change

Speed	e	f	Design Radius	Deviate %	Deviate radius	Deviate Speed	Speed % Change
30	0.04	0.2	250	10	225	28	5.1%
35	0.04	0.17	389	10	350	33	5.1%
40	0.04	0.16	533	10	480	38	5.1%
45	0.04	0.15	711	10	639	43	5.1%
50	0.04	0.14	926	10	833	47	5.1%
55	0.04	0.13	1186	10	1068	52	5.1%
60	0.04	0.12	1500	10	1350	57	5.1%

3.2.9 Rieker Superelevation

The above discussion assumes a superelevation value of 0.04. The Anderson Parkway data showed that MLS provides very good estimates of superelevation which is supported in a related study *(Shams et al. 2018).* Rieker CARS provides estimates of superelevation but the Anderson data shows that the superelevation data can deviate substantially from the actual superelevation. A representative from Rieker CARS indicated that while advisory speeds are accurate, individual model parameters and especially superelevation can have errors depending on vehicle driving speed, position in the lane, etc. Thus, the Rieker CARS superelevation values should be used with caution. For the Pickens County data, the *average* Rieker CARS superelevation values were higher than SCDOT and AASHTO design maximum values in many instances. When using the design method to estimate advisory speeds, a conservative estimate of superelevation may be more appropriate.

3.2.10 Comparison of Extraction Methods with Mobile LiDAR Data

Through comparisons of data extraction methods with selected MLS measured horizontal curves, data precision was determined to be superior for MLS collection methods. While extremely accurate, Mobile LiDAR data is not used any further in this research because of its very limited availability. It was only included in this research for comparison purposes. In addition to its high cost, Mobile LiDAR requires extensive post processing of immense point clouds to extract useful attributes. It is noteworthy that Mobile LiDAR has multiple applications beyond the type of highway curve data collection discussed in this study

3.3 Superelevation

The researchers initially considered using superelevation derived from Rieker data, however, as discussed in 3.2.9, the accuracy was highly variable. Instead, the researchers decided to use a GIS approach using statewide South Carolina Department of Natural Resources LiDAR data. Most of South Carolina's LiDAR data meets USGS level 2 quality standards depending on flight year **(Figure 3-11)**. Vertical accuracy is expected to be within 10 cm for levels 1 and 2, and 20 cm for level 3. Point spacing is <= 0.35 meters for level 1, <= 0.71 meters for level 2, and <= 1.41 meters for level 3. The LiDAR dataset is a vast point cloud that required the use of

Clemson's high performance Palmetto Cluster to greatly speed up processing. The researchers used curve buffers to filter most of the point cloud. Then, a segment was added perpendicular to each curve midpoint. Points within a rectangular buffer around this segment were processed using a RANSAC algorithm remove outliers and extract cross slopes. Longitudinal roadway grade within the rectangular buffer can also be extracted from the fitted plane **(Figure 3-12)**. The RANSAC algorithm *(Ruzgiene et al. 2018)* is robust to outliers which is a problem with the LiDAR data due to tree canopies and the spatial accuracy of the digital centerline. If the centerline does not fall in the middle of the road represented by the LiDAR, the segment might reach into or beyond the shoulder area. A sample of 60 curves were checked in the field using a digital level and average accuracy was +/- 0.8% superelevation (not % error). All of the curves selected were on low volume roads within 20 miles of Clemson. Many were in the vicinity of tree canopies. Clemson is in Pickens County. The flight year for the Pickens County aerial LiDAR data used in this research was 2011 and has a level 3 accuracy rating. It has since been determined that level 2 aerial LiDAR data is available for most counties including Pickens County. While the level 3 LiDAR data was used for the evaluation of extracted superelevation values, the researchers were still impressed with the results. While there are clear differences between the LiDAR and measured superelevation values, the researchers found that field measurements were highly variable depending on which lane was measured and where in the lane the measurement was taken. Because the average deviation in superelevation was less than 1% it was deemed suitable for use in determining statewide curve advisory speeds.

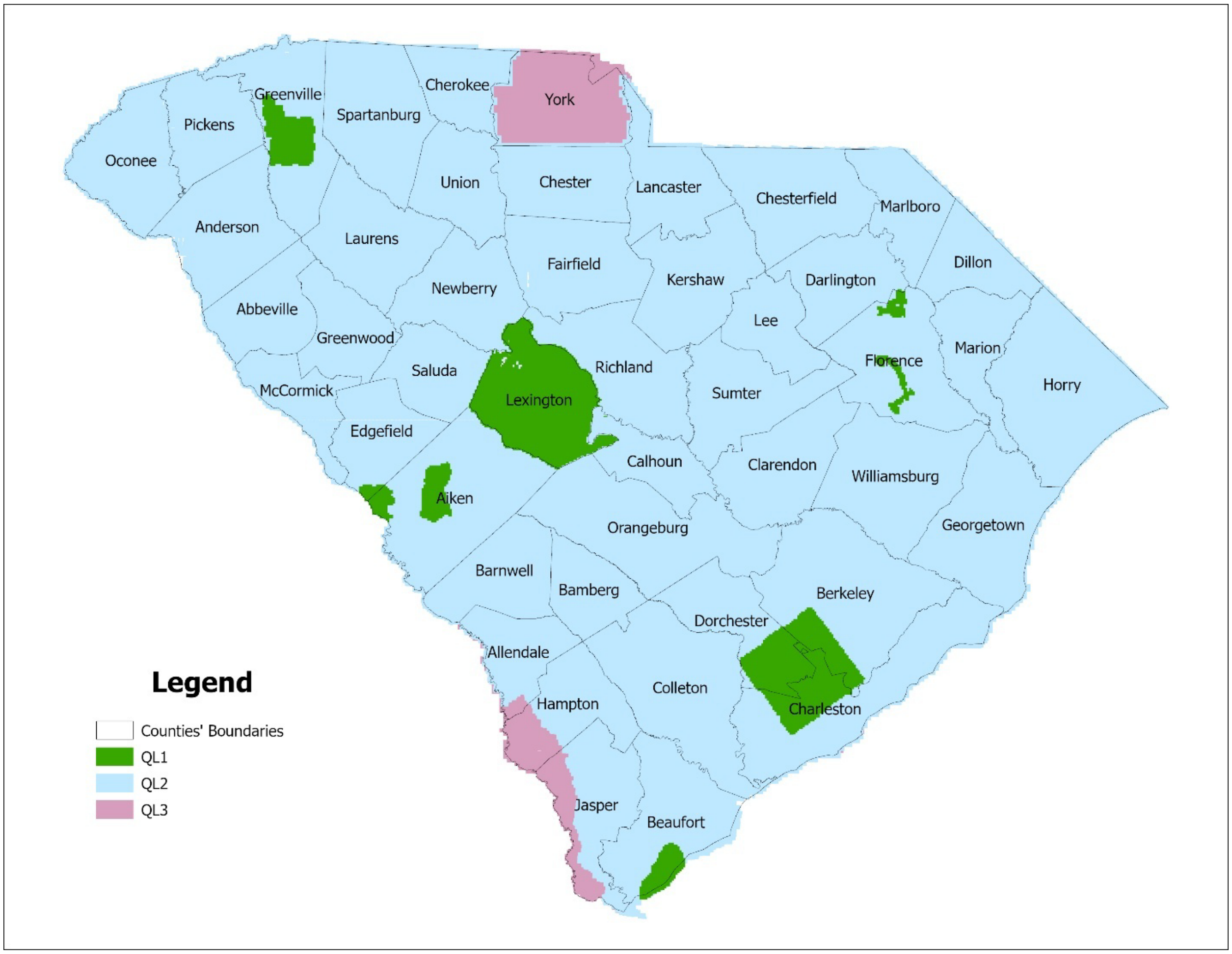

Figure 3-11 Quality level of available aerial LiDAR data in South Carolina

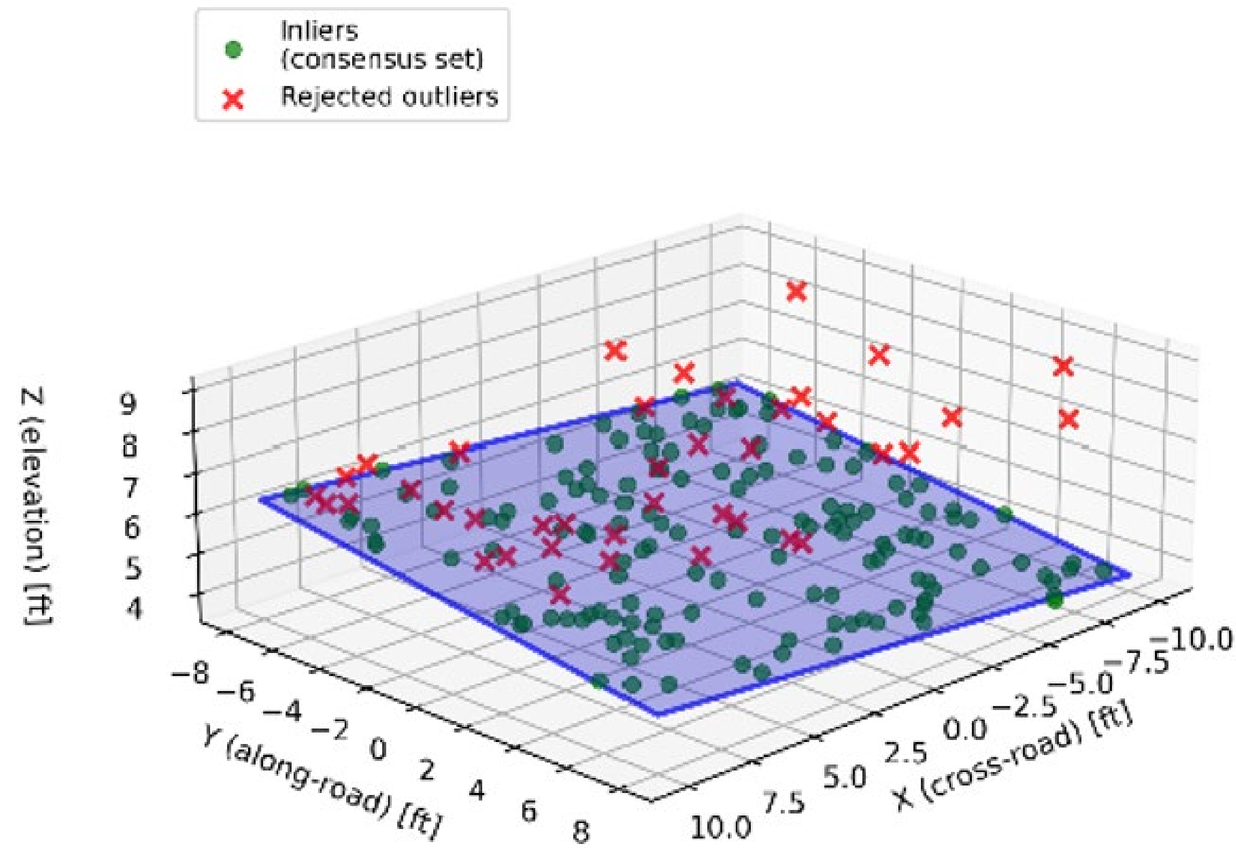

Figure 3-12 RANSAC roadway plane fitting to determine superelevation and grade

3.4 Posted Speed Limit

Posted speed limits are important traffic control devices for ensuring safe operating conditions on roads including highway curves. Posted speed limit data is a crucial data element for this project. It is used to determine safe advisory speeds based on MUTCD guidance and it is also used in the safety analysis for predicting crashes.

The SCDOT RIMS data includes posted speed limit as one of the attributes. Unfortunately, less than a third of the highway network has the speed limit attribute populated. **Figure 3-13** shows the coverage of RIMS segments with speed limit data. This coverage is far short of what is needed to do network wide curve advisory speed determination as well as the safety analysis. Thus, the researchers supplemented the RIMS speed data by extracting speed limits from the 51,200 speed limit signs in the SCDOT sign inventory. A second method using speed limits from crash reports was also developed to further improve the coverage of speed limit data.

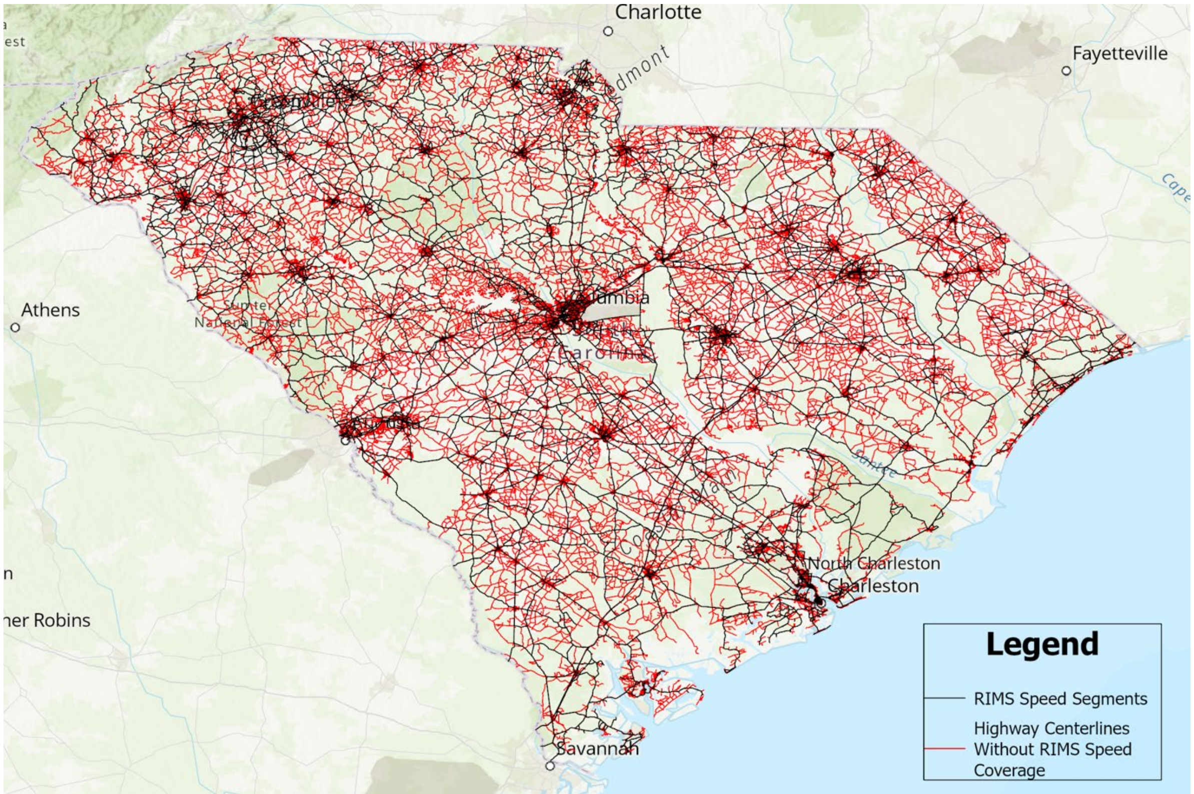

Figure 3-13 Coverage of the RIMS Segments with speed limit data

3.4.1 Extracting Posted Speed Limits from Signs

The process for extracting speed limits from signs involved developing a segmentation algorithm to partition roadway centerlines into continuous segments, each with a single, consistent speed limit. The approach follows the common U.S. convention that a posted speed on an undivided highway typically applies to both directions of travel. The core logic defines explicit breakpoints. Each route is split at its start and end points and at the location of every validated speed-limit sign, regardless of orientation, to produce continuous, non-overlapping coverage. To avoid creating spurious micro-segments from signs on opposite sides of the same roadway, signs within a small proximity threshold are grouped and treated as a single breakpoint.

A prerequisite for segmenting the road network is to determine, programmatically, the applicable travel direction for each speed-limit sign. We defined this “Target Direction” as Forward (increasing mileposts) or Reverse. For every segment between consecutive breakpoints, the speed limit is assigned using the predefined directional rules based on the sign inventory’s road direction and sign direction attributes.   A segment takes the speed from a Forward (FWD) sign at its starting breakpoint or from a Reverse (REV) sign at its ending breakpoint. Conflicts between FWD and REV signs trigger a manual review. If a segment is not governed by a sign at its immediate boundaries, for example an interval between two FWD-facing signs, it inherits the speed from the preceding segment. The result is a geospatial layer of road segments with assigned speed limits suitable for network-level analysis.

3.4.2 Extracting Posted Speed Limits from Crash Reports

The deterministic speed limit segmentation derived from the SCDOT speed-limit sign inventory performed well overall; however, detailed review revealed noticeable gaps in sign data, creating breaks along otherwise continuous corridors. In addition, many roads classified as local lacked posted speed-limit signs in the field, often because of low AADT or missing records. These gaps prompted development of an alternative approach. Crash data are especially useful where sign coverage is sparse and crashes occur often. Officers record the posted speed on crash reports, yielding location-specific observations that can be aggregated at scale. Using these records, speed limits may be inferred across much of the network and can supplement sign-based data where needed.

Over 1 million crashes from 2017–2024 were used for this analysis. Although spatially extensive, the crash data posed a modeling problem: they are discrete point observations with known noise and reporting error. Simple aggregation, for example, a moving window average or taking the most frequent speed per segment, does not enforce spatial continuity and is sensitive to outliers. We therefore adopted a Hidden Markov Model (HMM). An HMM is a stochastic model designed to infer the most likely sequence of underlying "hidden" states from a sequence of "observed" emissions. In this formulation, the hidden states Q are the true, unobserved posted speeds along a route, and the observations O are the speeds recorded on crash reports ordered by milepost. The transition matrix T specifies the chance that the true speed changes between successive crash locations, which should be small given the contiguity of speed zones. The emission matrix E gives the likelihood of observing a reported speed, conditional on the true speed, and thus captures reporting noise. Framed this way, the HMM filters noisy observations to infer the most probable sequence of posted speeds along each route, providing a defensible basis for network segmentation.

Figure 3-14 illustrates the HMM used in this study. Along a route, the true posted speed limits are represented as hidden states, which are relatively stable and change infrequently. The speeds recorded on individual crash reports are the observations and are treated as noisy emissions from those states. Two probability structures define the model: transition probabilities (horizontal arrows) give the chance that the true speed changes between successive points, and emission probabilities (vertical arrows) give the chance of observing a reported speed given the true speed. The HMM algorithm uses this framework to infer the most probable sequence of hidden states from the sequence of noisy observations.

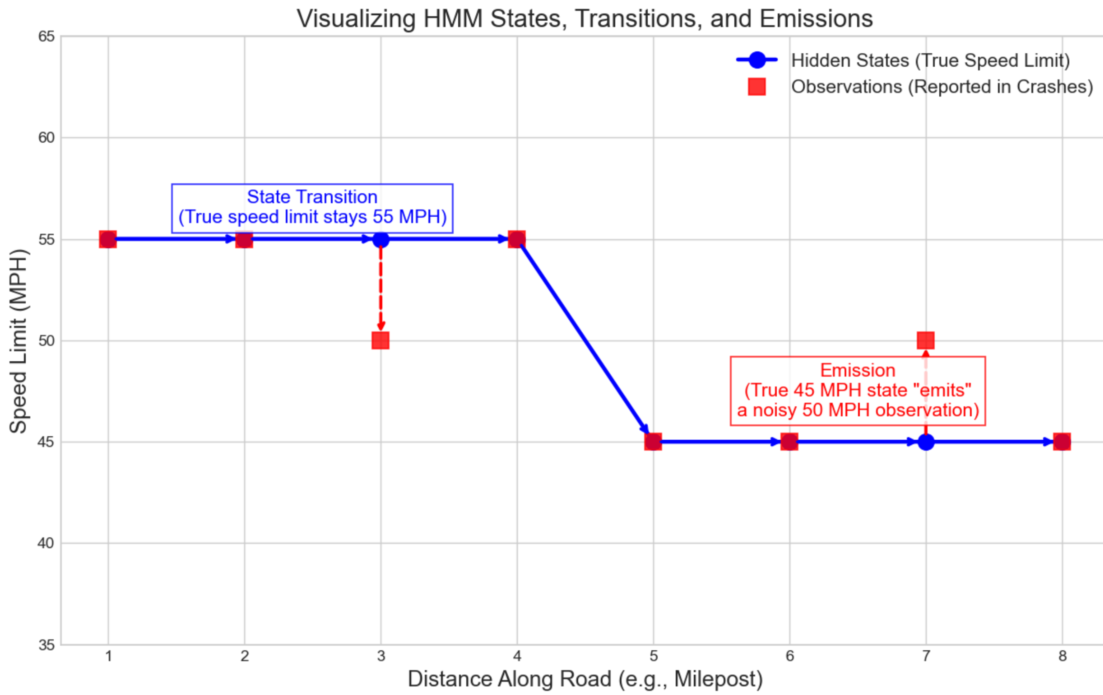

Figure 3-14 Conceptual diagram of the Hidden Markov Model for speed limit inference

Accurate use of an HMM is highly dependent on application of core parameters, which calibrates the model's assumptions to ascertain data tendencies. To determine an optimal core parameter combination, a rigorous calibration and validation process is required. To accomplish this HMM foundational computational element, a ground-truth dataset was established to serve as a benchmark for the model's results verification. A dataset of random samples was generated across the road network of three contiguous counties: Spartanburg, Anderson and Greenville. Then the research team used Google Street View to virtually drive each road segments to determine actual posted speed limit corresponding to each location. After post processing to resolve any outlying data issues, a dataset of 746 points was established for use as a ground truth sample to test subsequent HMM processing runs. After which, a systematic grid search was conducted to determine optimal model hyperparameters. Based on this analysis, the parameter set was established and included *minimum crashes per segment = 5* and *minimum segment length = 0.1 miles* for final statewide road network segmentation.

Based on preliminary model results, adjacent crash points with the same inferred speed limit were grouped to form initial segments. The boundaries between differing speed zones were then refined by setting the transition point to the midpoint between the last crash location of the preceding segment and the first crash location of the succeeding segment. Next a refinement loop was initiated to address segmentation fragmentation. Any segment with a length less than the calibrated threshold of 0.1 miles was iteratively merged with its adjacent segment. To ensure that less certain segments were absorbed by more statistically robust ones, short segments were systematically merged with neighboring segments exhibiting higher crash counts. This process was repeated until all remaining segments satisfied the minimum length requirement. Furthermore, to create an approximate confidence score, segments with at least three crashes and at least 0.1 miles in length were labeled as “HIGH” confidence and others were labeled as “LOW”. Additionally, to ensure complete coverage, the first segment of each route was extended to a route’s starting mile point and last segment to a route ending mile point, with these extensions being assigned a “LOW” confidence score.

The final output of this workflow is a comprehensive geospatial dataset of road segments, containing data such as route identifier, inferred speed limit, start and end mile points, segment length, number of crashes used in inference, and a confidence metric based on whether the segment meets the minimum crash and length thresholds. The final output included over 38,055 miles of segments, of which more than 32,000 miles were classified as high confidence.

To maximize both accuracy and network coverage, we built a hierarchical combined posted speed limit inventory using a hybrid of the different methods. The base layer consists of road segments with speeds populated with the sign inventory method. These results were compared with the RIMS inventory for these segments. When the two methods were determined to be in agreement, the posted speed limits for these segments were considered as high-confidence. The next level of confidence was based on the sign inventory without the RIMS inventory. Remaining gaps and any conflicts were filled with segments from the HMM analysis of crash data. The outcome is a single, GIS-ready statewide layer. **Figure 3-15** shows the complete coverage. Of South Carolina’s 44,037 state highway miles, we were able to populate posted speeds for approximately 41,500 miles (~94%).

To determine the accuracy of the methodology, a random sample of 209 points were generated across different roadway functional classes throughout the state. Actual posted speed limits were determined from Google Street View. Our hybrid method had an overall accuracy level of 88%. In comparison, for the segments in the sample that had RIMS posted speed limits, the accuracy was 86%. The HMM method gave an accuracy of just under 80%. This is to be expected because of the subjective nature of officers identifying what the posted speed limits are in the crash reports. In rural areas, it may not be obvious because of a lack of posted speed limit signage. Of 85,494 crashes with posted speed limit segmentation, 34,327 (40%) of the crashes had reported posted speed limits inconsistent with the speed limit segmentation.

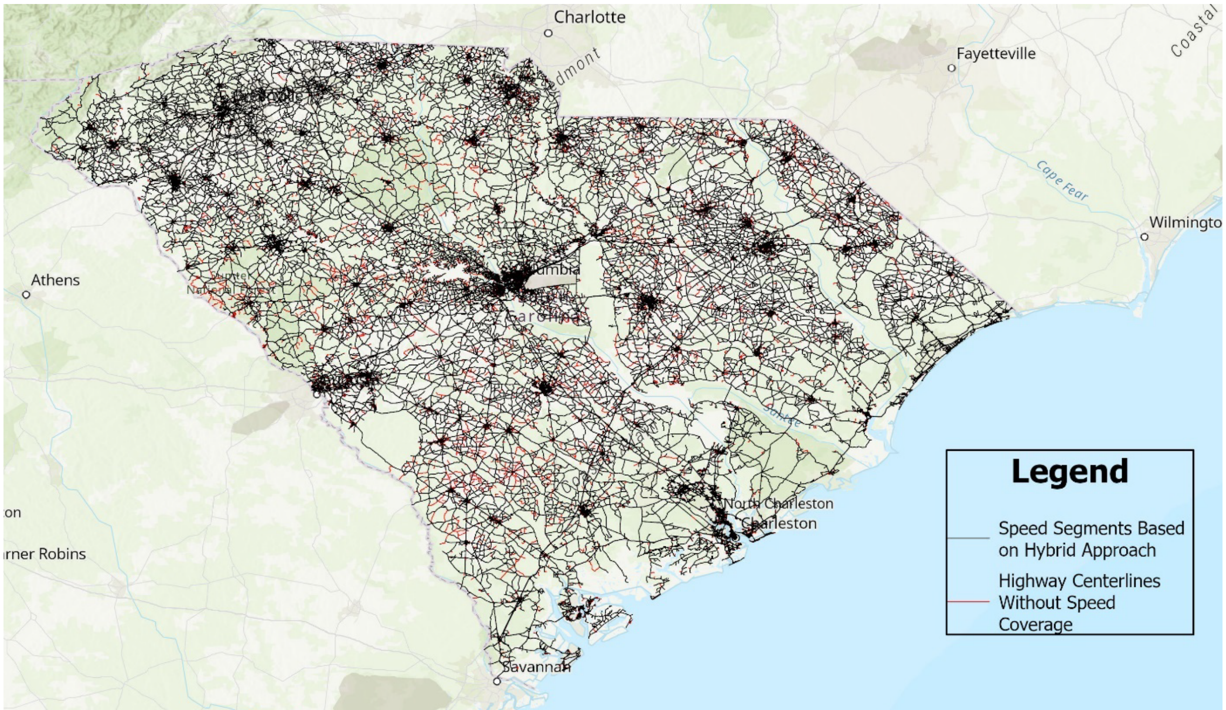

Figure 3-15 Coverage of segments created based on hybrid approach

CHAPTER 4: IDENTIFICATION OF HIGHWAY CURVE ADVISORY SPEEDS

4.1 Workflow for Determining Highway Curve Advisory Speeds

This chapter discusses a GIS-based workflow for determining signing needs and compliance for horizontal curves. The workflow is based on using the design method applied to curve attributes to determine the advisory speed for a curve. The method is similar to the highway information system (HIS) approach discussed in a Kentucky study *(Green et al. 2016)*; however, their method requires the collection of curve parameters using field data collection (e.g., MANDLI) and populating the data within the GIS. The methodology used in this research provides a GIS-based analytic alternative to field collection. The development of this data was discussed in Chapter 3.

A diagram showing the workflow and screening methodology is presented in **Figure 4-1.** The workflow includes data needs, preprocessing, advisory speed calculation, and determining signage requirements. The workflow calculates advisory speed using two variations of the design method: 1) the AASHTO design equation *(Kronicz, 2016)*, and 2) the TTI design equation *(Milstead, 2011)*. The survey indicated that both design equation methods are used to determine advisory speeds depending on a state's preference, adopted procedures, and policies. The advisory speeds are compared to the posted speed limit to determine signage requirements based on MUTCD guidance. A comparison was also made between the advisory speeds and signage requirements of the GIS approach with those determined by Rieker CARS.

The first variation is the AASHTO *(2018)* design equation method, based on equation *4-1* which is generally used to estimate roadway design speed. This equation was also presented in Chapter 2. It is repeated here for clarity.

$$R = \frac{v^2}{15(e+f)} \qquad (4\text{-}1)$$

In this equation, R (feet) is the radius of the curve, v (mph) is the design speed, e (ratio to 1) is the design superelevation rate, and f is the design friction coefficient. If the radius of a curve is known, design speed can be calculated by substituting values for R, e, and f. This equation can also be used for determining highway curve advisory speed *(Glennon et al. 1985; MUTCD, 2023),* which is used in this study along with the posted speed limit to determine highway curve signage requirements. The equation is applied through a batch process in ArcGIS using each of the parameters in equation *4-1* solving for v.

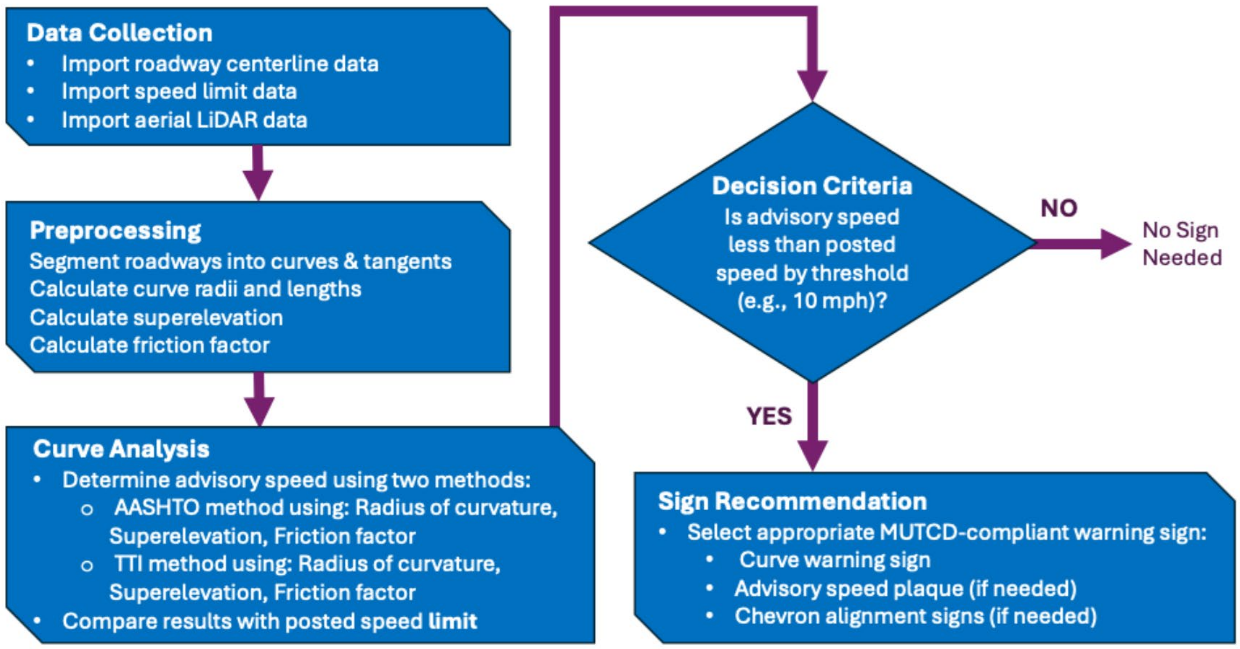

Figure 4-1 Workflow and screening methodology for determining highway curve advisory speeds for South Carolina state highways

The second variation is the TTI design method discussed in *(Milstead, 2011)*. Advisory speed is calculated from the following equation using curve design parameters (radius and superelevation). The 85th percentile speed of the tangent approaching the curve is also needed.

$$V_{c,85} = \left(\frac{15.0R_p\,(0.196 - 0.00106V_{t,85} + 0.000073V^2_{t,85} - 0.0150\mathrm{I}_{tk} + e/100)}{1 + 0.00109R_p} \right)^{0.5} \qquad (4\text{-}2)$$

R_p = travel path radius, ft;

$V_{c,85}$ = 85th percentile curve speed, mph, which is the suggested advisory speed;

$V_{t,85}$ = 85th percentile tangent speed, mph;

e = superelevation rate, percent;

I_{tk} = indicator variable for trucks (= 1.0 if model is used to predict truck speed; 0.0 otherwise)

For this research, truck speeds are used for determining the TTI design method advisory speeds, which is the suggested approach *(Milstead, 2011)*.

4.2 Selecting Curves

Curved roads for a state are vast and include everything from meandering roads in neighborhoods to realignments at intersections. Filtering of curve data is necessary to facilitate identification of curves requiring signage based on MUTCD. The GIS is ideally suited for this sort of filtering. For neighborhoods, signs with a speed limit of less than 30 mph can be filtered out because advisory speeds are rarely less than 20 mph.

Filtering curves based on length of curve is tricky. The AASHTO Greenbook recommends the minimum length of curve to be $L_{min} = 15\ V$ where V is design speed. A minimum design speed of 20 mph gives a 300-foot minimum length of curve. Choosing this number as a threshold will remove curves in mountainous terrain that should be included. **Figure 4-2** shows a location in a mountainous region of South Carolina with multiple curves less than 300 ft long. The highlighted curve is just over 100 ft. Thus, to be conservative we chose a minimum curve length of 100 ft to filter out curve fragments while leaving short curves in mountainous regions.

Curves with a radius of greater than >1500 were also removed. This is because the advisory speed for a 1500 ft radius curve is likely greater than 60 MPH depending on superelevation. Because the maximum speed limit of any road in the state is 70 MPH, there will be no curves with that magnitude of radius that would require curve signage.

Figure 4-2 Section of road in SC with tight curves. The highlighted curve has a length just over 100'

4.3 Design Equation Attributes

4.3.1 Curve Attributes

The curve attributes required by the methodologies include curve radius and superelevation. The statewide curve radius data was derived from two different methodologies (Rieker CARS and GIS-based automated method) and discussed in **Section 3-2**. Both methods were needed because the Rieker data were only available for a subset of roads.

Section 3-3 discussed the development of a superelevation database using aerial LiDAR data. This database was conditionally used in the methodologies depending on the magnitude of superelevation. Typical maximum superelevation values in South Carolina are 8% for higher speed roads. To be conservative, the aerial LiDAR value was used if the curve's superelevation was less than 4% and a value of 4% was used where the LiDAR value was greater than 4%. This conservative value was determined from the literature and through discussions with SCDOT engineering support services.

4.3.2 Friction Coefficient and Tangent 85th Percentile Speed

The highway curve side friction factor used in the AASHTO design equation method is based on driver comfort thresholds rather than the impending point of skidding. The factor varies with design speed and can be determined from AASHTO design guidelines *(2018)*. In this study, the side friction factor used is based on the posted speed limit, which is conservative unless the advisory speed is greater than the posted speed limit. In the latter case, curve warning signs will not be mandated regardless of the side friction factor used.

The tangent 85^{th} percentile speed is used in the TTI design method to determine highway curve advisory speed. The TTI design method allows the use of posted speed limit as the tangent 85^{th} Percentile speed. SCDOT has limited posted speed limit data in their road characteristics database. **Section 3-4** discusses how a posted speed limit database was developed as part of this project. This was the data that served as the tangent 85^{th} percentile speed used in the TTI design method and also to represent posted speed limits to determine signage requirements.

4.4 Identification of Horizontal Curve Advisory Signage using GIS

The algorithm was run for two different data stratifications. The first stratification was all of the selected curves based on the discussion in **Section 4-2**. This resulted in over 40,000 curves. The second stratification was the Rieker data set of approximately 9000 curves. This was done so that a direct comparison of advisory speed can be made between the Rieker data and the GIS generated advisory speeds. In practice, advisory speeds are typically rounded down to the nearest 5 mph increments. For comparison purposes, rounding was not done here.

4.4.1 Comparison of GIS Generated Advisory Speeds with the Rieker Speeds

Figure 4-3 shows a comparison of the GIS generated advisory speeds based on the AASHTO design equation and the Rieker advisory speeds. The graph includes a model that predicts the Rieker advisory speeds from the AASHTO design equation. A perfect model would have a y intercept of 0, a coefficient of 1, and no residuals. For this model, the constant is statistically significant even though it is only -0.0942 mph. The coefficient is 1.0297. Even though there are clearly residuals, the model itself is nearly ideal if two datasets are the same. The R^2 is 0.8427. There are some notable outliers in the graph. One outlier occurs where the AASHTO design equation advisory speed is 70 mph while the Rieker advisory speed is 22 mph. The curve radius is 1192 ft indicating that the Rieker advisory speed is artificially low. The posted speed limit is only 25 mph which has a higher corresponding friction coefficient resulting in a higher advisory speed. The modeling approach allows for artificially high advisory speeds due to the friction coefficient if the advisory speed is greater than the posted speed limit. The friction factor is conservative if the advisory speed is less than the posted speed limit which is appropriate for curve signage requirements.

Figure 4-4 shows a comparison of the GIS generated advisory speeds based on the TTI equation for trucks and the Rieker advisory speeds. The graph includes a model that predicts the Rieker advisory speeds from the TTI design equation. For this model, the y intercept is -11.083 and the coefficient is 1.4223. The R^2 is 0.8359. The graph shows that the TTI advisory speeds are systematically higher than the Rieker advisory speeds when the TTI advisory speeds are lower than 50 mph.

Figure 4-5 shows a comparison of the GIS generated advisory speeds based on the AASHTO design equation and the TTI equation advisory speeds. The graph includes a model that predicts the TTI equation advisory speeds from the AASHTO design equation. For this model, the y intercept is 12.34 and the coefficient is 0.6269. The R^2 is 0.756. The graph shows that the TTI advisory speeds are systematically higher than the AASHTO advisory speeds when the TTI advisory speeds are lower than 40 mph.

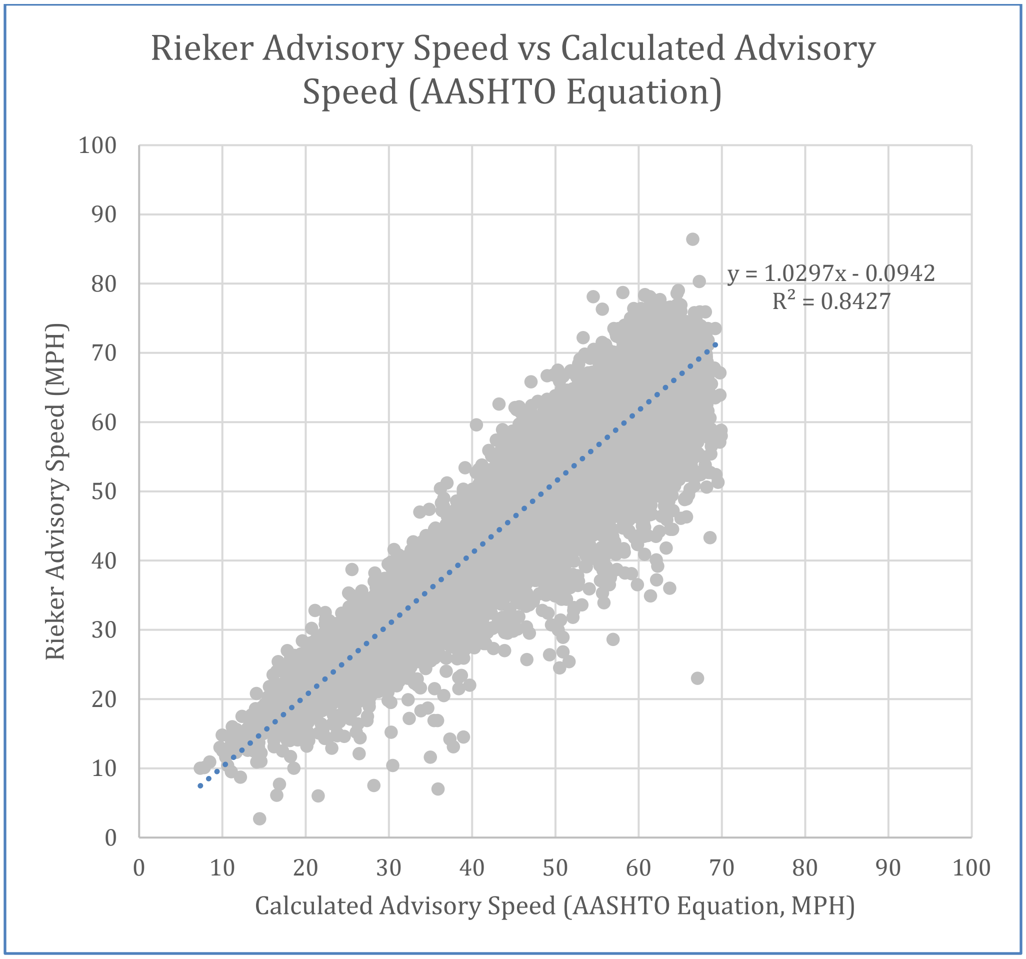

Figure 4-3 Rieker minimum advisory speed vs GIS generated advisory speed (AASHTO)

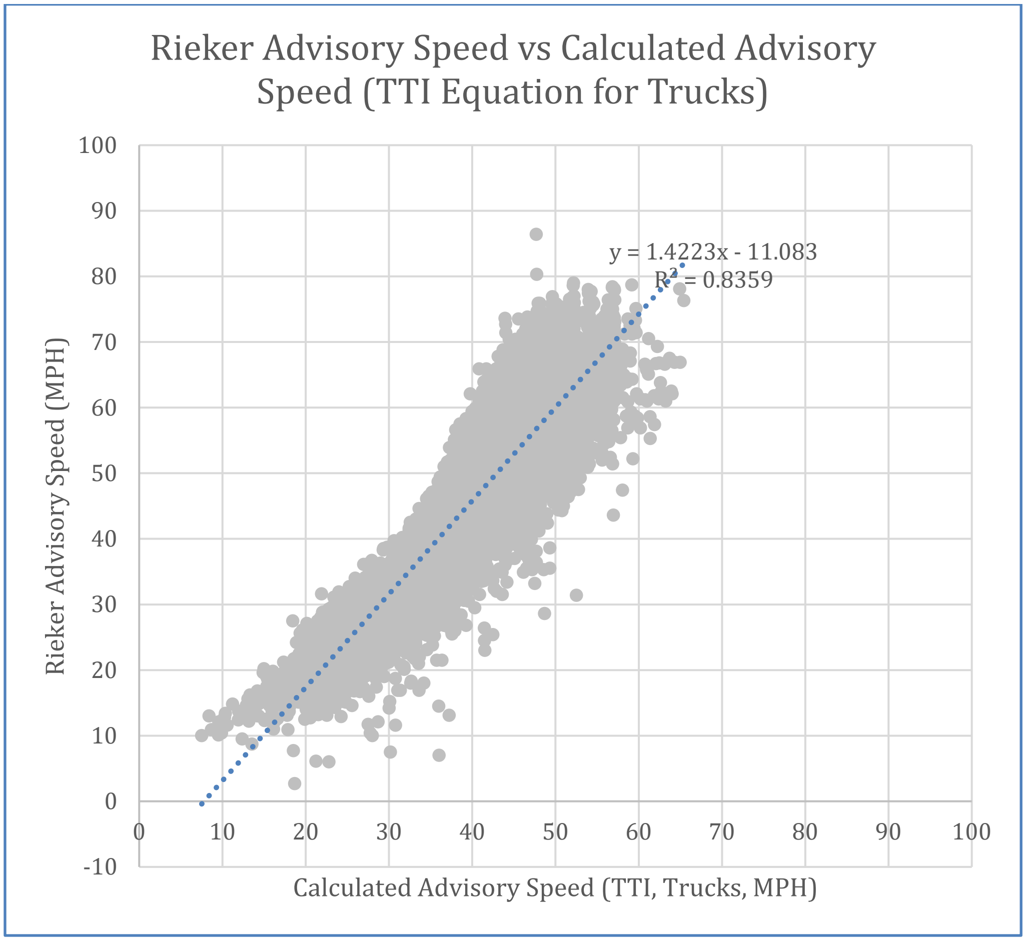

Figure 4-4 Rieker minimum advisory speed vs GIS generated advisory speed (TTI)

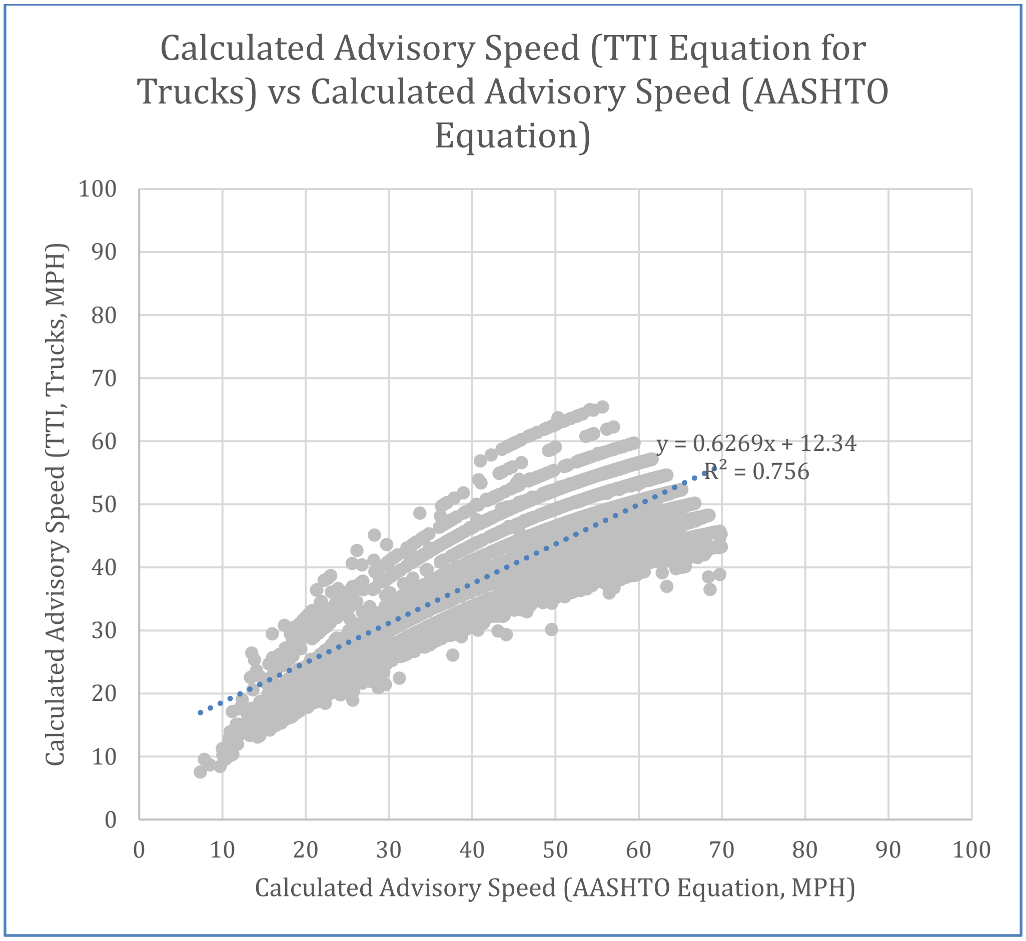

Figure 4-5 GIS generated (TTI) vs GIS generated advisory speed (AASHTO)

A paired samples t-test presented in Table 4-1 indicates that a statistically significant difference exists between each combination of AASHTO advisory speed, Rieker minimum advisory speed, and TTI advisory speed.

Table 4-1 Paired t-test results of the comparison between advisory speed methods

	Mean	Std. Deviation	Std. Error Mean	t	df	Two-Sided p
AASHTO - Rieker_Minimum_Advisory_Speed	-1.32	5.71	0.05	-24.08	10893	0.00
AASHTO - TTI (Trucks)	5.40	6.60	0.06	85.33	10893	0.00
Rieker_Minimum_Advisory_Speed - TTI (Trucks)	6.72	7.00	0.07	100.10	10893	0.00

The mean absolute percentage deviation (MAPD) is a common metric of model prediction accuracy. It is especially useful in this comparative analysis because it is easily understood irrespective of the magnitude of the speed. As previously established in Equation *4-3*.

$$MAPD = \frac{100}{n}\sum_{t=1}^{n}\left|\frac{A_t - F_t}{A_t}\right| \qquad (4\text{-}3)$$

Where:

- n is the number of fitted points;
- A_t is the reference value for observation t;
- F_t is the forecasted or comparison value.

The MAPD between the AASHTO equation advisory speeds and the Rieker equation advisory speeds is 9.4%. The MAPD between the Rieker and the TTI advisory speeds is 14.8% and between the AASHTO and TTI advisory speeds is 14.3%.

4.4.2 Comparison of GIS Generated Advisory Signage with SCDOT Actual Signage

The primary use of the calculated advisory speed is to determine applicable usage of traffic control devices related to horizontal alignment based on MUTCD guidelines. **Figure 4-6** shows two tables from the 2023 MUTCD summarizing the sign requirements and recommendations based on the difference in advisory speed and posted speed limit, traffic volumes, and roadway functional class. For local roads, curve signage is not mandated regardless of the speed difference. Roads with pavement markings and an AADT less than 4000 also do not require curve signage. For comparison, the 2009 MUTCD used a hard cutoff of 1000 AADT for mandating horizontal-alignment signs. Below 1000 AADT, it is based on engineering judgement.

Rieker data was collected in South Carolina in 2019 and was available for approximately 25,000 curves. Out of those 25,000 curves, mandated signage was identified for about 3000 curves based on 2009 MUTCD standards. **Table 4-2** shows the results of a comparison between the Rieker required sign data and the actual signage at the corresponding curves. SCDOT maintains a sign inventory that includes GPS locations of each sign along with the sign type, the year installed, and the facing direction. The researchers geocoded the signs into the GIS. Then, a buffer was created about each curve and overlaid with the signs to assign each sign to a corresponding curve. The facing direction of the sign was also considered. The coding system used in the table is as follows:

0 No signage
1 Curve warning sign
2 Curve warning sign and advisory speed sign
3 Curve warning sign, advisory speed sign, and chevron signs
4 Only chevron signs
5 Only advisory speed sign
6 Chevon signs and advisory speed sign
7 Chevron and curve warning signs

Table 4-2 shows that the vast majority of the curve locations that required signs based on Rieker data did not actually have signs. For example, the Rieker data indicated that 2,228 locations required a curve warning sign, an advisory speed sign, and chevron signs (code 3). Based on the SCDOT sign inventory, 171 of the locations actually had the required signage. A closer look indicated that the primary reason for this is that the Rieker speed limit data used to determine the difference between speed limit and advisory speed was not correct in the majority of the locations and was usually much higher than the actual posted speed limit. Thus, the calculated differences in speeds were much higher than they should have been resulting in the excessive number of required signs.

Table 2C-4. Application of Traffic Control Devices for Changes in Horizontal Alignment

A - Determination of the Need for Devices for Changes in Horizontal Alignment[1]

Roadway Type	AADT			
	Less than 1,000	1,000-2,999	3,000-3,999	Greater than 3,999
Freeways and Expressways	Required	Required	Required	Required
Arterial or Collector without Pavement Markings	Optional	Recommended	Required	Required
Arterial or Collector with Pavement Markings[2]	Optional	Recommended	Recommended	Required
All other roadways	Optional	Optional	Optional	Optional

[1] If devices are determined to be needed, the selection of the device(s) is based on Chart B below.

[2] An arterial or collector is considered to have pavement markings when either a center line, edge lines, or both are present.

B - Selection of Devices for Changes in Horizontal Alignment

Speed Differential[3]	Devices for Change in Horizontal Alignment[3]
5 mph	Pavement markings or advance horizontal alignment warning sign on paved roadways. Advance horizontal alignment warning sign on unpaved roadways.[4]
10 mph	Advance horizontal alignment warning sign
15 mph	Delineators[5] and advance horizontal alignment warning sign
20 mph or more	Chevrons[5] and advance horizontal alignment warning sign

Table 2C-6. Use of Advisory Speed Plaque for Horizontal Alignment Changes

Speed Differential	Use of Advisory Speed Plaque (W13-1P)[1]
5 mph	Optional
10 mph	Recommended
15 mph or more	Required

[1] See Section 2C.59

Figure 4-6 MUTCD Curve signage selection criteria (6)

Table 4-2 Curve comparison of Rieker required sign locations compared to field inventory sign data

		Existing Signs (Inventory)							
Standard	Inventory	0	1	2	3	4	5	6	7
Rieker MUTCD 2009	0	0	0	0	0	0	0	0	0
	2	407	51	203	53	28	20	6	7
	3	1392	105	407	171	89	33	7	24

Table 4-3 shows a comparison between the actual highway curve sign inventory and the GIS-generated required signage based on the AASHTO design equation and the TTI equation for locations that the Rieker data indicated that signs were required. This data includes recalculated Rieker requirements based on the Rieker advisory speed but corrected speed limit data. Both 2009 and 2023 MUTCD selection criteria are used. The table shows that results for each method are comparable. Results also show that there are many fewer required sign locations based on the 2023 MUTCD criteria. That is because of the higher AADT threshold in the 2023 MUTCD, as well as local roads not being required in the 2023 MUTCD.

Table 4-3 Curve comparison of field inventory signage w/AASHTO, TTI, adjusted Rieker

		Existing Signs (Inventory)							
Standard		0	1	2	3	4	5	6	7
MUTCD 2009 AASHTO	0	1395	141	517	167	86	49	10	26
	2	116	3	45	30	16	3	2	2
	3	278	12	48	27	15	1	1	3
MUTCD 2023 AASHTO	0	1606	153	587	209	113	51	13	29
	1	55	2	8	8	1	1	0	1
	2	44	1	4	5	3	1	0	0
	3	84	0	11	2	0	0	0	1
MUTCD 2009 TTI	0	1454	143	540	181	96	51	11	27
	2	161	3	33	27	14	1	2	2
	3	174	10	37	16	7	1	0	2
MUTCD 2023 TTI	0	1631	154	591	212	114	52	13	30
	1	74	1	6	7	2	0	0	0
	2	32	1	6	4	1	1	0	1
	3	52	0	7	1	0	0	0	0
MUTCD 2009 Rieker Advisory	0	1407	139	521	169	92	50	10	24
	2	133	5	43	25	10	2	1	5
	3	249	12	46	30	15	1	2	2
MUTCD 2023 Rieker Advisory	0	1610	152	583	209	113	52	11	29
	1	60	3	12	7	2	0	1	1
	2	44	1	7	7	2	1	1	1
	3	75	0	8	1	0	0	0	0

The researchers also looked at GIS generated sign requirements for the large stratification of 41,420 highway curves in South Carolina. The stratification was discussed previously and includes curves with a radius of less than 1500’ and length of greater than 100’. **Table 4-4** shows a comparison of the SCDOT sign inventory with the GIS generated required signage for all curves in the large stratification. The table indicates that South Carolina has a vast number of curve locations that have signage even though the MUTCD does not require them based on the GIS screening approach using the AASHTO and TTI equations. They may be recommended but that threshold was not checked. Further, both the 2009 and 2023 MUTCD allow DOTs and municipalities discretion for the usage of curve signage based on engineering judgement.

Table 4-4 Curve comparison of field inventory signage w/AASHTO, TTI (expanded dataset)

		Existing Signs (Inventory)							
Standard	Inventory	0	1	2	3	4	5	6	7
MUTCD 2009 AASHTO	0	25070	3734	8537	794	526	872	71	154
	2	393	28	132	62	40	8	5	7
	3	698	37	103	77	49	11	3	9
MUTCD 2023 AASHTO	0	28092	3991	9211	926	607	904	78	168
	1	171	8	16	8	7	3	1	2
	2	106	3	9	7	4	3	0	0
	3	213	2	12	2	3	4	0	1
MUTCD 2009 TTI	0	25311	3744	8612	824	552	877	75	158
	2	402	29	90	59	34	5	2	5
	3	448	26	70	50	29	9	2	7
MUTCD 2023 TTI	0	28202	3996	9221	929	612	905	79	170
	1	173	4	12	8	6	3	0	0
	2	81	2	8	5	2	3	0	1
	3	126	2	7	1	1	3	0	0

4.4.3 Discussion of Comparative Results

The comparative analysis shows that the GIS screening method for determining highway curve advisory speeds using the AASHTO equation yields a close prediction to the advisory speed generated with the Rieker methodology (intercept of a linear fit close to 0, coefficient close to 1, $R^2 = 0.84$; absolute value of the difference in means < 1.5 mph [although statistically significant]). Direct substitution of the advisory speed generated by the TTI equation for the advisory speed would be less successful (intercept of a linear fit close to -11, coefficient close to 1.4, $R^2 = 0.83$; absolute value of the difference in means > 6.5 mph [statistically significant]) are comparable to the Rieker methodology. The TTI equation predicts higher advisory speeds than the others for advisory speeds under 50 MPH for Rieker and under 45 MPH for AASHTO. The SCDOT sign inventory indicates that over 99% of highway curve advisory speed signs actually in use in the state are 45 MPH or less as shown in **Figure 4-7**.

As far as MUTCD mandated signage, the GIS screening method using the AASHTO equation produces nearly identical results to the recalculated Rieker signage requirements using both 2009 and 2023 MUTCD criteria. This is not surprising considering the similarity between the advisory speeds of the AASHTO equation and those generated by Rieker. **Figure 4-8** shows a revised version of Figure 4-3 with data points color coded if the advisory speed is less than the posted speed limit by at least 10 MPH which mandates signage. The grey points require no signage.   The green points require signage based only on the AASHTO design equation. This occurs predominately where the Rieker advisory speeds are significantly higher than the AASHTO speeds. Conversely, the orange points require signage based only on the Rieker advisory speeds. The blue points require signage based on both approaches. The TTI equation which predicts 85th percentile truck curve speed is less conservative than the AASHTO and Rieker methods, and has signage requirements universally lower than both the AASHTO and Rieker methods.

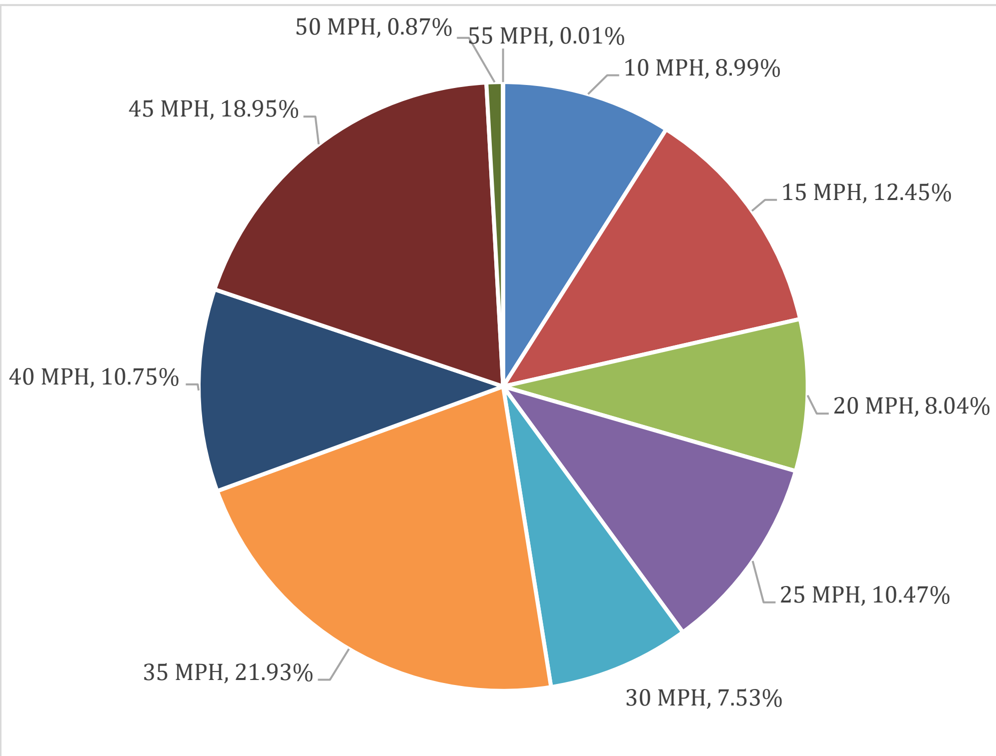

Figure 4-7 Breakdown of advisory speed signage in South Carolina

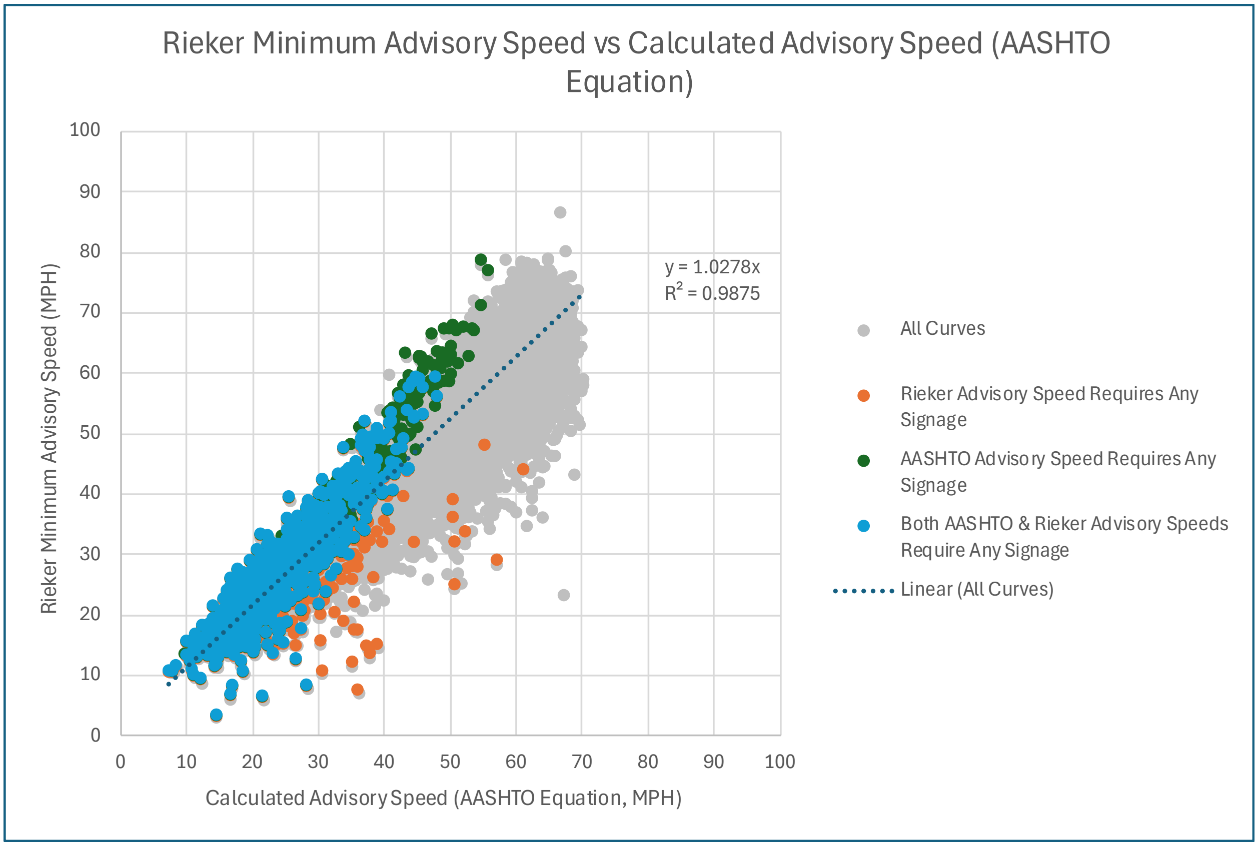

Figure 4-8 Rieker and AASHTO advisory speeds with corresponding signage requirement

4.5 Using the Results

A list of locations in South Carolina that potentially meet curve signage requirements but do not have signage has been provided to SCDOT in a digital file. A field study should be conducted to verify their need based on the MUTCD criteria and engineering judgement. Crash history should also be considered to determine the appropriateness of the existing signs and the possible need for additional signs. **Figure 4-9** shows a location in which curve warning signs are mandated based on the Rieker and AASHTO design methodologies but is not mandated based on the TTI equation. Because the TTI equation is an acceptable method from a compliance standpoint, it would be at the discretion of SCDOT to determine if signage is needed. This assumes that the generated radius and superelevation data are representative of the curve.

Figure 4-9 Curve location that meets mandatory sign requirements based on two out of three methods

CHAPTER 5: SAFETY ANALYSIS OF HIGHWAY CURVES

5.1 Introduction

Most of the studies that have analyzed crash frequency on curves have been limited to samples. In this chapter, we look at a statewide screening methodology for analyzing geometric factors influencing crashes on the population of curves on two lane roads in South Carolina. Using the innovative data sources discussed in Chapter 3 combined with crash data, models are developed to predict crashes on curves based on geometric factors, traffic volume, and posted speed limits. Finally, CMFs are estimated for an array of changes in the parameters studied.

5.2 Preparing for the Safety Analysis

5.2.1 Populating Data into GIS

The Highway Safety Manual and subsequent curve prediction models in the literature have effectively established radius, length of curve, and superelevation as significant factors in the determination of crash outcomes. Due to a significant correlation between radius and length of curve if the deflection angle is consistently applied, only radius and superelevation are included in the model parameters and length is not. Given findings of significance of downhill grades per (*Bauer and Harwood, 2014)* and (*Saleem and Persaud, 2017)*, grade is also considered. Beyond these variables, numerous parameters were also available from the RIMS data.

Radius data was discussed in **Section 3-2** and superelevation and grade data were discussed in **Section 3-3**. The direction of the grade was also captured from the aerial LiDAR data and was recorded in terms of the center line mile markers. Positive grades go uphill in relation to increasing mile markers. Conversely, downhill grades in relation to increasing mile markers are negative. Other curve attributes important to the analysis include AADT, functional class from RIMS, and posted speed limit (**Section 3-4**).

5.2.2 Selecting and Stratifying Curves

Curves were filtered based on radius as discussed in **Section 4-2**. Because of the very different contributing factors of crashes at intersections, curves within 300 ft of intersections were filtered.

Part C of the HSM *(2010)* provides predictive models for estimating expected average crash frequency at an individual site based on Safety Performance Functions (SPFs). SPFs exist for numerous road group types, so the first step in HSM analysis requires determination of the road group type for each segment. The HSM road groupings have been used in this project to classify the various roadway segments for analysis purposes. The roadway segments are grouped based on either rural or urban environments, number of lanes, and median type. In **Table 5-1**, roadway group types were identified using three characters. The first character (R or U) describes the rural or urban environment (land use context), the second character (2, 3, 4, or 5) describes the number of lanes and the last character (D, U, T) shows the median type which is either divided or undivided or two way left turn lane. The number of curves of each type used in the analysis is shown in the last column in **Table 5-1**. The apparent lack of curves in some of the road groups is because of the filtration process. Thus, the research focuses on models for R2U and U2U which have sufficient sample sizes.

Table 5-1 Roadway group types and definition in Highway Safety Manual, 2010

Road Group Type	Description	Rural/ Urban	Number of Lanes	Divided/ Undivided	# of curves
R2U	Rural two-lane undivided	Rural	2	Undivided	14561
R4D	Rural four-lane divided	Rural	4	Divided	19
R4U	Rural four-lane undivided	Rural	4	Undivided	8
U2U	Urban two-lane undivided	Urban	2	Undivided	3061
U3T	Urban 2+TWLTL* lane	Urban	2+TWLTL*	Undivided	70
U4D	Urban four-lane divided	Urban	4	Divided	16
U4U	Urban four-lane undivided	Urban	4	Undivided	11
U5T	Urban 4+TWLTL* lane	Urban	4+TWLTL*	Undivided	56
*TWLTL = Two Way Left Turn Lane					

5.2.3 Crash Preprocessing and Assigning Crashes to Curves

Eight years of crash data from 2017-2024 was used in the analysis (**Section 3-1**). The preprocessing of crashes is also discussed in **Section 3-1**. Adding crash information to curves was accomplished by first assigning crashes to curves and then joining the crash data to the curve. The researchers used a GIS approach to assign crashes to curves. A buffer was created around each curve that extended 100 ft before and after the curves. This was done to try to capture vehicle crashes that may have been related to the curve but traveled beyond it before coming to a stop. Crashes within the 100 ft curve buffer and on the same route were linked to that curve (**Figure 5-1)**.

Figure 5-1 Associating crashes with curves using a curve buffer

5.3 Safety Analysis using GIS

5.3.1 Statistical Analysis of Curve Crashes

In this section, models are developed to predict the contribution of individual curve characteristics to crash incidence and determine the statistical significance of this contribution. The stratification of the highway curves is the same as discussed in the previous section. Models were only developed for the R2U and U2U stratifications because of their sample size. R2U roads have the most mileage in the state and the highest percentage of curves.

Vehicle crashes are random, discrete, and non-negative. As such, commonly used models to study traffic crashes are the Poisson and negative binomial regression models. Another reason for their popularity is their ability to identify effectively a broad range of risk factors for crashes and thus provide valuable information for traffic engineers to select mitigation measures. Between the Poisson and negative binomial models, the Poisson model was deemed not appropriate for this study because the mean and variance of the crashes-per-highway curve distribution are not approximately equal. For this reason, the negative binomial regression model is employed to identify geometric parameters and other characteristics that affect curve-related crashes. The negative binomial model is shown in Equation 5-1 below.

$$\ln \lambda_i = \beta X_i + \varepsilon_i \qquad (5\text{-}1)$$

where:

λ_i is the expected number of crashes for curve *i*,

X_i is a vector of explanatory variables,

β is vector of estimable coefficients, and

$\exp(\varepsilon_i)$ is a gamma-distributed error term with mean one and variance α.

The negative binomial estimation results of crashes for R2U and U2U are shown in **Table 5-2**. The first column in the table shows the final model variables. It is noteworthy that superelevation is not included because its impact on model performance was not significant. Column 2 shows the variables' estimated coefficients. A positive coefficient is interpreted as increasing crashes and a negative coefficient as decreasing crashes. The third column shows the standard errors for the regression coefficients. The last column shows p-values for the null hypothesis that an individual predictor's regression coefficient is zero, given that the rest of the predictors are in the model.

Note that the coefficients for the variables are very similar indicating that both R2U and U2U have similar crash performance. The negative coefficients for radius indicate that an increase in radius will decrease crashes. Conversely, an increase in posted speed limit will result in increased crashes. For R2U, the absolute value of grade is significant and has a negative coefficient. This indicates that a steeper grade, either uphill or downhill results in a reduction of crashes. This is counter intuitive for downhill where literature has shown that downhill curve sections of have a higher proportion of run-off-the-road crashes *(Baur and Harwood, 2014)*. The absolute value of grade was used because, for multicar crashes, it may not be clear the direction of travel of the vehicle at fault. Because of this, the researchers decided to develop a model for single car crashes and used actual grade in the direction of travel to see the effects of grades on crash experience.

Table 5-2 Negative binomial estimation results for crashes on curves (R2U right, U2U left)

R2U Total Crashes	N=14561			U2U Total Crash		N=3061	
Parameter Estimates				Parameter Estimates			
Parameter	B	Std. Error	Sig.	Parameter	B	Std. Error	Sig.
(Intercept)	-5.793	0.1166	<.001	(Intercept)	-5.352	0.1817	<.001
lnAADT	0.754	0.0137	<.001	lnAADT	0.704	0.0215	<.001
Abs_Grade	-0.014	0.0069	0.042				
Speed_Limit	0.026	0.002	<.001	Speed_Limit	0.027	0.004	<.001
Radius	-0.001	4.33E-05	<.001	Radius	-0.001	7.15E-05	<.001

Because of the similarity of the estimates for R2U and U2U curves in **Table 5-2**, the researchers decided to combine the data. **Table 5-3** shows the negative binomial estimation results after combining the R2U and U2U curve data. The estimates are again very similar to the estimates in **Table 5-2**. The absolute value of grade was included in the analysis however it was not significant for the combined dataset and is therefore not shown in the table. With regard to the constant, it indicates that the expected number of crashes is zero over 8 years. (actual value for λ_i is 0.00331; ln(0.00331) = -5.711). Lastly, it is noted that the dispersion parameter for the negative binomial is significantly greater than 0, and thus, indicating that the negative binomial model is more suitable than the Poisson model for analyzing curve crashes.

Table 5-3 Negative binomial estimation results combined (R2U and U2U)

N = 17622		Total crashes		
Parameter Estimates				
Parameter	B	Std. Error	Sig.	Exp(B)
(Intercept)	-5.711	0.0962	0.000	0.003
lnAADT	0.759	0.0106	0.000	2.136
Abs_Grade				
Speed_Limit	0.024	0.0016	0.000	1.024
Radius	-0.001	3.6312E-05	0.000	0.999

The safety performance function for combined R2U and U2U that predicts crashes on curves as a function of volume is shown in **Figure 5-2**. This SPF is based on the negative binomial model presented earlier that is solved for different AADT values. It assumes mean values of the significant variables. The SPF applies to curves less than 1500' radius and beyond 300' from any intersection.

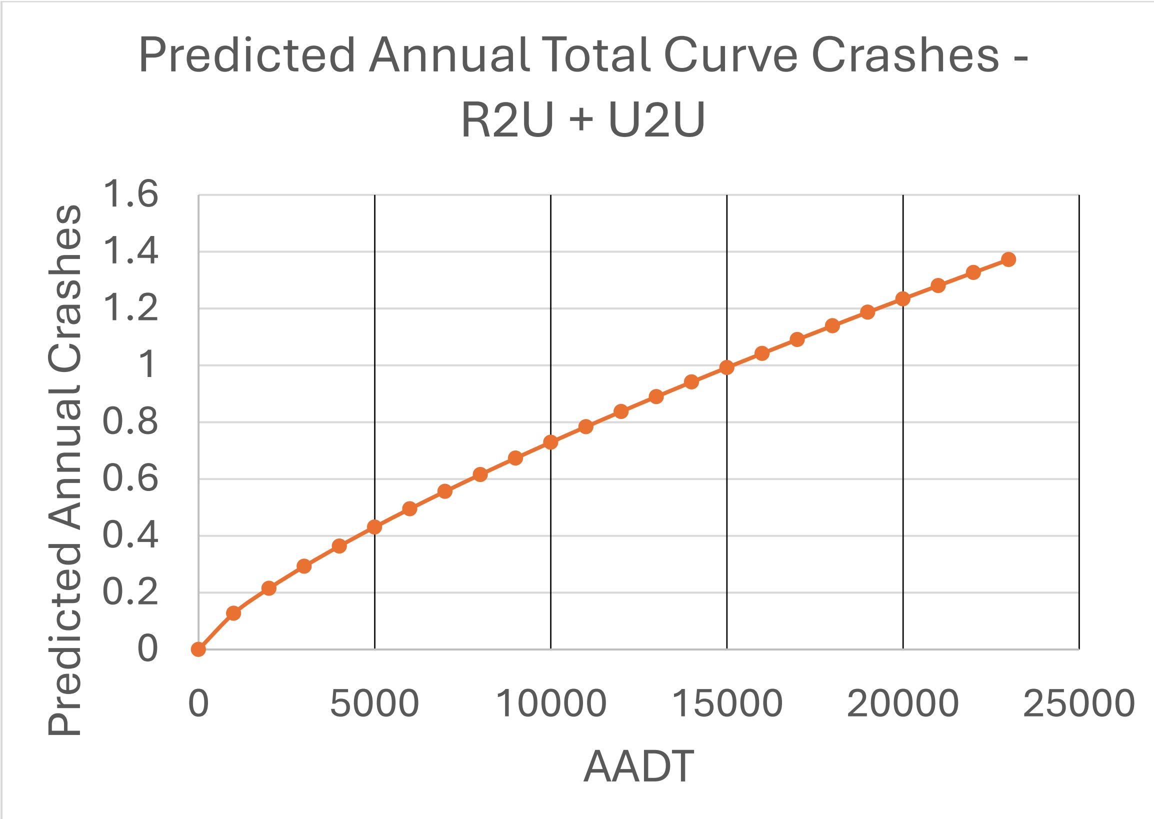

Figure 5-2 SPF for R2U and U2U curves

5.3.2 <u>Development of Crash Modification Factors</u>

Crash modification factors (CMFs) capture the relationship between a change in a specific highway geometric design element (e.g., curve radius) and safety. It is a multiplicative factor or function used to compute the expected number of crashes after implementing a given countermeasure at a specific site. Thus, given a CMF, this value would be multiplied by the expected crash frequency prior to treatment. A CMF greater than 1.0 indicates an expected increase in crashes, while a value less than 1.0 indicates an expected reduction in crashes after implementation of a given countermeasure. For example, a CMF of 0.9 indicates an expected safety benefit; specifically, a 10% expected reduction in crashes. On the other hand, a CMF of 1.1 indicates an expected degradation in safety; specifically, a 10% expected increase in crashes.

This study estimates the CMFs directly from the coefficients of the developed negative binomial model, as proposed by (*Lord and Bonneson, 2023*). This approach of estimating CMFs assumes that each model variable is independent and, thus, not influenced by the value of any other variable. It also assumes that the relationship between the change in the variable value and the change in crash frequency is exponential (as indicated by the negative binomial model). The CMFs are estimated using Equation 5-2 as follows.

$$CMF_j = e^{\left(\beta_j \times \left(x_j - y_j\right)\right)} \qquad (5\text{-}2)$$

Where:

x_j = range of values or a specific value investigated (e.g., radius, grade, etc.) for CMF_j;

y_j = baseline conditions or average conditions for the variable x_j (when needed/available); and

β_j = regression coefficient associated with the variable *j*.

The following sections present derived crash modification factors for the statistically significant parameters using Equation 5-3 for crash modification factors based on curve radius, R, and Equation 5-4 for Speed Limit.

<u>Curve Radius</u>

$$CMF_R = e^{(-0.001\times(R_a-R_b))} \quad (5\text{-}3)$$

Where

R_a = radius in feet after modification.

R_b = radius in feet before modification.

The CMF is applicable to curve radii of 2-lane roads ranging from 100’ to 1500’ and was developed based on curve data of 17,622 records with a mean radius of 829’. This CMF suggests that increasing the curve radius will decrease crashes. As an example, increasing the radius by 200’ from 400’ to 600’ *(R_a-R_b=200)* will result in a crash reduction of 17.8% (CMF=0.82). **Figure 5-3** shows a graph of how the CMF changes with a corresponding change in radius.

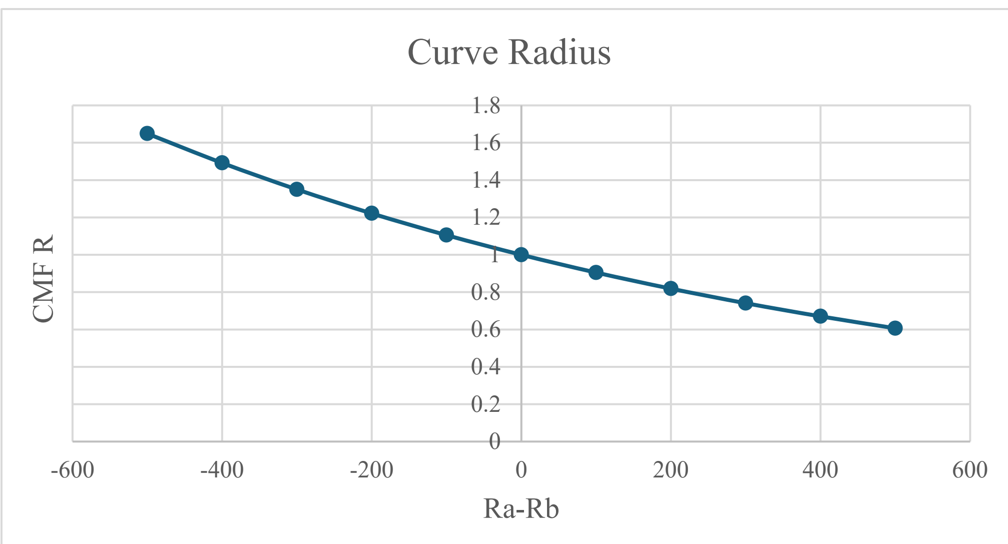

Figure 5-3 CMF for change in radius

<u>Curve Posted Speed Limit</u>

$$CMF_{SL} = e^{(0.024\times(SL_a-SL_b))} \quad (5\text{-}4)$$

Where

SL_a = posted speed limit in MPH after modification.
SL_b = posted speed limit in MPH before modification.

The CMF is applicable to 2-lane roads and was developed based on curve data of 17,622 records with a mean posted speed limit (rounded down to the nearest 5 MPH) of 40 MPH'. This CMF suggests that increasing curve posted speed limit will increase crashes. As an example, decreasing the posted speed limit by 10 mph from 50 mph to 40 mph *(SL_a-SL_b=-10)* will result in a crash reduction of 21% (CMF=0.79). **Figure 5-4** shows a graph of how the CMF changes with a corresponding change in posted speed limit.

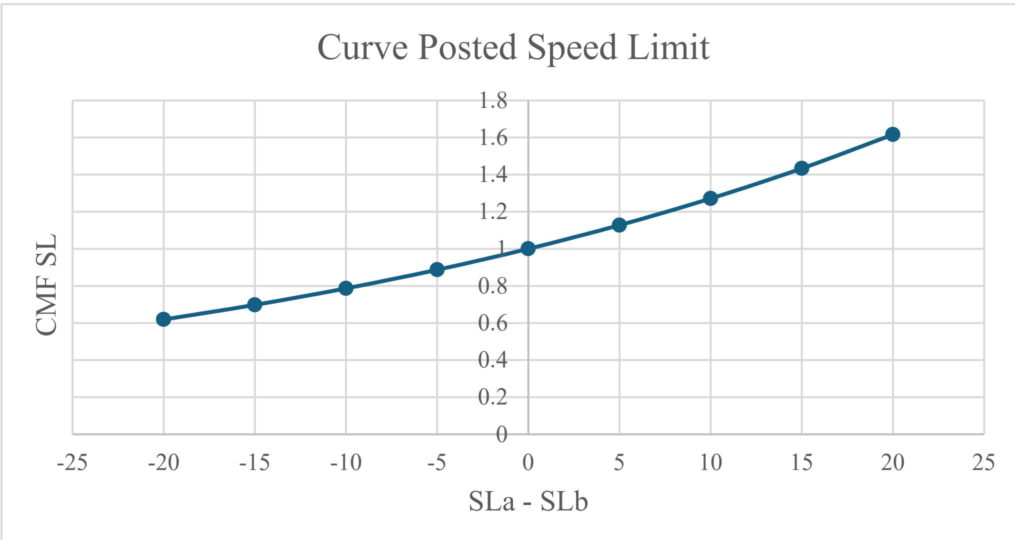

Figure 5-4 CMF for change in posted speed limit

5.3.3 <u>Development of a Crash Modification Factor for Grade</u>

Research has shown that downhill grade can influence run-off-the-road crashes on highway curves. The researchers were interested in developing a CMF to reflect this for single vehicle crashes. Crash reports in South Carolina contain the direction of travel. The researchers used this information and the curve orientation to assign the single vehicle crashes to the downhill or uphill direction of the curve. The curves had to be split by direction, thus doubling the size of the database so that each curve had an uphill record and a downhill record (opposing direction). After assigning crashes to a direction, the researchers created models to predict single vehicle crashes for R2U, U2U, and combined R2U plus U2U curves. Grade was only significant at p=.05 for R2U curves. For U2U, p=0.082. Regardless, the combined model was still used to determine the CMF, as shown in Equation 5-5.

<u>Grade (single vehicle crashes)</u>

$CMF_G = e^{(0.07\times(G_a-G_b))}$ (5-5)

Where
G_a = grade (%) after modification.

G_b = grade (%) before modification.

The CMF is applicable to 2-lane roads and was developed based on curve data of 35,244 records. This CMF suggests that increasing grade will reduce crashes. As an example, increasing grade by 4% from -4% to 0% *(G_a-G_b=4)* will result in a crash reduction of 24.5% (CMF=0.755). **Figure 5-5** shows a graph of how the CMF changes with a corresponding change in grade.

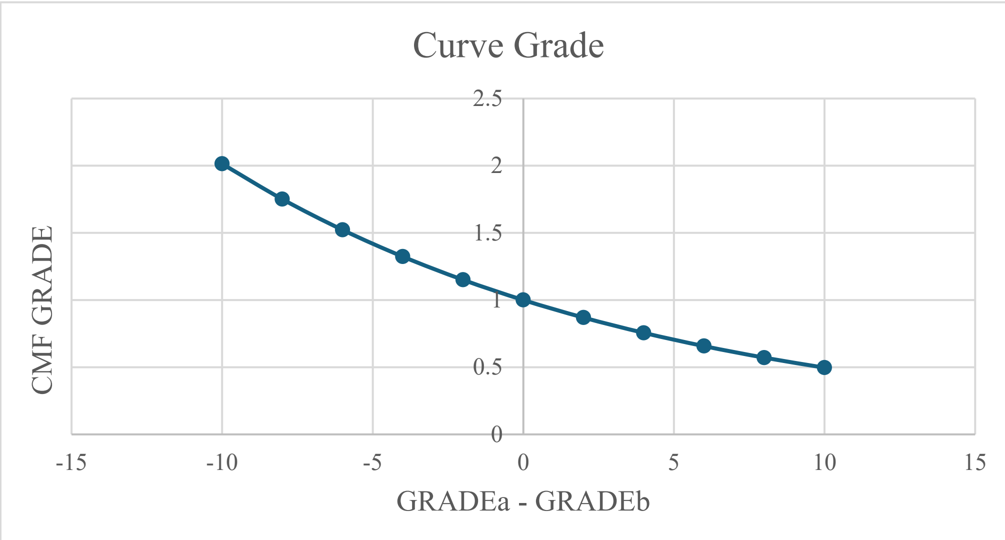

Figure 5-5 CMF for change in grade

5.3.4 Crash Severity

The researchers also developed a negative binomial model for crash severity. For this analysis, fatal and severe crashes were combined. All crashes were considered—not just single vehicle crashes. **Table 5-4** shows the results of the analysis for R2U and U2U curve sections. A few things to note. First, superelevation is significant for R2U while the absolute value of grade is not. Next, the radius coefficient is the same as the coefficient for all crashes. This indicates that the radius CMF developed for total crashes on curves can also be used for serious crashes.

Table 5-4 Negative binomial estimation results for severe crashes on curves

R2U Total Crashes		N = 14561		U2U Total Crash		N = 3061	
Parameter Estimates				**Parameter Estimates**			
Parameter	B	Std. Error	Sig.	Parameter	B	Std. Error	Sig.
(Intercept)	-9.511	0.4776	<.001	(Intercept)	-9.223	0.7278	<.001
lnAADT	0.704	0.0518	<.001	lnAADT	0.664	0.0831	<.001
Speed_Limit	0.048	0.0084	<.001	Speed_Limit	0.047	0.0145	0.001
Radius	-0.001	0.0002	<.001	Radius	-0.001	0.0003	0.002
Superelevation	-0.031	0.0155	0.043				

Because of the similarities between the model coefficients for R2U and U2U, a combined model was also created to determine a severe crash CMF for the posted speed limit using Equation 5-6.

Curve Posted Speed Limit (Severe Crashes)

$CMF_{SL} = e^{(0.043 \times (SL_a - SL_b))}$ (5-6)

Where
SL_a = posted speed limit in MPH after modification.
SL_b = posted speed limit in MPH before modification.

The CMF is applicable to 2-lane roads and was developed based on curve data of 17,622 records with a mean posted speed limit (rounded down to the nearest 5 MPH) of 40 MPH. This CMF suggests that increasing curve posted speed limit will increase severe crashes at a higher rate than for total crashes. As an example, decreasing posted speed limit by 10 MPH from 50 MPH to 40 MPH *(SL_a-SL_b=-10)* will result in a severe crash reduction of 35% (CMF=0.65). The corresponding crash reduction for total crashes is only 21% (CMF=0.79). **Figure 5-6** shows a graph of how the CMF changes with a corresponding change in posted speed limit.

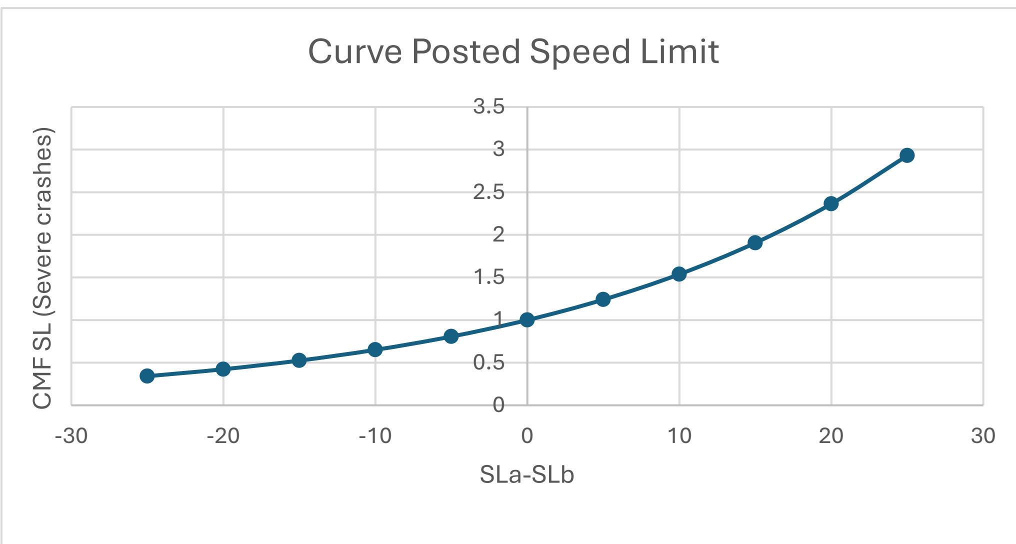

Figure 5-6 CMF for change in speed limit

The model for severe crashes indicates that superelevation is significant for R2U curves. A CMF was developed based on the model, shown in Equation 5-7.

Superelevation (Severe Crashes)

$CMF_{SE} = e^{(-0.031 \times (SE_a - SE_b))}$ (5-7)

Where:
SE_a = Superelevation in percent after modification.
SE_b = Superelevation in percent before modification.

The CMF is for severe crashes and is applicable to 2-lane *rural* roads and was developed based on curve data of 14,561 records with a mean superelevation of 4.29%. This CMF suggests that increasing superelevation will reduce severe crashes. As an example, increasing superelevation from a normal crown of 2% to a typical maximum of 8% *(SE_a-SE_b=6)* will result in a severe crash reduction of 17% (CMF=0.83). **Figure 5-7** shows a graph of how the CMF changes with a corresponding change in superelevation.

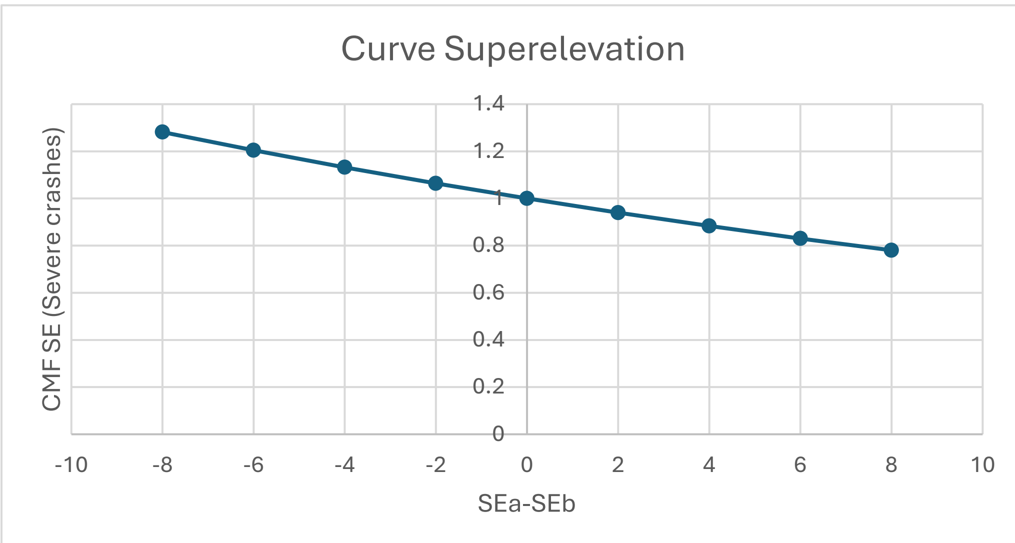

Figure 5-7 CMF for change in superelevation

5.3.5 Summary

This chapter has investigated the relationship between geometric design features of highway curves and the frequency and severity of crashes. The negative binomial crash analysis indicated that traffic volume, radius, and posted speed limit were significant estimators for total crashes, severe crashes, and single vehicle crashes. Grade was significant for single-vehicle crashes. Superelevation was significant for R2U severe crashes. Crash modification factors were developed for all of the significant parameters except for traffic volume.

CHAPTER 6: IDENTIFICATION OF HIGH CRASH LOCATIONS AND COUNTERMEASURE STUDY

6.1 Identification of Curves with the Highest Frequency of Crashes

Using specialized curve buffers discussed in Chapter 5, crashes within 100' feet of curves were associated with each curve for 8 years of crash report data. The researchers identified 200 curves in the R2U and U2U roadway type categories with the greatest frequency of crashes. Each of these curve locations were viewed in Google Earth and Google street view to look at specific curve characteristics including geometry, clear zone, signage, side slopes, and presence of trees. The characteristics of crashes that occurred on each curve were noted.

6.2 Highway Curve Countermeasures

This section discusses potential countermeasures to reduce highway crashes on curves. There is a primary emphasis in this chapter on rural roads. This is because research has shown that rural roads show stronger crash modification factor reductions for most curve countermeasures. This is especially true for curve realignment and guard rail countermeasures due to high rates of run-off-road and fixed object crashes. Urban roads often have lower CMF impact for the same countermeasure due to lower speeds, more congestion, and different crash profiles. Further, the literature shows that CMFs for curves in urban settings are less frequently studied, and results are often site specific.

Tables 6-1 and 6-2 identifies potential countermeasures for R2U and U2U roads respectively. The references and guidance for the countermeasures and crash modification factors are as follows:

1. This research
2. FHWA Rural Roadway Departure Guide
3. FHWA Report # FHWA-21-071
4. CMF Clearinghouse
5. NCHRP Report 641(guidance)
6. MUTCD (guidance)

Typical benefit-cost ratios are from the literature where the benefit is related to a reduction in cost if the crash did not happen or if the severity of a crash is reduced, and cost is related to the cost of implementing the countermeasure. Most countermeasures can be combined with the expected overall effect on safety being a the product of the CMFs.

Table 6-1 Potential countermeasures for R2U roads

Countermeasure	Crash Type	Crash Severity	CMF	Typical B/C	Source
Increase Curve Radius	All crashes	All severities	See Chapter 5	3:1 – 8:1	1
Chevron Alignment Signs	Curve-related crashes	All severities	0.65–0.90	High	3,4,6
Dynamic Curve Warning Signs	Curve-related crashes	All severities	0.87	6:1 – 12:1	3,4
Advisory Speed Signs w/Curve Warning Signs	Curve-related crashes	All severities	0.70–0.87	20:1 – 40:1	4
High-Friction Surface Treatment	Wet-weather curve crashes	All severities	0.65–0.75	20:1 – 60:1	3,4
Shoulder Rumble Strips	Roadway departure	All severities	0.78–0.86	30:1 – 50:1	3,4
Centerline & Shoulder Rumble Strips	Roadway departure crashes	Fatal & injury	0.78	30:1 – 50:1	3,4,5
Install Guardrails (Urban Arterials)	Run-off-road crashes	Fatal & serious injury	0.74–0.85	2:1 – 6:1	4
Safety Edge Treatment	Run-off-road crashes	All severities	0.64	40:1 – 60:1	3
Curve Posted Speed Limit	All crashes	All severities	See Chapter 5	High	1,6

Table 6-2 Potential countermeasures for U2U roads

Countermeasure	Crash Type	Crash Severity	CMF	Typical B/C	Source
Increase Curve Radius	All crashes	All severities	See Chapter 5	3:1 – 8:1	1
Chevron Alignment Signs	Curve-related crashes	All severities	0.65–0.90	High	3,4,6
Dynamic Curve Warning Signs	Curve-related crashes	All severities	0.87	6:1 – 12:1	3,4
Advisory Speed Signs w/Curve Warning Signs	Curve-related crashes	All severities	0.70–0.87	20:1 – 40:1	4
High-Friction Surface Treatment	Wet-weather curve crashes	All severities	0.65–0.75	20:1 – 60:1	3,4
Shoulder Rumble Strips	Roadway departure	All severities	0.78–0.86	30:1 – 50:1	3,4
Centerline & Shoulder Rumble Strips	Roadway departure crashes	Fatal & injury	0.78	30:1 – 50:1	3,4,5
Install Guardrails (Urban Arterials)	Run-off-road crashes	Fatal & serious injury	0.74–0.85	2:1 – 6:1	4
Safety Edge Treatment	Run-off-road crashes	All severities	0.64	40:1 – 60:1	3
Curve Posted Speed Limit	All crashes	All severities	See Chapter 5	High	1,6
Curve Posted Speed Limit	All crashes	Fatal & serious injury	See Chapter 5	High	1,6

6.3 Applying Suggested Countermeasures to Curves

Using the curve characteristics along with the crash information for each curve with the highest crash frequency, potential countermeasures were identified. In some cases, missing signs were identified by looking at multiple years of Streetview images. Replacing these signs was identified as a high priority countermeasure. Priority levels were assigned to all of the curves. The resulting list of curves along with potential countermeasures and a priority level was provided as a digital file to SCDOT.

Figure 6-1 shows a location initially identified as high priority because 22 curve crashes have occurred at this location from 2017 through 2024. The picture is from July, 2016. A closer look at this location indicated that SCDOT actually improved curve safety at this location with the addition of chevron signs, shoulder improvements, and rumbled edge lines in 2021 **(Figure 6-2)**. Of the 22 crashes, only 2 occurred during the three year period (2022-2024). Other curve locations that showed a similar changing trend in crash occurrence were tagged as having a potential intervention and were looked at in greater detail.

Figure 6-1 Fork Shoals Rd in Simpsonville, July 2016

Figure 6-2 Fork Shoals Rd in Simpsonville, June 2021 with safety improvements

6.4 Recommended SCDOT Workflow

The researchers developed a workflow that SCDOT can use to do periodic statewide safety screening of highway curves. The workflow is shown in **Figure 6-3**. It is a greatly simplified workflow from what the researchers used because the curve buffers can be reused. When overlaid with crash data, these buffers can be used to identify curves with greatest crash frequency. Once identified, the researchers can use Google Earth and Street View to do a virtual roadside safety audit of the curve. Site visits should be made at the discretion of the district engineers. Low-cost countermeasures such as signage should be considered for systemic safety projects. Scheduled repaving should include Safety Edge Treatment as well as rumbled striping of longitudinal lines.

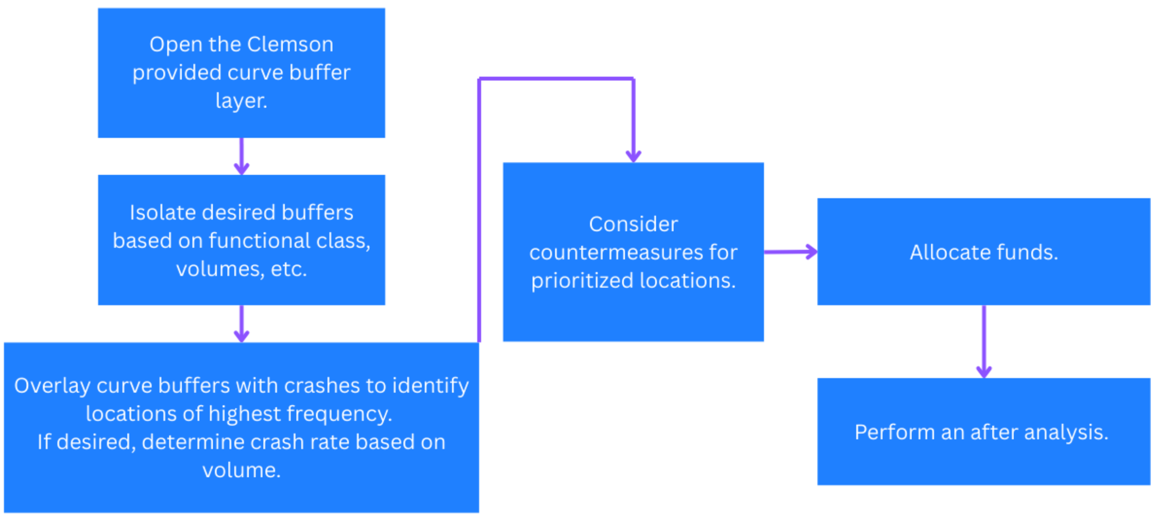

Figure 6-3 Workflow for statewide safety screening of highway curves

CHAPTER 7: CONCLUSIONS AND RECOMMENDATIONS

7.1 Highway Curve Safety

This research focused on different aspects of highway curve safety. More than 25% of fatal crashes in the US occur on horizontal curves and a recent study indicated that nearly 20% of fatal crashes in South Carolina occur on horizontal curves. Further, the crash rate for curves is approximately three times higher than other highway sections. A significant contributing factor to curve related crashes is excessive vehicle speed. This research identified and achieved several objectives including identifying potential locations of compliance issues related to curve signage and also identifying curve locations of highest crash frequency that can benefit from potential countermeasures. The research required innovative data development methods vital to the research. The next few sections highlight the achievements of this research including research products and benefits, and recommendations.

7.2 Identification of Horizontal Curve Advisory Signage

The GIS based workflow discussed in Chapter 4 is a method for determining signing needs and compliance for horizontal curves. The workflow is based on using the AASHTO design equation and the TTI equation to determine the advisory speed for a curve. The workflow uses the GIS centerline database discussed in Chapter 3 that was populated with curve attributes using automated methods. Curve radius was GIS generated but also leveraged Rieker radius data where available. Super elevation data was extracted from statewide LiDAR data in the vicinity of the highway curves using a RANSAC algorithm that was field tested for accuracy. The survey of state highway agencies indicated that while some states use an automated GIS method to extract radius data from their digital centerline, super elevation data was field collected. The GIS automated method for determining advisory speeds is novel and efficient, requiring no additional field data collection. It provides comparable advisory speed results to Rieker CARS. The method was used to screen thousands of curves for mandatory signage requirements. The Rieker mandatory signage requirements were updated to reflect more appropriate posted speed limits. It is recommended that SCDOT uses a combination of the Rieker and GIS automated method results combined with field study to determine any signage needs or changes based on MUTCD criteria and engineering judgement. Crash history should also be considered to determine the appropriateness of the existing signs and the possible need for additional signs.

7.3 Safety Analysis of Horizontal Curves using GIS

The safety analysis of this research investigated the relationship between geometric design features of highway curves and the frequency and severity of crashes. Using a combination of empirical crash data, geometric parameters, posted speeds limit, and traffic volume, statistical models were applied to identify key predictors and their effect on highway curve crash outcomes. The analysis used a population sample of curves in South Carolina that was only limited by the radius and proximity to intersections. While every state has spatially located crash data, geometric curve features such as radius, grade, and superelevation are not readily available on a large scale. The survey of states conducted as a part of this research indicated that less than half (12 of 28) of the states have radius as one of their curve attributes and even fewer (eight) have superelevation. Most of the states that maintained this data indicated that they used expensive field data collection methods to collect radius and superelevation data. This project used innovative GIS-based processing methods and aerial LiDAR data sources discussed in Chapter 3 to generate the geometric data.

The negative binomial crash analysis indicated that traffic volume, radius, and posted speed limit were significant estimators for total crashes, severe crashes, and single vehicle crashes. Grade was significant for single-vehicle crashes. Superelevation was significant for R2U severe crashes (fatal and incapacitating injury). Crash modification factors were developed for all of the significant parameters except for traffic volume. It is recommended that SCDOT use these CMFs when considering countermeasures to enhance highway curve safety.

7.4 Benefits of This Research and Research Products

The results of the research will have significant benefits for SCDOT and the traveling public, as well as other DOTs. These benefits fall into several major categories. Direct benefits to SCDOT include increased safety on highway curves through highly targeted countermeasures. Enhanced safety includes reduced crash frequency, reduced crash rates, and reduced crash severity. Crash severity is especially problematic on highway curves. This final report includes a workflow that can be followed by SCDOT to facilitate future highway curve safety analysis and prioritize investment in highway curves to enhance safety in the most efficient manner. Having a better understanding of contributing factors to crashes on highway curves and identifying best design practices through a data driven approach will ensure best use of resources to enhance safety. Based on 2023 data, traffic crashes in South Carolina annually equate to $7.7 billion in economic losses. The results of this research should provide measurable evidence-based benefits to the motoring public by enhancing safety and providing cost savings to the state of South Carolina.

There are several products of this research that should be of great benefit to SCDOT. The products include the aforementioned workflow and crash countermeasures for highway curves. Other products are discussed in the next section.

7.5 Research Products

This research project includes several useful products that can assist SCDOT to enhance curve safety. In addition to the contents of this report, several digital files have been provided to SCDOT. They include:

A table of locations of highway curves that may not meet 2023 MUTCD standards for mandated highway curve signage. The list includes three categories of signage: 1) curve warning; 2) curve warning with advisory speed; and 3) curve warning with advisory speed and chevron signs. The 2023 MUTCD allows the use of delineators in certain circumstances in lieu of chevron signs. The list is derived from nearly all highway curves in the state—not just Rieker Curves. The list includes curve attributes and hyperlinks to the curve locations so they can be quickly viewed in Google Maps.

Tables of highest crash frequency of R2U and U2U curves with potential countermeasures. The tables include notes about select curves and, for some, an indication that there was a possible intervention that caused a change in the crash trend. The tables also include curve attributes, number of crashes by year, number of fatal and severe crashes, and hyperlinks to the curve locations.

Linear referenced curve database of attributes. This database includes curve radii for 54,000 highway curves with a radius between 100' and 1500' in the state. The radii were derived from the Rieker data as well as a consultant's GIS derived radii. It involved a great deal of "cleaning" of the raw curve data. Issues with the curve radii data still exist in many instances however the cleaned database is much improved. Another attribute is curve superelevation data that was extracted from aerial LiDAR data using a RANSAC method developed by the researchers. Sample field verification indicated that the LiDAR superelevation data was within one percent on average of actual superelevation values. An additional attribute that was extracted from the LiDAR data using a similar method is curve highway grade including the direction of the grade relative to the mile marker values.

ArcGIS feature class of improved highway curve signage with improved geocoding. The speed limit and curve signage provided by SCDOT underwent a positional accuracy assessment as discussed in **Section 3-1**. Milepoints were corrected for 12,500 signs (24% of the provided signs) and geographic coordinates were corrected for 4,500 signs (9% of the provided signs).

Speed limit database. Out of 44,000 miles of state highway mileage, posted speed limits are available for 13,200 miles. The accuracy of these posted speed limits is estimated at 86%. Using a hybrid methodology developed by the researchers, the database has posted speed limits for over 41,500 miles of state highway with an estimated accuracy of 88%.
.
ArcGIS feature class of curve buffers. When overlaid with crash data, these buffers can be used to identify curves with greatest crash frequency based on the curve safety analysis workflow presented in Chapter 6.

7.6 Recommendations

The research recommendations revolve around all of the products of this research. In the near-term, SCDOT should focus on MUTCD sign compliance by making use of the list of locations that may be in need of signage. An obvious benefit is enhanced safety from new signage. New signage should also be an initial consideration at curves with a high frequency of crashes if signage is listed as a potential countermeasure.

The tables of highest frequency of R2U and U2U crashes should be scrutinized and prioritized for potential funding of countermeasures. The potential reduction in crashes will be of significant benefit to SCDOT and the traveling public. Periodic use of the curve safety workflow can be used to identify future curve safety needs while also provide "after" data for monitoring the effectiveness of countermeasures.

The researchers strongly recommend that SCDOT takes advantage of the data products of this research including curve attributes, greatly expanded posted speed limit data, and the improved curve sign inventory. The availability of these data should be communicated department wide to maximize the utility of the data.

REFERENCES

American Association of State Highway and Transportation Officials (AASHTO). A Policy on Geometric Design of Highways and Streets. Washington, D.C., 2018.

Albin, R.; Brinkly, V.; Cheung, J.; Julian, F.; Satterfield, C.; Stein, W.; Donnell, E.; McGee, H.; Holzem, A.; Albee, M.; Wood, J.; Hanscom, F. (2016). Low-Cost Treatments for Horizontal Curve Safety, *Report No. FHWA-SA-15-084.*

Babić, D., and Brijs, T. (2021). Low-cost road marking measures for increasing safety in horizontal curves: A driving simulator study. *Accident Analysis & Prevention*, *153*, 106013.

Bauer, K. M and Harwood, D. W (2014). *Safety Effects of Horizontal Curve and Grade Combinations on Rural TwoLane Highways. FHWA-HRT-13-077* Washington, DC: Federal Highway Administration.

Buddhavarapu, P., Banerjee, A., and Prozzi, J. A. (2013). Influence of pavement condition on horizontal curve safety. *Accident Analysis & Prevention*, *52*, pp. 9–18.

Chang, J., D. Findley, C. Cunningham, and M. Tsai. Considerations for Effective Lidar Deployment by Transportation Agencies. Transportation Research Record, Vol. 2440, 2014, pp. 1–8.

Dixon, K. K., and Rohani, J. W. 2008. SPR 641: Methodologies for Estimating Advisory Curve Speeds on Oregon Highways. Technical Report, Oregon Department of Transportation, Salem, Oregon.

Donnell, E. T., Porter, R. J., Li, L., Hamilton, I., Himes, S., and Wood, J. (2019). *Reducing roadway departure crashes at horizontal curve sections on two-lane rural highways*. Washington, DC: Federal Highway Administration.

Du, Y., Y. Li, S. Jiang, and Y. Shen. Mobile Light Detection and Ranging for Automated Pavement Friction Estimation. Transportation Research Record, Vol. 2673, No. 10, 2019, pp. 663–672

Elvik, R. International Transferability of Accident Modification Functions for Horizontal Curves. Accident Analysis & Prevention, Vol. 59, 2013, pp. 487–496. https://doi.org/ 10.1016/j.aap.2013.07.010.

FHWA. *Horizontal Curve Safety—Safety | Federal Highway Administration*. https://safety.fhwa.dot.gov/roadway_dept/countermeasures/horicurves/, March 14, 2022.

Fitzpatrick, K., D. Lord, and B.-J. Park. Horizontal Curve Accident Modification Factor with Consideration of Driveway Density on Rural, Four-Lane Highways in Texas. Journal of Transportation Engineering, Vol. 136, No. 9, 2010.

Farzinpour, Farhad, W. Sarasua, W. Davis, and P. Murray-Tuite. A Comparison of Methods for Collecting Highway Horizontal Curve Attributes. Transportation Research Board, Annual Meeting Conference Proceeding, 2025.

Farzinpour, F., W. Sarasua, J. Yang, and Y. Yang. A Curve Warning System to Enhance Transportation Safety in Rural Areas. Presented at Joint CATM and CR2C2 Annual Symposium, Greensboro, NC, 2024.

Ferrer-González, E., Agüera-Vega, F., Carvajal-Ramírez, F., & Martínez-Carricondo, P. UAV photogrammetry accuracy assessment for corridor mapping based on the number and distribution of ground control points. *Remote Sensing, 12*(15), 2447, 2020. https://doi.org/10.3390/rs12152447

Federal Highway Administration. *Motorcycle safety on rural curves: Countermeasure strategies*. Washington, DC: U.S. Department of Transportation, 2021.

Ghalehni, S. A., and Boroujerdian, A. M. (2023). Model of encroachment into opposite lanes in horizontal curves of rural roads. *IATSS Research*.

Glennon, J.C.; Neuman, T.R.; Leisch, J.E. (1985). Safety and Operational Considerations for Design of Rural Highway Curves. *Report No. FHWA-RD-86-035,* Federal Highway Administration, Washington, DC.

Gooch, J.P.; Gayah, V.V.; Donnell, E.T. (2018). Safety Performance Functions for Horizontal Curves and Tangents on Two Lane, Two Way Rural Roads. *Accid. Anal. Prev., 120,* pp. 28–37.

Green, E., K. Agent, and E. Lammers. Development of an Improved Method for Determining Advisory Speeds on Horizontal Curves. Publication KTC-16-14/SPR15-507-1F. Kentucky Transportation Cabinet, 2016.

Guan, H., J. Li, Y. Yu, C. Wang, M. Chapman, and B. Yang. Using Mobile Laser Scanning Data for Automated Extraction of Road Markings. ISPRS Journal of Photogrammetry and Remote Sensing, Vol. 87, 2014.

Holgado-Barco, A., D. Gonzalez-Aguilera, P. Arias-Sanchez, and J. Martinez-Sanchez. An Automated Approach to Vertical Road Characterisation Using Mobile LiDAR Systems: Longitudinal Profiles and Cross-Sections. ISPRS Journal of Photogrammetry and Remote Sensing, Vol. 96, 2014, pp. 28–37.

Highway Safety Manual with Supplement. American Association of State Highway and Transportation Officials, Ed. 1, 2010; 2014.

Himes, S., and Donnell, E. (2020). Safety effects of horizontal curve reliability index. *Transportation Research Record*, *2674*(9), pp. 627–636.

Hummer, J. E., W. Rasdorf, D. J. Findley, C. V. Zegeer, and C. A. Sundstrom. Curve Collisions: Road and Collision Characteristics and Countermeasures. Journal of Transportation Safety & Security, Vol. 2, No. 3, 2010, pp. 203–220.

Indiana Design Manual, Ch. 43 Indiana DOT, 2013.

Li, Z., M. Chitturi, A. Bill, and D. Noyce. Automated Identification and Extraction of Horizontal Curve Information from Geographic Information System Roadway Maps. Transportation Research Record: Journal of the Transportation Research Board, Vol. 2291, 2012, pp. 80-92

Lord, D. and Bonneson, A. (2007) Development of Accident Modification Factors for Rural Frontage Road Segments in Texas. Transportation Research Record, 2023, 20-27.

Khan, G., Bill, A. R., Chitturi, M., and Noyce, D. A. (2012). Horizontal curves, signs, and safety. *Transportation Research Record*, *2279*(1), pp. 124–131.

Kronicz, J. Using GIS to Identify and Characterize Horizontal Curvature. Presented at the 2016 Pennsylvania GIS Conference, State College, PA, 2016.

Ma, L., T. Wu, Y. Li, J. Li, Y. Chen, and M. Chapman. Automated Extraction of Driving Lines from Mobile Laser Scanning Point Clouds. Advances in Cartography and GIScience of the ICA, Vol. 1, 2019, pp. 1–6.

Manual on Uniform Traffic Control Devices. FHWA. U.S. Department of Transportation, 2009.

Manual on Uniform Traffic Control Devices. FHWA, U.S. Department of Transportation, 2023.

MassDOT Project Development Guide, Chapter 4 – Horizontal and Vertical Alignment, MassDOT, 2024.

Milstead, R., X. Qin, B. Katz, J. Bonneson, M. Pratt, J. Miles, and P. Carlson. Procedures for Setting Advisory Speeds on Curves. Publication FHWA-SA-11-22. FHWA, U.S. Department of Transportation, 2011.

Montana DOT Road Design Manual, Ch 3, Montana DOT, 2016.

NHTSA. *MMUCC guideline: Model minimum uniform crash criteria fourth edition.* (report no. dot hs 811 631). Washington, DC: National Highway Traffic Safety Administration, 2012.

Peng, J., Chu, L., and Fwa, T. F. (2021). Determination of safe vehicle speeds on wet horizontal pavement curves. *Road Materials and Pavement Design*, *22*(11), pp. 2641–2653.

Persaud, B.; Retting, R.A.; Lyon, C. (2000). Guidelines for identification of hazardous highway curves. Transp. *Res. Rec. J. Transp. Res. Board, 1717,* pp. 14–18.

Rasdorf, W.; Findley, D.J.; Zegeer C.V.; Sundstrom, C.A.; Hummer, J.E. (2010). Curve Crashes: Road and Collision Characteristics and Countermeasures. *Journal of Transportation Safety and Security, Southeast Transportation Research Center.*

Russo, F.; Busiello, M.; Dell'Acqua, G. (2016). Safety performance functions for crash severity on undivided rural roads. *Accid. Anal. Prev., 93*, pp. 75–91.

Ruzgienė, B., and W. Förstner. Ransac for Outlier Detection. Geodeziji ir Kartografija, Vol. 31, No. 3, 2005, pp. 83-87

Saleem T., B. Persaud. Another look at the safety effects of horizontal curvature on rural two-lane highways. Accid Anal Prev. 2017 Sep;106:149-159. doi: 10.1016/j.aap.2017. 04.001. Epub 2017 Jun 13. PMID: 28618353.

Shalkamy, A., L. Karsten, S. Gargoum, and K. El-Basyouny. A Framework to Detect Horizontal Curves and Assess Their Geometric Properties from Remotely Sensed Point Clouds. International Journal of Remote Sensing, Vol. 41, No. 21, 2020, pp. 8328–8351.

Shams, A., W. Sarasua, A. Famili, W. Davis, J. Ogle, L. Cassule, and A. Mammadrahimli. Highway Cross-Slope Measurement Using Mobile LiDAR. Transportation Research Record, Vol. 2672, No. 39, 2018

Sil, G., et al. Operating Speed Prediction Models for Horizontal Curves on Two-Lane Rural Highways. Journal of Transportation Engineering, 2020.

SCDPS. *Traffic Collision Fact Books.* Blythewood, SC: South Carolina Department of Public Safety, 2021.

Stewart, T. (2022). *Overview of Motor Vehicle Crashes in 2020* (DOT HS 813 266). Washington, DC: National Highway Traffic Safety Administration.

Torbic, D. J., Harwood, D. W., Gilmore, D. K., Pfefer, R., Neuman, T. R., Slack, K. L., & Hardy, K. K. (2004). *Guidance for implementation of the AASHTO strategic highway safety plan. NCHRP 500. Volume 7: A guide for reducing collisions on horizontal curves*.

Tsai, Y., P. Yu, T. Liu, Z. Yang, and A. Steel. An Enhanced Network-Level Curve Safety Assessment and Monitoring Using Mobile Devices. Publication FHWA-GA-21-1917. Georgia Department of Transportation, 2021.

USDOT. Achieving the Vision of Zero Roadway Deaths Through the Safe System Approach. US Department of Transportation, No. 2, 2022, https://www.transportation.gov/utc/achieving-vision-zero-roadway-deaths-through-safe-system-approach.

Ural, S., Shan, J., Romero, M. A., & Tarko, A. Road and roadside feature extraction using imagery and LiDAR data for transportation operation. *ISPRS Annals of Photogrammetry, Remote Sensing and Spatial Information Sciences, II-3/W4*, 2015, pp.239–246. https://doi.org/10.5194/isprsannals-II-3-W4-239-2015

Wang, K.; Simandl, J.K.; Porter, M.D.; Graettinger, A.J.; Smith, R.K. (2016). How the choice of safety performance function affects the identification of important crash prediction variables. *Accid. Anal. Prev., 88,* pp. 1–8.

Zegeer, C. V., Stewart, J. R., Council, F. M., Reinhurt, D. W., and Hamilton, E. (1992). Safety effects of geometric improvements on horizontal curves. *Transportation Research Record*. 1356, pp. 11-19

Zou, F.; Sarasua, W.; Ogle, J.; Stanley, M.; Brown, K.; Michalaka, D.; Lloyd, J.; Murray-Tuite, P.; Davis, W.; Wade, L. (2022) Site Characterization for Fatal Crashes in South Carolina. *Presented at Transportation Research Board 101st Annual meeting (Paper #22-04907)*

Zulkipli, M. A., & Tahar, K. N., Multirotor UAV-based photogrammetric mapping for road design. *International Journal of Optics*, Article ID 1871058, 2018. https://doi.org/10.1155/2018/1871058

APPENDIX A

Survey of State Agencies

Note: Omitted questions were related to the person completing the survey including their title and contact information.

Q2 - Please enter your State or Commonwealth

Please enter your State or Commonwealth

Colorado

Maine

South Carolina

Washington

Florida

Tennessee

Oregon

North Dakota

Nebraska

Maine

Louisiana

Arkansas

Nevada

Texas

Pennsylvania

Vermont

Arizona

Wyoming

New York

Indiana

Montana

Indiana

Ohio

Michigan

Mississippi

South Dakota

Kentucky

Missouri

Delaware

Q9 - What methods do you use to determine safe advisory speeds for roadway curves? Please select all that apply.

Field	Choice Count
Compass method	1
Safety based method	3
Accelerometer (in-house)	5
Design equation method	12
Ball-bank method (in-house)	22
Direct method based on speed data	3
Other (specify)	2
GPS Method	
Not sure	
Rieker or similar curve advisory speed reporting service	7

Q10 - Because you chose more than one method in the previous question, what is your primary method for determining safe advisory speeds for roadway curves? (select one) - Selected Choice

Field	Choice Count
Compass method	0
Safety based method	0
Accelerometer (in-house)	0
Design equation method	5
Ball-bank method (in-house)	11
Direct method based on speed data	0
Rieker or similar curve advisory speed reporting service	2
Other (specify)	1
GPS Method	

Q11 - Does your statewide road characteristics database include curve attributes such as radius, length, or included angle (delta)?

Q12 - What curve information does your road characteristics database include? Please select all that apply. - Selected Choice

Field	Choice Count
Radius	12
Start or PC mile point	11
End or PT mile point	10
Length	14
Delta (included angle	7
Design speed/Advisory speed	6
super elevation/cross slope	8
Other (describe)	4
Degree of curvature	

Q13 - How does your organization collect radius data? Please select all that apply. - Selected Choice

Field	Choice Count
Mobile LiDAR	2
Automated processing of GIS map data	4
As-built plans	7
Rieker	0
A manual method using imagery such as Bing or Google	3
Derived from compass method (calculated using include angle and curve length	2
Other (describe)	5
Derived from GPS data	
ARAN	
Not sure	

Q14 - How is radius data used? Please select all that apply. - Selected Choice

Field	Choice Count
Pre-construction project planning	8
Safety analysis (crash occurrence on curves)	10
Prioritizing locations for setting advisory speeds (screening purposes)	7
Setting advisory speeds using the design equation	8
Other (describe)	0

Q15 - You indicated in the previous question that you use the radius data to set advisory speeds using the design equation. How is superelevation determined? - Selected Choice

Field	Choice Count
Field collected regardless of method	5
A conservative value is assumed. If so, please state the value in % (e.g. 4%)	0
Other (describe)	2

Assumed value based on roadway functional classification

Q16 - Does your organization maintain a sign inventory?

25 Responses

Q17 - What signs are included in your inventory? Please select all that apply.

21 Responses

Field	Choice Count
Regulatory signs	19
Warning signs	20
Guide signs	18
Other signs	17

Q18 - With regard to speed limit signage which of the following best describes your speed limit sign inventory.

19 Responses

Field	Choice Count
Relatively complete	15
Incomplete coverage (Only primary roads are included or data is missing for many roads)	2
Some data may be inaccurate or outdated.	4
Other (describe)	0

Q19 - Does your road characteristics database include posted speed limit?

26 Responses

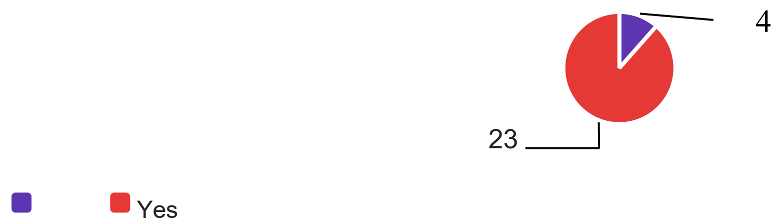

Q20 - What is the primary source for speed limit data in your road characteristics database? Please select all that apply. - Selected Choice

Field	Choice Count
Sign inventory if available	10
Field reconnaissance	10
As built plans	5
Google street view or other video logging source including in-house	10
Other (describe)	9

When speed limits are updated

Not sure

State rules for speed limits

Strip map roadway library

Q21 - What best describes your speed limit data in your road characteristics database? Please select all that apply. - Selected Choice

23 Responses

Field	Choice Count
Relatively complete	17
Incomplete coverage (Only primary roads are included or data is missing for many roads)	1
Some data may be inaccurate or outdated.	6
Other (describe)	2